DYSREGULATION OF CELL GROWTH AND APOPTOSIS NETWORKS THROUGH ALTERED MRNA DECAY IN MALIGNANT AND VIRUS-INFECTED CELLS

A DISSERTATION

SUBMITTED TO THE FACULTY OF THE GRADUATE SCHOOL OF THE UNIVERSITY OF MINNESOTA

BY

LIANG GUO

IN PARTIAL FULFILLMENT OF THE REQUIREMENTS FOR THE DEGREE OF DOCTOR OF PHILOSOPHY

PAUL R. BOHJANEN MD, PhD &

IRINA VLASOVA-ST. LOUIS MD, PhD

August 2018

Acknowledgements

I would like to thank many people in helping me to complete this thesis. First of all, I would like to acknowledge my thesis committee for their insightful comments and encouragement: Dr. Clifford Steer, MD, Dr. James Lokensgard, PhD, Dr. Jose Debes, MD, Dr. Irina St. Louis, MD PhD, and Dr. Paul Bohjanen MD PhD. Especially, I would like to express my sincere gratitude to my advisors, Drs. Irina St. Louis and Paul Bohjanen, for their guidance and support throughout my PhD study. It has been a privilege to work with and learn from them. They are and will always be my mentors and friends.

I also would like to thank all the past and present lab members, particularly, Dr. Daniel Beisang, for his feedback and cooperation. I also thank Dr. Cavan Reilly, who provided help in analyzing the data for many of my projects.

In addition, my sincerest thanks go to the Comparative and Molecular Biosciences Graduate Program in the College of Veterinary Medicine for their support. I am also grateful to the Institute for Molecular Virology Training Program for their financial support.

Last but not least, I would like to thank my friends and family, for their unfailing support and encouragement along the way.

Dedications

This dissertation is dedicated to my husband, Eric Espland, and our cats, Mimi and Olly.

Abstract

Gene expression in eukaryotic cells is tightly regulated at various levels, including transcription, post-transcriptional RNA modification, RNA localization, RNA stability, translation, and post-translational modification. Alterations in mRNA stability are particularly unique; regulation of mRNA stability enables the rapid and precise change in the expression of genes *en masse* in a coordinated fashion in response to different cellular conditions. An important feature of both chronic viral infections and the development of cancers is dysregulated cell growth and prevention of the death of damaged cells. Dysregulation of signaling transduction networks that control cellular division and apoptosis occurs in both viral infection and development of malignancy, and this dysregulation involves a variety of gene regulatory mechanisms, including transcription, post-transcriptional regulation, translation and post-translation modification. Post-transcriptional regulatory mechanisms that control gene expression in viral infection and malignancy, especially mRNA decay, are not well understood. The work presented in this thesis focuses on investigating the dysregulation of gene expression networks that control cell growth and apoptosis at the level of mRNA decay in two disease states: viral infection and malignancy. In particular, this work describes how dysregulation of cell growth and apoptosis networks contributes to the pathogenesis of viral infection and malignant transformation.

The first project presented in Chapter 2 was to elucidate the network of transcripts that are regulated by the RNA binding protein CUGBP1 and Etr3 Like Factor 1 (CELF1) in malignant T cells. CELF1 is an important RNA decay

regulator which binds to the GU-rich element (GRE) within its target transcripts and mediates rapid degradation of the transcripts. We performed immunoprecipitation using an anti- CELF1 antibody, followed by identification of co-purified transcripts using microarrays. We found that CELF1 is bound to a distinct set of target transcripts in the H9 and Jurkat malignant T-cell lines, compared with primary human T cells. CELF1 was not phosphorylated in resting normal T cells, but in malignant T cells, phosphorylation of CELF1 correlated with its inability to bind to GRE-containing mRNAs that served as CELF1 targets in normal T cells. Lack of binding by CELF1 to these mRNAs in malignant T cells correlated with stabilization and increased expression of transcripts. Several of these GRE-containing transcripts that encode regulators of cell growth were also stabilized and up-regulated in primary tumor cells from patients with T-cell acute lymphoblastic leukemia. Interestingly, transcripts encoding numerous suppressors of cell proliferation that served as targets of CELF1 in malignant T cells, but not normal T cells, exhibited accelerated degradation and reduced expression in malignant compared with normal T cells, consistent with the known function of CELF1 to mediate degradation of bound transcripts. Overall, CELF1 dysfunction in malignant T cells led to the up-regulation of a subset of GRE-containing transcripts that promote cell growth and down-regulation of another subset that suppress cell growth, producing a net effect that would drive a malignant phenotype.

The next two projects presented in Chapter 3 and 4 were to explore the network of cellular transcripts with altered stability following infection of

mammalian cells with hepatitis C virus (HCV) and reovirus, respectively. We utilized RNA-immunoprecipitation followed by RNA sequencing on cell lysates from human hepatoma cells expressing a HCV subgenomic replicon, and found that the viral nonstructural protein 5A (NS5A), a protein known to bind to viral RNA, also bound specifically to human cellular transcripts that encode regulators of cell growth and apoptosis, and this binding correlated with transcript stabilization. An important subset of human NS5A-target transcripts contained GRE, sequences known to destabilize mRNA. We found that NS5A bound to GU-rich elements in vitro and in cells. Mutation of the NS5A zinc finger abrogated its GU-rich element-binding and mRNA stabilizing activities. Through this project, we identified a molecular mechanism whereby HCV manipulates host gene expression by stabilizing host transcripts in a manner that would promote growth and prevent death of virus-infected cells, allowing the virus to establish chronic infection and lead to the development of hepatocellular carcinoma.

In the reovirus project, we utilized oligonucleotide microarrays to measure cellular mRNA decay rates in mock- or reovirus-infected murine L929 cells. Our analysis detected a subset of cellular transcripts that were coordinately induced and stabilized following infection with the reovirus isolates c87 and c8, isolates that also induced inhibition of cellular translation in infected cells. The induced and stabilized transcripts encoded multiple regulators of TGF-β signaling, including components of the Smad signaling network and apoptosis/survival pathways. The coordinate induction through mRNA stabilization of multiple genes that encode components of TGF-β signaling pathways represents a novel

mechanism by which the host cell responds to viral infection.

In summary, the work presented in this dissertation demonstrates that posttranscriptional gene expression networks that control cell growth and apoptosis are dysregulated in malignant cells (Chapter 2) as well as in cells infected with viruses such as HCV (Chapter 3) or reovirus (Chapter 4). Manipulation of cellular gene expression networks by HCV allows establishment of chronic infection and prevents apoptosis, eventually leading to development of liver cancer. In contrast, reovirus, which kills infected cells and does not induce chronic infection, also leads to perturbation in cell survival/apoptosis networks, perhaps as a cellular response to viral infection.

Table of Contents

List of Tables

List of Figures

List of Abbreviations

AP2A2	AP-2 complex subunit alpha-2
APA	Alternative polyadenylation
ARE	AU-rich element
AREBP	AU-rich element binding protein
AUF1	ARE/poly(U) binding/degradation factor 1
AURKB	Aurora kinase B
BAG	BCL2-associated athanogene
BBB	Beta-globin expression plasmid
BCL10	B-cell lymphoma/leukemia 10
CCR4	Carbon catabolite repression 4
CCR5/7	C-C motif chemokine receptor 5/7
CDC73	Cell division cycle 73
CDK11A/B	Cyclin-dependent kinase 11A/B
CDKN1A	Cyclin dependent kinase inhibitor 1A
CEBPB	CCAAT/enhancer-binding protein beta
CELF1	CUGBP and Etr3-Like Factor 1
CENPA	Centromere protein A
CENPF	Centromere protein F
COX2	Cyclooxygenase 2
CUGBP1	CUG triplet repeat, RNA binding protein 1
CVB3	Coxsackievirus B3
CXCL-8	Interleukin-8
DCP2	Decapping enzyme 2
DcpS	Scavenger decapping enzyme
dsRNA	Double-stranded RNA
EBV	Epstein-Barr virus
EBVR1/2	EBV-encoded RNA 1/2
EDEN-BP	Embryo deadenylation element binding protein
EIF4G3	Eukaryotic translation initiation factor 4 gamma 3
EIFEBP1	Eukaryotic initiation factor 4E binding protein 1
ERK	Extracellular signal-regulated kinase
FCE	Fold change in enrichment
Fos	AP-1 transcription factor subunit
FPKM	Fragments per kilobase of transcript per million
G2E3	G2/M-phase specific E3 ubiquitin protein ligase
GAPDH	Glyceraldehyde-3-phosphate dehydrogenase
GFP	Green fluorescence protein
GPCR	G-protein-coupled receptor

GRE	GU-rich element
GREBP	GU-rich element binding protein
HA	Human influenza hemagglutinin
HCV	Hepatitic C virus
HOXC10	Homeobox protein Hox-C10
HPRT	Hypoxanthine phosphoribosyltransferase
HSP70-1	Heat shock 70-kDa protein-1
HSV	Herpes simplex virus
HuD	Human antigen D
HuR	Human antigen R
IFN-γ	Interferon gamma
IL1/2/6	Interleukin-1/2/6
IL1RB	Interleukin 1 receptor type II
IP	Immunoprecipitation
JUN	AP-1 transcription factor subunit
KBTBD7	Kelch repeat and BTB domain-containing protein 7
KSHV	Kaposi's sarcoma-associated herpesvirus
LLP	λ-protein phosphatase
MAP3K5	Mitogen-activated protein kinase kinase kinase 5
MAPK	Mitogen-activated protein kinase
MED24	Mediator of RNA polymerase II transcription subunit 24
mRNA	Messenger RNA
NDRG3	N-myc downstream-regulated gene 3
NGR3	Nogo receptor family member 3
Not	Negative on TATA
NS5A	Non-structural protein 5A
PABP	PolyA biniding protein
PAN2/3	PolyA nuclease 2/3
PARN	PolyA ribonuclease
PIAS1	E3 SUMO-protein ligase
PKC	Protein kinase C
QPCR	Quantitative polymerase chain reaction
RBP	RNA binding protein
RNA-IP	RNA-immunoprecipitation
RNA-SEQ	RNA sequencing
RRM	RNA-recognition motif
RT-PCR	Reverse transcription polymerase chain reaction
SIAH1	E3 ubiquitin-protein ligase
SMAD7	Mothers against decapentaplegic homolog 7
SOCS5	Suppressor of cytokine signaling 5

SOX	Shut-off alkaline exonuclease
SSN	Smad signaling network
STAT5	Signal transducer and activator of transcription 5
T-ALL	T-cell acute lymphoblastic leukaemia
TERF2	Telomeric repeat-binding factor 2
TGF-β	Transforming growth factor beta
TNF-α/β	Tumor necrosis factor alpha/beta
TNFRSF4	TNF receptor superfamily member 4
TNFSF10	Tumor necrosis factor (ligand) superfamily, member 10
TTP	Tristetraprolin
UTR	Untranslated region
VEGF	Vascular endothelial growth factor
VHS	Virion host shutoff
XRN1	5'-3' exoribonuclease 1
ZMAT3	Zinc finger matrin-type protein 3
ZNF436	Zinc Finger Protein 436

Preface

Some of the work presented in the following chapters has been published or submitted for publication. This work is the collaborative efforts from many authors. Chapter 1 is a compilation of two reviews published in Future Virology and Current Trends in Immunology, respectively. Both reviews were published in conjunction with Paul Bohjanen and Irina Vlasova-St. Louis. My role in these two publications was to write and edit the manuscript, as well as produce associated tables and figures.

Chapter 2 has been published in the journal RNA in conjunction with Paul R. Bohjanen, Mai Lee Moua, Ammanuel Taye and Irina A. Vlasova-St. Louis. In conjunction with Ammanuel Taye, I performed 2D electrophoresis and western blotting to generate figure 2.3. In conjunction with Mai Lee Moua, I performed RNAIP and qRT-PCR to generate figure 2.5 and table 2.6.

Chapter 3 has been published in the journal Nucleic Acids Research in conjunction with Suresh D. Sharma, Jose Debes, Daniel Beisang, Bernd Rattenbacher, Irina Vlasova-St. Louis, Darin L. Wiesner, Craig E. Cameron, and Paul R. Bohjanen. I performed data analysis and complied data for supplementary tables 1-3. I generated figures 3.1, 3.2, 3.6B, and supplementary figure 2. I performed experiment and generated supplementary table 4. I participated in writing and editing the manuscript.

The data in Chapter 4 is submitted for publication in the journal PLOS ONE. The work is done in conjunction with Jennifer A. Smith, Michelle Abelson, Irina A. St-Louis-Vlasova, Leslie A. Schiff and Paul R. Bohjanen. I participated in

the data analysis and compiled the data. I generated figures 4.1. I participated in writing and editing the manuscript.

Chapter 1:

Introduction

Mammalian cells have developed mechanisms to detect cellular damage that trigger death of damaged cells. Cellular damage that triggers cell death can be due to viral infection or other genetic damage that leads to the development of malignancy. In order for malignancy to develop or for viruses to establish chronic infection, cellular pathways that induce cell death must be disrupted to allow continued growth of damaged cells. This dissertation focuses on understanding mechanisms by which cell death and cell growth pathways are dysregulated in malignancy or viral infection.

Viruses are small infectious pathogens that must replicate inside host cells. After entering the cell, viruses release their genetic materials and take control of the cellular gene expression factory to produce viral proteins for viral replication. Most infected cells eventually die because of host organism's immune response, or cell lysis due to excessive viral burden, or apoptosis triggered by damage caused by infection as an innate antiviral defense mechanism. However, viruses such as hepatitis C virus (HCV) and human papilloma virus (HPV) develop methods to alter the cell functions in order to keep the infected cell alive and establish chronic infection. The mechanisms that some viruses used to promote cell growth and limit apoptosis are similar to those seen in malignancies, and in fact, some chronic viral infections eventually transform infected cells to malignant cells (1, 2). Enormous amounts research studies have investigated the mechanisms that cancer or viruses exploit to regulate cell functions at transcriptional or post-translational levels, yet this research has yielded only a scant number of clinical treatments. On the other hand, not many

studies have looked at the post-transcriptional aspect of regulation in the pathogenesis of viral infection or cancer. In particular, the role of mRNA decay is not well understood. This dissertation aims to filling this knowledge gap by focusing on understanding the dysregulation of cellular growth and apoptosis networks through altered mRNA decay in malignant and virus-infected cells.

Apoptosis, a process of intentional, programmed cell death, plays a role in many different physiological processes, including normal human development, as well as serving as a critical mechanism of protection against certain diseased states, such as infection and malignancy. When a cell is virally infected, the cell can undergo apoptosis through one of two ways: intrinsic or extrinsic. The extrinsic pathway involves cytosolic viral proteins fragments being loaded onto MHC Class I molecules and sent to the cell membrane, where circulating cytotoxic CD 8^+ T cells identify the protein fragments as foreign, and undergo a complex series of events that result in apoptosis of the infected cell. Intrinsic apoptosis is when the infected host cell detects the damage caused by the invading virus, and triggers a cascade of event that ultimately lead to death of the cell from within (1).

Similar to virally infected cells, malignant cells are subject to much of the same apoptosis mechanisms, albeit with some differences. Tumor cells do not produce true “foreign” proteins, but as seen in virally infected cells, DNA damage and subsequent expression of aberrant proteins trigger apoptosis. The main difference, however, is that DNA damage is much more prominent in tumor cells than virally infected cells (1).

Apoptosis, therefore, represents a monumental obstacle that must be overcome in order to establish chronic viral infection and in the development of malignancy. Both viral infected cells and cancer cells have shown to have altered genes or expression of genes that are major regulators of cell growth and apoptosis. These genes that are often associated with cancer, including proto-oncogenes and tumor suppressors. Proto-oncogenes, such as c-Myc and Ras, encode proteins that promote cell division or prevent cell death under normal conditions; Tumor suppressors, such as Rb and p53, produce proteins that normally inhibit cell division and induce cell death. Thus, controlled cell growth and cell death in normal cells are maintained by proto-oncogenes and tumor suppressors. Mutations of either group of genes or abnormal expression of these genes would result in uncontrolled cell growth. For instance, proto-oncogenes encoded proteins are usually key players in the signaling cascades or pathways that stimulate cell growth, and when they are mutated, they become oncogenes. The oncogenes constitutively activate the signaling pathways, resulting in continuous cell growth.

The fundamental processes that drive the pathogenesis of chronic viral infection and malignancy, although seemingly unrelated, share some of the same basic features. In both chronic viral infection and tumorigenesis, each must accomplish some changes: 1) promotion of growth; 2) suppression of apoptosis; and 3) evasion of extrinsic immune system attacks. The similarities do not end there, as the actual mechanisms of achieving each of these ends can be quite similar as well.

The promotion of growth is a keystone in the establishment of both malignancies and viral infections. In fact, both of these diseases involve some of the exact same key mediators of growth. For example, the proto-oncogene c-Myc has been implicated in both B-Lymphomas (3) as well as HTLV-1 infection (4). Besides, the inactivation of retinoblastoma (Rb) is a key component in the pathogenesis of both HPV infection (5) and many cancers, including its name sake retinoblastoma (6).

Similarly, the suppression of apoptosis is absolutely paramount in the pathogenesis of both viral infection and malignancy. Much like cellular growth, viruses and cancers act on some of the regulatory mechanisms to accomplish the suppression of apoptosis. For example, induction of the expression of Bcl-2, a well-known inhibitor of apoptosis, has been implicated in the establishment of latent EBV infection (7), as well as the development of chronic myelogenous leukemia (8).

In the attempt to evade extrinsic immune system attacks, certain viruses decrease the expression of MHC Class I molecules; however, NK cells detect cells with low levels of MHC expression and induce their apoptosis (9). Likewise, NK cells detect decreased amounts of MHC on tumor cells and induce their apoptosis (10).

The similarities between chronic viral infection and oncogenesis are so extensive that, in some case, infection with certain viruses has been directly associated with the development of certain human cancers. Some examples include, both Hepatitis B virus (HBV) and HCV can increase the patient's chance

of liver cancer, human papillomavirus (HPV) has been identified as an important cause of cervical cancer, and T-cell leukemia virus (HTLV-I) are found to cause T-cell lymphoma/leukemia. In fact, it is estimated that 15-20% of human cancers are associated with viral infection (11-13).

Our laboratory has been focusing on the mRNA decay aspect of the post-transcriptional regulation in many other systems, such as T cell activation, and we are interested in investigating its role in the dysregulation of cell growth and apoptosis networks in malignant and virus-infected cells.

Biochemistry of mRNA decay

In eukaryotic cells, gene expression is tightly regulated both transcriptionally and post-transcriptionally to assure correct protein production and normal cell function. One important aspect of post-transcriptional regulation is mRNA turnover, in which the cellular mRNA decay machinery works to coordinate the expression of genes by controlling the stability and lifespan of mRNAs through highly regulated mechanisms. The overall importance of mRNA stability in determining gene expression is highlighted by the studies investigating the impact of mRNA decay on gene expression, which estimate that 20-50% of the changes in gene expression in both yeast and mammalian cells upon stimulation are due to altered mRNA decay (14, 15).

Deadenylation-dependent RNA decay is the major cellular pathway for cytoplasmic mRNA turnover. Deadenylation is a process of 3' polyA tail shortening by cellular deadenylase enzyme complexes such as CCR4-NOT,

PAN2-PAN3, and PolyA ribonuclease (PARN). The removal of the polyA tail is usually the first and rate limiting step of mRNA decay (16). The deadenylated transcript is then subject to rapid exonucleolytic degradation, with decay occurring in either the 3'-to-5' direction by the cytoplasmic exosome and the scavenger decapping enzyme (DcpS), or in the 5'-to-3' direction by the cellular decapping enzyme DCP2 and exonuclease XRN1 (17-21). Specific mRNAs are deadenylated at different rates. This differential mRNA deadenylation is not a stochastic process but rather, a precisely controlled process for determining the life span of each mRNA. The mechanisms by which the cell selects mRNAs for deadenylation are not fully known (18, 22).

During recent decades, advanced techniques such as RNA immunoprecipitation, gene expression microarrays, next generation sequencing, and mass spectrometry have enabled researchers to identify *cis*-elements and *trans*-acting factors which determine mRNA stability. *Cis*-elements are sequences within mRNA molecules, often in the untranslated regions, that are bound by *trans*-acting factors, such as RNA binding proteins (RBPs) or microRNAs. Their interaction determines the transcription, location, translation, and stability of the mRNAs that harbor the *cis*-elements (23). The study of how these *cis*-elements and *trans*-acting factors mediate mRNA decay has unraveled a broader understanding of the mechanism of coordinately regulated deadenylation-dependent mRNA decay; mRNA decay rates are determined by the ability of *trans*-acting factors to recruit or repel components of the mRNA decay machinery. For example, upon binding to *cis*-elements, decay-promoting

RBPs can recruit deadenylases such as PARN to shorten the polyA tail of a mature mRNA, which then initiates the degradation cascade (24, 25).

mRNA decay networks

The interactions between *cis*-elements and *trans*-acting factors define different post-transcriptional regulatory networks. Different *trans*-acting factors collectively act on the *cis*-elements within a group of mRNAs that involve the same functional network, thus coordinating the gene expression post-transcriptionally (23, 26). Countless studies have been focusing on two important mRNA decay regulating *cis*-elements. These include AU-rich elements (AREs) and GU-rich elements (GREs), their associated *trans*-acting factors, and the post-transcriptional regulation of ARE- or GRE-containing transcripts in malignancy and viral infection.

ARE-mediated mRNA decay

The best-studied mRNA decay *cis*-element is the ARE, a sequence found in the 3’ UTR of certain transcripts that promotes rapid mRNA decay. The ARE was first identified in 1986 by Caput and colleagues using bioinformatic approaches. They found an evolutionarily-conserved adenine- and uridine-rich consensus sequence that is present in the 3' UTR of both human and mouse tumor necrosis factor (TNF) mRNAs (27). Later studies identified more AREs that functioned to mediate mRNA decay, and AREs were organized into three classifications that differ by their sequence composition and decay kinetics (28).

A subset of AREs, characterized by overlapping AUUUA pentamers, are enriched in secreted proteins, such as cytokines and chemokines. Notably, ARE-containing transcripts account for 5-8% of the human transcriptome (29), but they make up approximately 80% of transcripts within cytokine networks (30). The importance of AREs in regulating cytokine expression was first demonstrated by the mutation of AREs in cytokine mRNAs, such as TNF-α or IFN-γ, resulting in autoimmune-like inflammatory syndrome due to increased expression of these cytokines (31, 32). Many proto-oncogene transcripts, such as v-myc, c-fos, and c-jun, also contain AREs (33).

AREs regulate mRNA stability by interacting with a variety of ARE-binding proteins (AREBPs). Some AREBPs, such as tristetraprolin (TTP, also known as ZFP36) and ARE/poly(U) binding/degradation factor 1 (AUF1), promote transcript decay by recruiting cellular enzymes for deadenylation and degradation (20, 34), while other AREBPs, such as human antigen R (HuR, also known as ELAV-like protein 1) and ELAV-like protein 4 or human antigen D (HuD), stabilize transcripts when they bind to the AREs (35), possibly by preventing the binding of decay-promoting AREBPs (36). Some ARE-containing transcripts are targeted for degradation by cellular ribonucleases directly. For example, ZC3H12A initiates rapid degradation of several cytokine transcripts, such as TNFα, IL1b, IL2, IL6 and IL12b, by cleaving the stem loop mRNA structure that is proximal to the AREs (37). On the other hand, HuR also binds to AREs in these transcripts and many other pro-inflammatory cytokine transcripts, including IL13, IL17, VEGF, COX2, and several chemokines. Binding by HuR to the AREs in the

3'UTR of these transcripts leads to stabilization of the transcripts and consequently, increasing mRNA levels and often protein levels (38-42). In addition, microRNAs can directly bind to AREs and regulate the stability of the ARE-containing transcripts (43). These AREBPs and microRNAs work in concert to determine the biological outcome of the ARE-harboring transcripts (36). There are over 20 AREBPs from various families and that are spread widely throughout the cell, from nucleus to cytoplasm to subcellular structures such as stress granules and processing bodies. They are also active contributors or effectors in a variety of signaling transduction pathways.

GRE-mediated mRNA decay

GREs are recently discovered mRNA decay elements that are enriched in the 3'UTR of numerous short-lived transcripts. Inserting a GRE into the 3'UTR of a beta-globin reporter causes the otherwise stable reporter to become highly unstable, indicating that GRE is a functional mediator of mRNA decay (44). The RNA-binding protein CUGBP and Etr3-Like Factor 1 (CELF1) has been found to specifically bind to GREs and mediate the subsequent rapid degradation of the GRE-harboring transcripts (45). Later experiments found that CELF1 also binds to GU-repeat sequences and mediates the decay of their mRNA as well (46). Thus, the GRE has been defined as of the form UGUU(/G)UGUU(/G)UGU. Transcripts that contain GRE encode important regulators involved in cell growth, proliferation, apoptosis, and oncogenesis (47). The exact mechanism of GRE and CELF1 mediated mRNA decay is not completely understood. It is postulated

that in the cytoplasm, the GRE-containing transcript is recognized and bound by CELF1, which recruits deadenylases to initiate the rapid degradation of the transcript (25).

The GRE/CELF1 regulatory networks control a variety of important biological processes, such as cellular growth, differentiation, and activation. For example, upon T cell activation, CELF1 becomes phosphorylated and loses its ability to bind to GREs, the consequence of which is increased stability and expression of GRE-containing mRNAs that are involved in cell activation and proliferation (48). GRE-containing CELF1 target transcripts also preferentially undergo alternative polyadenylation in activated T cells, resulting in the permanent removal of the 3'UTR regions that harboring GREs and thus, the increased stability of these transcripts (49).

ARE- and GRE-mediated decay in cancer

Aberrant stabilization of ARE-containing cytokine transcripts in cancer

In malignant cells, some ARE-containing cytokine transcripts that are normally unstable in primary cells become constitutively stable, leading to overexpression of cytokines (50, 51). The aberrant stabilization of these ARE-containing transcripts may be due to abnormal expression, post-translational modification, or altered localization of AREBPs or irregular microRNA interactions in malignant cells (52, 53). Two AREBPs in particular, HuR and TTP, have been extensively studied regarding their role in ARE-mediated mRNA decay in malignant compared to normal cells. These two proteins potentially compete for

thousands of overlapping ARE-binding sites, but they have antagonistic effects (54, 55). HuR facilitates transcript stabilization and up-regulation upon binding to AREs (56), while TTP promotes degradation and down-regulation of ARE-containing transcripts (54). The dynamic competition between HuR and TTP for binding to AREs influences the outcome during biological processes and diseases. For example, early in T lymphocyte activation, the amount of cytoplasmic HuR is transiently increased to stabilize and up-regulate ARE-containing transcripts that encode activators of immune responses. In the later phase of activation, with the reduction of HuR and induction of TTP in the cytoplasm, TTP replaces HuR in binding to ARE-containing transcripts and mediates rapid transcript degradation, allowing the resolution of adaptive immune responses (36).

Remarkably, the balance between these two AREBPs is disturbed in many types of cancer. In some cancer cells, the function and expression of HuR is elevated but the function of TTP is nearly abolished, leading to increased production of cytokines that promote malignant phenotypes (57-61). In fact, high HuR/TTP ratio is associated with high levels of mitosis-related ARE-containing transcripts in many solid cancers (52), and single nucleotide polymorphisms in these two proteins often correlate with poor prognosis (62, 63). In cancer cells, increased cytoplasmic HuR levels due to overexpression or cytoplasmic localization and HuR phosphorylation are strongly associated with aberrant cell growth, proliferation, and chemo-resistance (64-67). For example, HuR is reported to regulate the stability and expression of pro-angiogenic and pro-

inflammatory cytokine expression through the AREs within their 3'UTRs (60, 61).

In contrast, the decay-promoting protein, TTP, is reported to be down-regulated or even absent in various cancers, which makes the cancerous cell unable to degrade ARE-containing mRNAs that are normally targeted by TTP (68). For example, TTP down-regulation or deficiency in many tumors accounts for the overexpression of pro-inflammatory and tumorigenic cytokines and growth factors, including IL1, 2, 6, 8, 10, 16, 17, and 23, IFNγ, TNFα/β, and VEGF (69-72). When TTP is exogenously overexpressed, the progression of tumor growth and metastasis is decreased in several cancer cell lines (73). In fact, the cancer drug Sorafenib, an inducer for TTP re-expression in melanoma cells, can reduce the expression of pro-angiogenic cytokines that contain AREs in their mRNA 3'UTRs (74).

Overall, abnormal expression of HuR and TTP seems to contribute to the malignant phenotypes in cancer cells. Future studies may focus on developing mechanisms or agents that can correct the imbalance of these two proteins to achieve favorable post-transcriptional regulation of ARE networks in cancer cells, which may potentially serve as therapies for various cancers.

Aberrant GRE-mediated decay of cytokine signaling transcripts in cancer

Numerous transcripts encoding the protein components of cytokine signaling cascades contain GREs, suggesting that the down-stream effects of cytokines are regulated through GREs. Presumably, the presence of GREs in transcripts encoding multiple cytokine signaling components is responsible for

rapid decay of these transcripts, limiting their expression, and allowing them to be regulated during immune responses. For example, post-translational modification of CELF1 through phosphorylation has been reported in activated T lymphocytes and some cancer cells (48, 75). Phosphorylation leads to decreased binding affinity of CELF1 to GRE sequences and consequently, increased stability and expression of GRE-containing transcripts (48), including numerous transcripts encoding components of cytokine signaling pathways [68]. In malignant T cells, CELF1 loses its binding ability to a subset of transcripts that are targeted in normal T cells. The loss of binding is probably due to hyper-phosphorylation of CELF1 since the target transcripts are present in both normal and malignant cells and the CELF1 expression level are similar in both cells. The consequence is the stabilization and up-regulation of GRE-containing target transcripts in these malignant cells, including transcripts encoding transcription factors (such as JUN, STAT5) and transcripts encoding cytokines or cytokine signaling molecules that control cell growth (such as IFNγ, IL15, IL1RB, CCR5 and 7) (75). Notably, while hyperphosphorylation of CELF1 in malignant cells blocked its ability to bind to a subset of GRE-containing transcripts, this hyper-phosphorylation caused CELF1 to gain the ability to bind to and mediate decay of another subset of GRE-containing transcripts. These transcripts encode proteins involved in suppressing proliferation such as SOCS5, TNFRSF4, and PIAS1 (75). The detailed description of this study is included as Chapter 4. The mechanism by which CELF1 hyperphosphorylation leads to switching binding preferences to target transcripts is not clear, and more experiments are needed

to investigate the impact of post-translational modification of CELF1 on GRE/CELF1 mediated mRNA decay in cancer.

Coordinated regulation of cytokine expression and signaling transduction by AREs and GREs

While AREs regulate the stability of cytokine transcripts, GREs controls the stability of transcripts encoding numerous components of cytokine signaling pathways, indicating that cytokine function is coordinately regulated by both AREs and GREs. The ARE binding protein HuR and GRE binding protein CELF1 shares many target transcripts, because HuR can also bind to GU-rich or poly U sequences. Therefore, HuR and CELF1 may compete for the GU- or U- rich binding sites and exert opposite effects on the stability of target transcripts (76, 77). The cytoplasmic abundance and binding affinity of these two proteins varies in different cell types or environmental cues, thus the stability of a given target transcript varies depends on whichever protein is predominant in the cell. Particularly, in cancer cells, cytoplasmic HuR overexpression and phosphorylation plus CELF1 hyper-phosphorylation push GU- or U- rich mRNAs to undergo the regulation by HuR, i.e. transcript stabilization (30, 75, 78, 79). Therefore, a plausible model is that in normal cells, CELF1 targets at numerous cytokine signaling transcripts for degradation through GRE-mediated decay. Whereas in malignant cells, CELF1 is hyper-phosphorylated and loses its binding ability to certain GRE-containing transcripts, in the meantime, HuR is overexpressed and phosphorylated that its binding affinity increases to both

AREs and GREs, resulting in increased stability and expression of some ARE- and GRE- containing transcripts as we seen in malignancy (80, 81). More evidence is required to confirm this model.

The crosstalk between ARE and GRE networks are evident in many cytokine signaling pathways. For instance, both HuR and CELF1 target transcripts involved in TNF signaling pathways that regulate apoptosis, such as the BCL2 superfamily (82, 83). HuR and CELF1 also co-regulate the IL1 receptor signaling transduction through targeting at different or the same transcripts in this pathway (40) (Figure 1). Another example, members of interferon type I, II and III family contain AREs and are controlled by the ARE/AREBP mediated decay, whereas the interferon receptors harbor GREs in their mRNAs and undergo GRE/CELF1 mediated decay. Moreover, many components of the interferon signaling pathway contain ARE, GRE or both and are subject to their regulation (84). Therefore, coordination of ARE and GRE networks are required for effective interferon responses.

Both ARE and GRE networks are participated in the post-transcriptional regulation of cytokine expression and signaling transduction in health and disease (85). AREs modulate the expression of many cytokines as well as components of the cytokine signaling pathways, and GREs are overrepresented in the mRNAs of cytokine receptors and signaling transducers, modulating their transcript stability. Table 1 shows some examples of ARE- and GRE-containing cytokine signaling transcripts. Malfunctions in ARE and GRE binding proteins, such as HuR, TTP, and CELF1, are highly correlated with dysregulated cytokine

production and signaling, and have strong implications on the initiation and progression of diseases like inflammation, autoimmune diseases, and cancer. Understanding the mechanism of ARE, GRE and their binding proteins mediated mRNA degradation and the interactions between ARE and GRE networks may shed light on the development of therapeutic strategies for these diseases.

ARE- and GRE-mediated decay in viral infection

Viral manipulation of host ARE-containing transcripts' stability

Viruses take advantage of AREs to differentially manipulate the expression of ARE-containing subsets of host transcripts. Viruses produce proteins or noncoding RNAs to inhibit or promote host mRNA degradation, either by affecting the activity of ARE associated *trans*-acting factors, or by directly binding to the ARE within host mRNAs. For example, herpes simplex virus (HSV) protein UL14, or virion host shutoff (vhs) protein, a viral encoded endonuclease that will be described in detail later, triggers global degradation of host mRNAs (86). Vhs preferentially cuts mRNAs in the translation initiation region towards the 5' end, but can also differentially target host ARE-containing transcripts and cleaves them in the 3'UTR (87). Experiments show that in HSV-infected cells, the ARE-binding protein TTP binds to vhs and guides it to cleave the 3'UTR of ARE-containing stress response mRNAs (88). In contrast to vhs, which promotes the decay of ARE-containing transcripts, adenovirus oncogene product E4orf6 stabilizes ARE-containing mRNAs via an α-helix structure that is also required for the oncogenic activity and ubiquitin E3 ligase assembly of E4orf6. In return, the

stabilized ARE-containing mRNAs contribute to the E4orf6 oncogenic activity. E4orf6 lacked oncogenic activity in HuR-knockdown cells that failed to stabilize ARE-containing mRNAs (89), suggesting that the oncogenic activity of E4orf6 depends on stabilization of ARE-containing transcripts by HuR.

Other examples of virus interacting with AREBPs are alphaviruses, including Sindbis virus, Ross River virus, and Chikungunya virus (90, 91). The 3'UTRs of Sindbis virus RNAs bind to HuR with high affinity, which causes the relocation of HuR from the nucleus to the cytoplasm and the sequestration of HuR in the cytoplasm. These changes are associated with the destabilization of cellular mRNAs that are normally targeted by HuR (90).

Interestingly, the coxsackievirus B3 (CVB3) genomic RNA contains AREs and is susceptible to ARE-mediated decay by host factors. To counteract this, CVB3 causes the infected cell to increase expression of the stress-inducible chaperon protein heat shock 70-kDa protein-1 (HSP70-1), a host protein involved in the stabilization of ARE-containing mRNAs (92, 93). In turn, the upregulation of HSP70-1 facilitates viral replication by promoting the stabilization of CVB3 genome via the ARE within the 3'UTR of the viral genomic RNA (92). Additional studies found that the decay promoting AREBP, AUF1, undergoes cytoplasmic redistribution and cleavage upon CVB3 infection (93, 94) which may further promote the stabilization of ARE-containing transcripts.

In addition to the AREBPs, viral factors can also compete with AREs to bind to AREBPs, abolishing their mRNA decay regulating capability. For example, cells infected with Epstein-Barr virus (EBV) produce large amounts of

two noncoding RNAs, EBV-encoded RNA 1 (EBER1) and EBER2. Experiments shown that EBER1 competes with ARE to bind to the p40 isoform of the decay-promoting AREBP, AUF1. Binding by EBER1 to AUF1 prevents AUF1 from binding to its ARE-containing target mRNAs, thus influencing the stability of these ARE-containing transcripts (95).

Numerous signaling pathways, particularly the p38/MK2 mitogen-activated protein kinase (MAPK) pathway, regulate the decay of ARE-containing transcripts by influencing the localization, abundance, and modification of AREBPs (26). Viral infection is a stimulus for activating the stress-inducible p38/MK2 signaling pathway in the infected cell, and the consequence is usually the stabilization of ARE-containing transcripts that normally decay rapidly. For example, Kaposi's sarcoma-associated herpesvirus (KSHV) G-protein-coupled receptor (vGPCR) is found to prevent the turnover of host ARE-containing transcripts through activating the p38/MK2 pathway, probably by interacting with MK2. vGPCR also disturbs processing body formation during lytic KSHV infection, the net effect of which is the promotion of the secretion of angiogenic factors from the infected cells (96). Another KSHV protein, kaposin B, binds to MK2 and activates the p38/MK2 pathway, leading to the stabilization of ARE-containing mRNAs that encodes cytokines such as interleukin (IL)-6, tumor necrosis factor α (TNF α), and interferon γ (IFN γ) (97, 98). The activation of p38/MK2 pathway by Kaposin B also induces accumulation of HuR, an ARE-stabilizing AREBP, leading to the overexpression of ARE-containing transcripts (99). Another example of viral manipulation of host signaling is the HSV-1

immediate early protein ICP27 which is responsible for stabilizing the ARE-containing transcripts through activation of the p38/MK2 pathway (100). In the case of hepatitis C virus (HCV) infection, interleukin-8 (CXCL-8) and other related ARE-containing mRNAs are stabilized via AREs within their 3'UTRs (101). A later study revealed that the stabilization of CXCL-8 transcript is triggered by HCV activated double-stranded RNA (dsRNA) signaling pathways, but the factors responsible for this mechanism are still unknown (102).

The AREBP, AUF1 is also a target of West Nile virus. Arginine methylation of AUF1 during West Nile virus infection facilitates viral replication and affects the ability of AUF1 to bind to RNA (103). Cleavage and cellular relocation of AUF1 plays a role in the infectious cycle of poliovirus or human rhinovirus (104). However, these studies did not further investigate the impact on host mRNA stability by the viruses, yet we can still speculate that the changes of these AREBPs upon infection would at least affect the decay of some, if not all, of their ARE-containing target transcripts.

Viral manipulation of host GRE-containing transcripts at the level of mRNA decay

Our laboratory, recently discovered that HCV non-structural protein 5A (NS5A) binds to GREs and regulates host mRNA decay (105). NS5A is a multi-functional protein that plays pivotal roles in both viral and cellular processes (106). Interestingly, NS5A is also an RNA-binding protein that can bind specifically to G- and U-rich sequences within the HCV genomic RNA (107). Cytoplasmic extracts from human hepatoma cells expressing an HCV

subgenomic replicon were immunoprecipitated using an anti-NS5A antibody, and copurified transcripts were identified using RNA-SEQ to identify host transcripts that were bound to NS5A. NS5A target transcripts identified in this manner were found to be enriched for GREs and GRE-like sequences within their 3'UTRs. Pathway analyses of these NS5A target transcripts shows that they participate in many important cellular processes and functions such as regulation of cell growth and apoptosis. Expression of NS5A led to stabilization of GRE-containing reporter transcripts that were otherwise unstable, suggesting that NS5A binding causes stabilization of GRE-containing transcripts. The stabilization and upregulation of host transcripts likely represents an example whereby HCV manipulates host gene expression to bypass antiviral responses, promote cell growth, and prevent cell death in order to establish chronic infection. This could eventually lead to the development of hepatocellular carcinoma since apoptosis is inhibited in chronically infected cells, and additional genetic damage could accumulate in these cells over time. Although the exact mechanism of the NS5A-mediated mRNA stabilization is not known, NS5A may compete with cellular CELF1 to bind to GREs, thus preventing CELF1-mediated rapid decay. The detailed description of this study is included as Chapter 2.

In the following chapters, we addressed some of the knowledge gaps regarding to the post-transcriptional regulation of gene expression at the level of mRNA decay and its impact on the cell growth and cell death signaling pathways in malignancy and viral infection. In chapter two, we performed RNA-

Immunoprecipitation followed by microarray in primary human T cells and the H9 and Jurkat malignant T-cell lines. We found that CELF1 dysfunction in malignant T cells led to the up-regulation of a subset of GRE-containing transcripts that promote cell growth and down-regulation of another subset that suppress cell proliferation, producing a net effect that would drive a malignant phenotype. In chapter three, we performed high-throughput RNA sequencing technique to generate expression and decay profiles of cellular transcripts and to identify NS5A target transcripts in Huh and Huh-HCV cells. By data analysis and a series of biochemical experiments, we propose that HCV NS5A stabilizes host growth-regulatory transcripts, possibly through interacting with GRE-mediated decay network and other unidentified mechanisms, to promote cell growth and prevent cell death. In chapter four, we utilized oligonucleotide microarrays to compare cellular mRNA decay rates in mock- or reovirus-infected murine L929 cells and discovered a subset of cellular transcripts that were induced and stabilized following infection with the reovirus isolates c87 and c8. These transcripts encoded multiple regulators of TGF- β signaling, including components of the Smad signaling network and apoptosis/survival pathways. Overall, the work presented in this thesis has furthered our understanding of the mechanisms and consequences of mRNA decay regulation in malignancy and viral infection, and added more evidence to enhance the biological importance of the GRE-mediated decay.

Chapter 2:

Altered CELF1 binding to target transcripts in malignant T cells

Paul R. Bohjanen, Mai Lee Moua, **Liang Guo**, Ammanuel Taye, and

Irina A. Vlasova-St. Louis

Introduction

Precise regulation of mRNA turnover is critical for normal gene expression during cell growth, activation, and differentiation (108, 109), and abnormal stabilization of growth-promoting transcripts can lead to malignant proliferation (110). Specific target sequences in mRNA can interact with RNA-binding proteins to coordinately regulate networks of transcripts involved in cell growth and development (45) or other biological processes (23, 111) . A well-characterized example is the AU-rich element, which interacts with RNA-binding proteins to coordinate gene expression over the course of immune responses (40, 55, 112-114). A more recently identified regulatory motif, known as the GU-rich element (GRE), is found in the 3′ untranslated regions (UTRs) of transcripts that encode regulators of cell growth, activation, differentiation, and apoptosis (44, 115). The GRE serves as the binding target of the protein, CUGBP and ELAV-like family member 1 (CELF1), which functions to mediate the rapid degradation of GRE-containing transcripts (116). During T-cell activation, GREs coordinate the degradation of transcripts involved in cell growth and apoptosis (48). The presence of GREs in the 3′UTRs of numerous transcripts have also been associated with rapid mRNA degradation during muscle cell differentiation (117) or Xenopus oocyte development (118). CELF1 has also been shown to coordinately regulate other post-transcriptional processes including alternative splicing and translation (for review, see (116, 119)).

We have shown that CELF1 binds to a network of GRE-containing transcripts in primary human T cells (48). As early as 6 h following T-cell

activation, the CELF1 protein becomes phosphorylated, which decreases its ability to bind to GRE-containing transcripts (48). CELF1 phosphorylation leads to stabilization and increased expression of GRE-containing mRNAs, consistent with a model whereby transient phosphorylation of CELF1 following T-cell activation leads to the coordinate stabilization and increased expression of a network of transcripts that function to accommodate cellular proliferation and activation during an immune response.

We hypothesize that dysregulation of the GRE/CELF1 network promotes uncontrolled cellular proliferation. In a genetic screen in mice, disruption of CELF1 was found to be a driver of colorectal cancer tumorigenesis (120), and CELF1 has been associated with proliferation and abnormal apoptotic responses in malignant cells (46, 121-123). Abnormal function or expression of CELF1 has been observed in liver cancer (124), breast cancer (125), and leukemia (126). Thus, dysregulation of CELF1 is a potential driver of cancer.

To determine whether dysregulation of the GRE/CELF1 network is found in T-cell malignancies, we compared target transcripts of CELF1 in normal human T cells and malignant T-cell lines. We found that similar sets of GRE-containing transcripts were expressed in normal T cells and malignant T-cell lines, but the subset of GRE-containing transcripts bound by CELF1 was altered in malignant T cells compared with normal T cells. In particular, many transcripts that encode regulators of cell proliferation were CELF1 targets in normal T cells, but were not CELF1 targets in malignant T cells. The decreased binding by CELF1 to these transcripts in malignant T cells correlated with the

phosphorylation of CELF1, as well as increased stability and overexpression of these transcripts. We also analyzed the expression and stability of several of these GRE-containing transcripts that encode growth regulators in cells from patients with primary T-cell leukemia (T-ALL), and found that these transcripts were stabilized and overexpressed in primary T-cell tumors compared with normal T cells. The increased expression of these regulators of cell growth may facilitate cellular proliferation in malignant T cells.

Surprisingly, we identified a subset of GRE-containing transcripts that were CELF1 targets in malignant T cells, but not in resting or activated normal T cells. These transcripts were expressed at lower levels and exhibited more rapid degradation in malignant T-cell lines compared with normal T cells. These CELF1 targets included numerous transcripts encoding cell cycle suppressors, and down-regulation of their expression in malignant T cells may further elevate cell proliferation. Overall, our data suggest that in malignant T cells, CELF1 undergoes a change in its RNA-binding behavior such that it loses the ability to bind to a subset of GRE-containing transcripts and gains the ability to bind to another subset. The net effect of this altered CELF1 binding in malignant T cells is predicted to up-regulate the expression of drivers of cell proliferation, down-regulate suppressors of proliferation, and promote a malignant phenotype.

Materials and Methods

Cell culture, stimulation, and preparation of cytoplasmic extracts

Culture of normal and malignant T-cell lines, stimulation of normal T cells with anti-CD3 and anti-CD28 antibodies, and preparation of cytoplasmic extracts were performed as described previously (55).

RNA-IP followed by microarray analysis or RT-PCR

RNA-IP, microarray analyses, and RT-PCR were performed as described previously (44, 46, 50). Three separate IP experiments were performed for microarray analyses for H9 and Jurkat cell lines, and IP experiments were performed from normal primary human T cells isolated from three different donors. The following antibodies were used for IP: anti-CELF1/CUGBP1 (3B1), anti-HA (F7, Santa Cruz Biotechnology), or anti-PABP (10E10, ImmuQuest). Microarray data were analyzed as described previously (48) using Partek Genomics Suite (Partek). Briefly, the output signals were normalized using the Partek Robust Multi-Chip Average analysis adjusted for the GC content of probe sequence (GCRMA). The genes that were differentially expressed among different cell types were identified using the analysis of variance (ANOVA) as implemented in the Partek Gene Expression tool, with the P-value adjusted using step-up (127) multiple test correction. mRNA transcripts were considered to be significantly differentially expressed if they obtained ANOVA P-value ≤ 0.005 and FDR ≤ 0.15. Transcripts were determined to be CELF1 targets if the difference between the log2 normalized signal from the microarrays hybridized with the cRNA from the anti-CELF1 RNA-IP and the anti-PABP RNA-IP was greater than the same value derived from the difference between the anti-HA RNA-IP and

anti-PABP RNA-IP, with $P \leq 0.005$, as determined by Fisher exact test of two factor variables, in either cell IP types.

A pathway analysis of CELF1 target transcripts in malignant T-cell lines was performed with the Ingenuity Pathway Analysis software (IPA, Ingenuity Systems, http://www.ingenuity.com). For conventional RT-PCR reaction, mRNA in the immunoprecipitated complexes and 50 ng of input fraction from >3 separate IP experiments were used in Superscript III reverse transcriptase (Invitrogen) reaction. cDNA were amplified using transcript-specific primers and PCR products were visualized on agarose gels. Forward and Reverse primers were designed to each mRNA of interest, using Primer-Blast software from National Center for Biotechnology Information, and posted in Supplemental Table 2 (http://www.ncbi.nlm.nih.gov/tools/primer-blast/).

Sequence analyses of CELF1 target transcripts

An algorithm, based on the Gibbs motif sampler, was used within the Partek Genomic Suite to detect de novo motifs in the 3′ UTRs of CELF1 target transcripts in the H9 and Jurkat malignant T-cell lines (128, 129). Logo sequence was used to represent the output motifs.

Two-dimensional gel electrophoresis and Western blotting

Two-dimensional gel electrophoresis followed by Western blotting to characterize CELF1 phosphorylation was performed as described previously (46). Briefly, for two-dimensional gel electrophoresis, 80 µg of cytoplasmic

lysates were diluted 1:1 with Rehydration buffer from BioRad and dialyzed against 2D gel buffer (7 M urea, 2 M thiourea, 2% CHAPS, 10 mM Tris) overnight at room temperature. The samples were then loaded onto 11-cm pH3–10 IPG strips (BioRad). Samples were focused using a BioRad Protean IEF cell device. Subsequently, IPG strips were loaded onto Bis–Tris 4%–12% pre-cast gels and run at 175 V using MOPS-SDS buffer. Gels were then blotted onto charged PVDF membranes. Western blots were performed probing with anti-CELF1 antibody and an anti-GAPDH antibody (Santa Cruz Biotechnology), or an anti-phospho-28S CELF1 antibody (Antagene).

In vitro binding by immunopurified CELF1 to a GRE-riboprobe

Binding by immunopurified CELF1 was performed as described in the Thermo Scientific IP protocol with slight modifications as described in Beisang et al (48). In brief, CELF1 was immunoprecipitated out of 100 µg of cytoplasmic lysate and samples were treated with λ-protein phosphatase (LPP) or were mock-treated. CELF1 was eluted from the beads by the addition of 0.5% SDS and heating at 65°C for 15 min. The immunoprecipitated material was then incubated for 30 min with 50 fmol of either the biotinylated GRE or mutant GRE-riboprobe, was treated with UV light (999 J) and was eluted from the beads, separated on a 4% acrylamide gel. The biotinylated RNA probe signal was visualized with the Chemiluminescent Nucleic Acid Detection Module from Thermo Scientific, following the manufacturer's instructions. The blots were then

stripped, and probed by Western blot with an anti-CELF1 antibody. Images were then quantified with ImageJ to determine the RNA:CELF1 ratio.

mRNA degradation assays

Primary tumor cells isolated from peripheral blood of four T-ALL patients via leukapheresis were stored frozen in liquid nitrogen. Cells were thawed in warm RPMI-1640 (Invitrogen), by centrifugation on a 25% of human serum albumin cushion and were cultured for 2–3 d in RPMI-1640, supplemented with human serum albumin (1.25 mg/mL), recombinant human IL2 and IL7 (10 ng/mL for both; R&D systems). To measure mRNA decay, Actinomycin D (10 μg/mL) was added to cultured cells and total cellular RNA was isolated at 0-, 1.5-, and 3-h time points. RT-QPCR using transcript-specific primers (see Supplemental Table 2) was used to quantitate the levels of individual mRNAs, which were normalized to the level of the expression of the HPRT transcript. For each transcript, normalized levels were used to calculate and compare transcript half-lives using GraphPad Prism 4 software, based on a linear first order exponential decay model ($P < 0.05$).

Results

CELF1 targets in malignant T cells were distinct from CELF1 targets in normal T cells

CELF1 binds to a network of transcripts that encode important regulators of cell growth and apoptosis, and we hypothesized that the regulation of this

network might be altered in malignant T cells. Previously, we performed immunoprecipitation (IP) of CELF1 from T-cell cytoplasmic extracts followed by analysis of coimmunoprecipitated mRNA using Affymetrix microarrays and identified 1309 CELF1 target transcripts in resting normal human T cells (48). The same approach was now used to identify target transcripts of CELF1 in the malignant T-cell lines, H9 (T-cell lymphoma), and Jurkat (T-cell leukemia). We found CELF1 associated with 260 probe IDs in H9 T cells and 360 probe IDs in Jurkat T cells, corresponding to 229 and 340 unique mRNA transcripts, respectively. A complete listing of transcripts associated with CELF1 in H9 T cells, Jurkat T cells, or primary human T cells is included in Supplemental Table 1. Among these transcripts, 149 were bound by CELF1 in both H9 and Jurkat malignant T-cell lines. A subset of transcripts that were CELF1 targets in both H9 and Jurkat malignant T-cell lines along with their stability, expression rates, and annotated biological functions is shown in Table 2.1.

In comparing the CELF1 target transcripts from normal T cells to CELF1 target transcripts from H9 or Jurkat malignant T-cell lines, we found relatively little overlap, despite the fact that most of the CELF1 target transcripts expressed in normal T cells were also expressed in these malignant T-cell lines. Of 1309 CELF1 target transcripts identified in normal T cells, 1044 were expressed in H9 T cells and 1112 were expressed in Jurkat T cells, but only 19 or 21 of these transcripts were found to be CELF1 targets in H9 T cells or Jurkat T cells, respectively, and only 12 were targets of CELF1 in both cell types (Figure 2.1A). Thus, in malignant T cells, the lack of binding by CELF1 to most transcripts that

were targets in normal T cells, was not due to absence of those transcripts, but was due to a decreased ability of CELF1 to bind to these transcripts in malignant T cells. A subset of transcripts that were CELF1 targets in normal T cells but not in the H9 or Jurkat T-cell lines is shown in Table 2.2.

To better analyze the relationship between transcript abundance and CELF1 binding in malignant compared with normal T cells, we calculated a fold change in enrichment (FCE) for each transcript on the microarrays defined as

FCE = (CELF1 · IP/Input) malignant/(CELF1 · IP/input) normal,

where the ratio of the microarray signal from the CELF1 IP to the microarray signal from input RNA for malignant T cells was divided by the same ratio for normal T cells. The FCE for all CELF1 target transcripts expressed in H9 or Jurkat T cells is included in Supplemental Table 1. The average FCE for all transcripts was 1.03 and 1.04 for H9 and Jurkat T cells, respectively, indicating that the overall distribution of transcripts with respect to CELF1 binding did not change when comparing malignant to normal T cells. In contrast, the average FCE of transcripts that were CELF1 targets in normal T cells, were 0.65 and 0.71 for H9 and Jurkat T cells, respectively, indicating that CELF1 exhibited decreased binding to target transcripts in both malignant cell lines (Figure 2.1B,C; Tc, hashed bars). Thus, correcting for transcript abundance in malignant T-cell lines compared with normal T cells indicated that the lack of association of CELF1 with these target transcripts in malignant T cells could not be explained by the absence of these transcripts, but was more readily explained by an inability of CELF1 to bind to those transcripts. Table 2.2 shows decreased FCE

values for a subset of transcripts that were CELF1 targets in normal T cells but not H9 or Jurkat T cells, even though they were expressed in each cell type.

Interestingly, the average FCE for transcripts that were CELF1 binding targets in malignant T-cell lines were 1.42 and 1.43 in H9 and Jurkat T-cell lines, respectively (Figure 2.1B,C: H9 and JK, empty bars). Table 2.1 shows the increased FCE values for a subset of the transcripts that were CELF1 targets in malignant T-cell lines. These data suggest that CELF1 could not bind to these transcripts in normal T cells, even though they were present in cytoplasm, but gained an ability to bind to these transcripts in malignant T cells. These results in malignant T cells are quite different from what we previously observed in normal activated T cells (48), where T-cell activation led to a similar decrease in binding by CELF1 to target transcripts from resting T cells, but CELF1 did not gain an ability to bind to a new subset of transcripts. Overall, we observed that binding by CELF1 to target transcripts was altered in malignant T cells compared with normal T cells, and CELF1 in malignant T cells gained an ability to bind to a new subset of target transcripts.

Normal and malignant T cells express similar amounts of CELF1, but with different phosphorylation patterns

We performed Western blot assays to assess the level of expression of the CELF1 protein in cytoplasmic extracts from resting normal T cells, normal T cells that were stimulated for 6 h with anti-CD3 and anti-CD28 antibodies, and Jurkat or H9 malignant T cells, and we found similar levels of expression in each

cell type or condition (Figure 2.2A, CELF1 and Figure 2.2B, left). CELF1 is known to be regulated through phosphorylation following T-cell activation (Beisang et al. 2012b), but CELF1 has 22 potential phosphorylation sites (PhosphoSitePlus database, Cell Signaling Technology), and the sites of phosphorylation following T-cell activation are not known. To screen for phosphorylation of CELF1 in malignant T cells, we blotted the same membranes with a commercially available antibody directed at a serine 28 phosphopeptide from CELF1 (Figure 2.2A, Phospho-S28 CELF1 and Figure 2.2B, right). We found only low levels of phosphorylation at S28 in normal resting T cells (rTc,) and normal stimulated T cells (sTc), but much higher levels in H9 and Jurkat (JK) malignant T cells, indicating that phosphorylation of CELF1 at this site differed between resting or activated normal T cells and these malignant T-cell lines.

To further characterize CELF1 phosphorylation in normal and malignant T cells, we performed two-dimensional (2D) gel electrophoresis, followed by Western blotting with an anti-CELF1 antibody (Figure 2.3). As seen previously, CELF1 was not phosphorylated in normal resting T cells (rTc), with the main position of the signal localized near pH 8.7, and stimulation of normal T cells with anti-CD3 and anti-CD28 antibodies caused the CELF1 signal to shift toward the right (pH 3.0), indicating phosphorylation of CELF1 (Figure 2.3, sTc). In H9 and Jurkat T cells, however, CELF1 exhibited a much more complex phosphorylation pattern with even further shift of the CELF1 signal to the right, demonstrating that CELF1 was hyperphosphorylated in the malignant T-cell lines compared with stimulated normal T cells.

Treatment of cytoplasmic extracts from H9 or Jurkat T cells with λ-phosphatase (LPP+) led to a shift of the CELF1 signal toward the unphosphorylated position, as was seen previously in cytoplasmic extracts from normal stimulated T cells (48). Overall, these results demonstrate that CELF1 is hyperphosphorylated in malignant T cells compared with normal stimulated T cells, with complex phosphorylation patterns suggesting multiple sites of phosphorylation.

Loss of binding by CELF1 to a subset of target transcripts in malignant T cells correlated with CELF1 phosphorylation and transcript stabilization

To test more directly whether the phosphorylation of CELF1 in malignant T-cell lines influenced RNA binding, we immunopurified CELF1 from cytoplasmic lysates from normal and malignant T cells and assessed CELF1 binding to a riboprobe containing a GRE or mutant GRE (Figure 2.4A with graphical representation in Figure 2.4B). CELF1 immunopurified from both malignant T-cell lines showed reduced binding to the GRE-riboprobe compared to CELF1 derived from normal resting T cells (cf. lanes 5 and 9 to lane 1). Treatment with LPP resulted in an increase in binding to the GRE-containing riboprobe by CELF1 immunopurified from malignant T-cell lines (cf. lane 5 to lane 7 and lane 9 to lane 11). In contrast, binding by CELF1 immunopurified from resting human T cells was unaffected by LPP treatment (cf. lanes 1 and 3). These results suggest that the binding by CELF1 to the GRE-riboprobe was inhibited in malignant T cells due to phosphorylation, and binding was restored when CELF1 was de-

phosphorylated in vitro.

We previously measured mRNA decay rates on a genome-wide basis in normal T cells and the Jurkat and H9 malignant T-cell lines (50), and we now compared transcript half-lives across these cell types (see Supplemental Table 1). We found that most transcripts that were CELF1 targets in normal T cells, but were not CELF1 targets in H9 or Jurkat T cells, were stabilized in the malignant T-cell lines. For example, of the 113 short-lived CELF1 target transcripts with median half-lives ≤90 min in normal T cells, 106 (93%) and 104 (92%) were stabilized in H9 and Jurkat T-cell lines, respectively ($P \leq 0.05$). None of these stabilized transcripts were CELF1 targets in malignant T-cell lines. The mRNA decay rates of a subset of these transcripts that were CELF1 targets in normal T cells but not in malignant T-cell lines are shown in Table 2.2: All of them were stabilized ($P \leq 0.05$) in malignant T cells compared with normal T cells. Our results suggest that CELF1 phosphorylation in malignant T cells leads to decreased CELF1 binding to GU-rich containing RNA transcripts, that were CELF1 targets in normal T cells, resulting in transcript stabilization in malignancy.

CELF1 targets in malignant T-cell lines exhibited accelerated mRNA degradation

Since binding by CELF1 is known to correlate with faster mRNA turnover (44), we evaluated the decay of transcripts that were CELF1 targets in malignant T cells but were not CELF1 targets in normal T cells. Compared with normal T cells, the decay rates of most CELF1 targets in malignant T cells were significantly shorter. Table 2.1 shows half-life values for a subset of transcripts

that were CELF1 targets in both H9 and Jurkat T cells, and all of these transcripts decayed significantly faster in malignant compared with normal T cells. Overall, our results suggested that CELF1 gained the ability to bind to a distinct subset of transcripts in malignant T cells, and this binding correlated with accelerated mRNA degradation.

To verify the relationship between CELF1 binding and mRNA decay that we found in our microarray data, we selected transcripts that were differentially bound to CELF1 in normal T cells and malignant T-cell lines to perform confirmatory assays (Figure 2.5). Cytoplasmic lysates from normal T cells (Tc), H9 T cells (H9), and Jurkat T cells (JK) were immunoprecipitated with no antibody (input, I), an anti-CELF1 antibody (C), an anti-poly(A) binding protein antibody (P) as a positive control, and an anti-HA antibody (H) as a negative control, and copurified RNA was isolated. This RNA was evaluated by reverse transcriptase PCR (RT-PCR) using transcript-specific primers (see Supplemental Table 2) to measure the binding by CELF1 to select transcripts (Figure 2.5, left panels). Normalized quantified results for the intensity of the CELF1 IP band for each transcript are shown in Figure 2.5, middle panels. We also used quantitative real-time PCR (QPCR) to measure mRNA decay rates of these same transcripts after treatment of cells with Actinomycin D (Figure 2.5, right panels) and determined if CELF1 binding correlated with mRNA decay.

The IP results confirmed that the AURKB, KBTBD7 and SIAH1 transcripts were enriched in the anti-CELF1 immunoprecipitates from malignant T cells compared with normal T cells (Figure 2.5, left and middle panels), and half-lives

of these transcripts in H9 and Jurkat cells were significantly shorter, with $P \leq 0.05$ for each transcript (Figure 2.5, right panels).

In contrast, the CEBPB, EIFEBP2, TNFSF10 transcripts were enriched in the anti-CELF1 immunoprecipitates from normal T cells compared with malignant T cells, and these transcripts decayed more rapidly in normal T cells compared with malignant T-cell lines ($P \leq 0.05$ for each transcript). These results confirm that CELF1 target transcripts exhibited accelerated decay, and CELF1 binding correlates with more rapid mRNA turnover, suggesting that altered CELF1 binding contributes to abnormal mRNA decay in malignant T cells.

GU-rich sequences were enriched in CELF1 target transcripts in malignant T-cell lines

CELF1 binds to GU-rich RNA sequences (for review, see (119)). We evaluated CELF1 target transcripts in malignant T cells to determine whether they contained defined CELF1 binding sequences. As described in Materials and Methods, a de novo motif search using Partek Genomic Suite software identified enrichment of G/UU-containing sequences in the 3′ UTR of CELF1 target transcripts from malignant T-cell lines (see motif logo in Supplemental Figure 1). The top two consensus sequences within this group of transcripts resembled the GRE. These results suggest that CELF1 in malignant T cells interacts with target transcripts through GRE sequences that are similar to known CELF1 target sequences in normal T cells and other cell types (47).

CELF1 targets in malignant T cells encode components of cell cycle networks

In normal T cells, CELF1 targets encode a variety of regulators of apoptosis and post-transcriptional regulatory networks (48). Since the subset of CELF1 target transcripts in malignant T cells is distinct from the subset of CELF1 targets in normal T cells, we analyzed the functions of the CELF1 target transcripts identified in H9 and Jurkat T cells. The most highly enriched CELF1 target transcripts in H9 and Jurkat malignant T-cell lines are listed in Table 2.1, and the proteins encoded by these transcripts function as cell cycle and apoptosis regulators or regulators of metabolism.

We evaluated biological processes and molecular functions for CELF1 target transcripts in H9 or Jurkat T cells, and found enrichment of a cluster of mRNAs encoding proteins with roles in cell cycle regulation. A simplified regulatory network of cell cycle control proteins encoded by GRE-containing CELF1 targets in malignant T cells is shown in Figure 2.6. This network shows CELF1 target transcripts that regulate cell cycle progression throughout the G1, S, G2, and M phases, including genes that are expressed at higher levels during G1/S and G2/M cell cycle checkpoints (Ingenuity Knowledge Database) and components of cyclin-driven pathways that play important roles in cell development, differentiation, and tumorigenesis (Pathways Analysis, Ingenuity Systems). Many of the transcripts shown are known to be abnormally expressed in cancer. Among them are regulators of DNA transcription and replication: NDRG3 (130), STAT5B (131), CENPF (132), G2E3 (133), ZNF436 (134), ZNF678 (http://www.proteinatlas.org/search/), ZMAT3 (135), AP2A2 (136),

MED24 (137); and proteins that control cellular senescence and mitotic arrest (JUND (138), TERF2 (139), NGR3, CENPA (140), PAFAH1B1 (141), CDK11A/B (142, 143)), negative regulators of G1 phase and G1/S transition (CDK1 (144), ZNF346, CDC73 (145)) and cytokinesis (SIAH1 (146), AURKB (147)). A functional analysis (Table 2.3) showed that CELF1 targets in malignant T cells were linked to cancer, neurological diseases, and developmental abnormalities in the category of diseases and disorders. In the category of molecular and cellular function, CELF1 targets were linked to cell cycle, cellular organization, and cell death and survival. In the category of physiological system development and function, CELF1 targets were linked to abnormal tumor morphology. In summary, our analysis suggested that the abnormal function of CELF1 in malignant T cells leads to misexpression of a network of GRE-containing transcripts.

Coordinate stabilization and up-regulation of CELF1 target transcripts in primary T-ALL

We found that numerous short-lived CELF1 target transcripts in normal T cells were not CELF1 targets in malignant T-cell lines, and the lack of CELF1 binding correlated with transcript stabilization. To determine whether stabilization of these same transcripts also occurred in primary T-cell tumors, we measured transcript levels and decay rates of 17 mRNA transcripts in primary T acute lymphoblastic leukemia (T-ALL) cells (Table 2.4). These mRNAs were CELF1 targets in normal T cells but were not CELF1 targets in H9 or Jurkat T cells. Actinomycin D was added to primary T-cell tumor cells isolated from peripheral

blood from four T-ALL patients, normal human T cells from four donors, and H9 T cells or Jurkat T cells from three independent cell passages; mRNA decay rates were measured using QRT-PCR. The QRT-PCR results confirmed our microarray data: transcripts that were CELF1 targets in normal T cells but not in H9 or Jurkat T cells, were stabilized and up-regulated in these T-cell lines. Furthermore, we found that these same transcripts were also stabilized and up-regulated in primary T-ALL cells (Table 2.4). These results support our hypothesis that a subset of GRE-containing transcripts is stabilized and up-regulated in primary human T-ALL tumors likely due to escape from CELF1-mediated degradation.

Discussion

We found that the GRE/CELF1 network, which normally functions to coordinate cellular proliferation during the course of normal T-cell activation, is dysregulated in malignant T cells. Altered binding by CELF1 to target transcripts in malignant T cells led to abnormal stabilization of a network of transcripts that promote cell proliferation and abnormal destabilization of transcripts that encode cell cycle checkpoint regulators or suppressors of proliferation.

CELF1 was phosphorylated in the H9 and Jurkat malignant T-cell lines (Figures 2.2, 2.3), and this phosphorylation correlated with decreased binding by CELF1 in malignant T-cell lines to its binding targets in normal T cells (Figure 2.1). In fact, most CELF1 target transcripts expressed in normal T cells were not CELF1 targets in malignant T-cell lines, even though they were expressed in the

malignant T-cell lines. The lack of binding by CELF1 in malignant T-cell lines to transcripts that were CELF1 targets in normal T cells was not due to differences in the amount of CELF1 in the different cell types (see Figure 2.2A), but appeared to be due to phosphorylation of CELF1 (Figure 2.3), similar to what was observed in activated normal T cells (48). In normal T cells, CELF1 appears to be transiently phosphorylated following T-cell activation as part of the normal T-cell activation program, whereas in malignant T cells, CELF1 appears to be constitutively phosphorylated, with a more complex phosphorylation pattern. Also, we found CELF1 phosphorylation at serine 28 in malignant T cells but not in resting or activated normal T cells, indicating that the site of phosphorylation of CELF1 differs in normal and malignant T cells. PKC α/βII-dependent phosphorylation of CELF1 at serine 28 is involved in murine heart development (148), but the role of phosphorylation of CELF1 at serine 28 in T cells has not been evaluated. Finding that CELF1 was phosphorylated at S28 in malignant T cells, but not in activated normal T cells suggests that different kinases that phosphorylate CELF1 at serine 28, or other positions, are expressed or activated in malignant T cells. Although there is very little data regarding the role of PKC isozymes in CELF1 function, several studies have demonstrated the involvement of PKC isozymes in controlling cellular signaling and proliferation in malignant cells (for review, see (149)). PKCβII, for example, plays a critical role in cancer cell proliferation, survival, and invasion. It is possible that cancer cells constitutively express kinases, such as PKCβII, that phosphorylate CELF1 and alter its binding to target transcripts. Activation and proliferation in normal T cells

is driven by PKCθ and other kinases, including MAP kinases and PI3 kinase (for review, see (150)). Possibly, these kinases induced by T-cell activation lead to transient phosphorylation of CELF1, affecting the network of GRE-RNAs only for the amount of time needed for cellular activation and proliferation before T cells return to a quiescent state. At this point, further work is needed to define the sites of CELF1 phosphorylation in malignant T cells and during activation of normal T cells, but based on our findings, it appears that different kinases are involved, and CELF1 is hyperphosphorylated in malignant T cells relative to activated normal T cells.

Involvement of kinase signaling in regulating CELF1 binding to RNA is supported by our observation that immunopurified CELF1 from malignant T-cell lines or activated normal T cells exhibited decreased binding to a GRE-containing riboprobe, compared to immunopurified CELF1 from resting normal T cells (Figure 2.4). Treating immunopurified CELF1 from malignant T cells or activated normal T cells with LPP led to increased GRE binding in vitro, suggesting that phosphorylation of CELF1 caused inhibition of binding (Figure 2.4; (48)). Thus, for the large subset of GRE-containing transcripts that were CELF1 targets in normal T cells, lack of binding by CELF1 in malignant T cells was likely due to phosphorylation of CELF1. In contrast, we found that CELF1 acquired an ability to bind to a new subset of target transcripts in malignant T cells even though all cytoplasmic CELF1 was present in a phosphorylated form (Figure 2.3). The mechanism by which CELF1 gained an ability to bind to these target transcripts is unknown. Perhaps, hyperphosphorylation of CELF1 led to

changes in its affinity such that it lost the ability to bind to most GRE-containing target transcripts, but gained the ability to bind to a new set of GRE-containing transcripts. Sequence analysis of these new CELF1 target transcripts from malignant T cells revealed that they contain GRE sequences that are similar or identical to previously characterized GRE sequences, and therefore, the mechanistic details for preferential binding by CELF1 to these target transcripts are yet to be uncovered. Hyperphosphorylation of CELF1 in malignant T cells may lead to altered RNA-binding characteristics through changes in the CELF1 protein conformation, alterations in the functional activities of individual RNA-recognition motifs (RRMs), or the ability of CELF1 to associate with sequences that flank the GRE or other nearby sequences such that CELF1 gains new binding characteristics. Binding by CELF1 to RNA occurs via multiple RRMs (151, 152), and phosphorylation within one or more RRMs may change its binding characteristics. Although, all RRM motifs have been shown to bind to short GRE sequences with comparable affinity in vitro (153), preferential binding to RNA by one, two or all three motifs could dictate differences in sequence-binding preferences. Alternatively, other binding proteins, microRNAs, or adjacent RNA *cis*-elements might interact with CELF1 and change its ability to bind to target mRNA. Further work is needed to understand why CELF1 binds to RNA differently in normal and malignant T cells.

We previously used microarrays to measure the decay rates of transcripts expressed in primary human T cells, H9 T cells, and Jurkat T cells (50), and now analyzed this data to determine whether differential binding by CELF1 to specific

transcripts correlated with rates of mRNA degradation and transcript abundance. We found that many transcripts that were targets of CELF1 in normal T cells but not in the H9 or Jurkat malignant T-cell lines were stabilized and up-regulated in the malignant T cells. This finding suggests that CELF1 bound to these transcripts in normal T cells and mediated their degradation, but since CELF1 did not bind to these transcripts in malignant cell lines, they were stabilized and their expression increased (Table 2.2). Thus, it appears that phosphorylation of CELF1 led to its functional inactivation, resulting in a failure of CELF1 to mediate the decay of a large set of GRE-containing transcripts in malignant T-cell lines. We have recently shown that numerous GRE-containing transcripts undergo shortening through alternative polyadenylation following T-cell activation, and similar transcript shortening has been shown to occur in malignancy (49, 154). Thus, some of the transcripts that were targets of CELF1 in normal T cells but not in malignant T cells may have lost their GRE sequences due to alternative polyadenylation.

For a subset of the transcripts that were CELF1 targets in normal T cells but not malignant T cells that are involved in cell growth regulation, we measured mRNA degradation rates and abundance in primary T-ALL cells from four patients using QRT-PCR. We found that these transcripts were stabilized and up-regulated compared with normal T cells, similar to what was seen in malignant T-cell lines (see Table 2.4). Although the small numbers of cells available did not allow us to perform RNA-IP or CELF1 phosphorylation experiments using T-ALL cells, the pattern of transcript stabilization and expression showed that numerous

GRE-containing transcripts that were CELF1 targets in normal T cells were stabilized and up-regulated in primary tumor cells. Up-regulation of these transcripts in malignant T cells would be expected to facilitate cell growth and proliferation and would likely contribute to the malignant phenotype.

The dysregulation of CELF1 through inappropriate phosphorylation in malignant T cells appears to contribute to abnormal growth and promotes the malignant phenotype by blocking CELF1 binding and thereby stabilizing and increasing the expression of a large subset of GRE-containing transcripts. At the same time, CELF1 gains the ability to bind to and mediate the degradation of another subset of GRE-containing transcripts that encode checkpoint control proteins and suppressors of proliferation. Many of the CELF1 target transcripts identified in malignant T-cell lines encode regulators of cell cycle transitions (Figure 2.6), including important suppressors of cell proliferation such as JUND, CDKN1A, SIAH, AURKB, and others. Rapid CELF1-mediated degradation of these target transcripts in malignant T cells would favor growth and proliferation by shortening cell cycle checkpoint phases and expediting cell cycle phase transitions (155). Overrepresentation of CELF1 targets in malignant T cells among disease specific categories, such as cancer, reinforces the role for these transcripts in driving or promoting cancer pathogenesis. CELF1-mediated degradation of these transcripts in malignant T cells would decrease their expression and facilitate a proliferative state.

Overall, our results support a model whereby dysregulated kinases or kinase signaling pathways lead to phosphorylation of CELF1, which facilitates the

development of the malignant phenotype by increasing the stability and expression of transcripts involved in cell proliferation. Acquisition of CELF1 binding to another set of transcripts in malignant cells leads to the degradation and down-regulation of transcripts encoding cell growth suppressors. Thus, CELF1 dysregulation in malignant T cells leads to the up-regulation of a subset of GRE-containing transcripts that promote cell growth, and down-regulation of another subset that suppresses cell growth, producing a net effect that would drive a malignant phenotype.

Chapter 3:

The hepatitis C viral nonstructural protein 5A stabilizes growth-regulatory human transcripts

Liang Guo, Suresh D. Sharma, Jose Debes, Daniel Beisang, Bernd Rattenbacher, Irina Vlasova-St. Louis, Darin L. Wiesner, Craig E. Cameron, and Paul R. Bohjanen

Introduction

For viruses to survive and replicate, they often control the host cellular environment by manipulating host gene expression. It is becoming increasingly clear that viral manipulation of host posttranscriptional regulatory mechanisms plays critical roles in viral pathogenesis. For example, Kaposi's sarcoma herpes virus globally down-regulates expression of host cellular transcripts by expressing the shut-off alkaline exonuclease (SOX), which mediates transcript degradation (156). Herpes simplex virus selectively degrades certain host transcripts through a viral endonuclease (157) but stabilizes and up-regulates a specific subset of host cellular transcripts through the viral ICP27 protein (100). By utilizing posttranscriptional mechanisms, viruses are able to selectively manipulate the expression of host transcripts to create a cellular environment that inhibits antiviral host defense mechanisms and allows the establishment of viral infection.

Hepatitis C virus (HCV), which belongs to the family *Flaviviridae* family of viruses (158), is a RNA virus with a 9.6 kb RNA genome of positive polarity that encodes structural and nonstructural proteins required for HCV replication (159). HCV infects approximately 184 million people worldwide (160) and causes hepatitis, liver cirrhosis and hepatocellular carcinoma (161). The mechanisms leading to liver cirrhosis and cancer in the HCV-infected individual are not understood. In the current era, cure of HCV infection with new antivirals is possible, but even patients with virological cure have an increased risk of

developing hepatocellular carcinoma (162, 163). Therefore, understanding the molecular progression of HCV infection to hepatocellular carcinoma is a priority.

Due to its small genome, HCV must use the host protein synthesis machinery to produce viral proteins required for viral replication. One of these viral proteins, non-structural protein 5A (NS5A), is multifunctional and influences many viral and cellular processes. The entire protein-protein interaction network of the HCV proteome was mapped by high throughput yeast two hybrid screening, and NS5A was found to interact with proteins functioning in focal adhesions, gap-junctions and host cellular signaling pathways (106). NS5A also influences cell cycle control by interacting with p53 and modulation of p21 (164-167). During viral genome replication, NS5A interacts with the RNA-dependent RNA-polymerase NS5B (168, 169), an interaction that is essential to maintain the HCV subgenomic replicon in Huh 7 cells (168, 170). NS5A also binds to G- and U-rich sequences in HCV genomic RNA (107). The amino terminal domain 1 and the adjacent unstructured region of NS5A interacts with HCV genomic RNA (169) and modulates its template selection (171). Crystal structures of domain 1 show a RNA-binding zinc finger which coordinates a Zn^{2+} ion (172, 173). We hypothesized that NS5A functions to regulate the expression of host genes at posttranscriptional levels through its ability to bind to G and U rich RNA sequences.

We previously described a GU-rich element (GRE) that is enriched in the 3' untranslated region (UTR) of rapidly degraded cellular transcripts expressed in primary human T cells (44). GRE-containing transcripts encode numerous proto-

oncogene proteins and other proteins involved in cell growth regulation or apoptosis (116). Insertion of the GREs from JUN, JUNB or TNFRSF1B mRNAs into the 3' UTR of a beta-globin reporter transcript conferred instability onto the otherwise stable beta-globin transcript. Further investigation showed that the CUGBP1 and ETR-3 - Like Factor 1 (CELF1) protein functions as a GRE-binding protein and mediates the decay of GRE-containing transcripts (44), perhaps by recruiting other enzymatically active proteins to the transcript. The Xenopus homologue of CELF1, EDEN-BP, also binds to GREs and is involved in deadenylation of mRNA during oocyte maturation (174). In mammalian cell extracts, CELF1 interacts with poly A ribonuclease and mediates transcript deadenylation (25). The GRE and CELF1 define a posttranscriptional mechanism for coordinately regulating the expression of multiple transcripts involved in cellular growth and apoptosis, and we hypothesized that HCV manipulates this mechanism through its NS5A protein to create a cellular environment that prevents cell death and promotes growth of virus-infected cells.

In this report, we demonstrate that the HCV NS5A protein does indeed bind to host transcripts, including a large set of GRE-containing transcripts and mediates their stabilization. Expression of a subgenomic HCV replicon in the Huh 7.5 human hepatoma cell line led to binding by NS5A to host GRE-containing transcripts, which correlated with the stabilization of these transcripts. NS5A expressed exogenously in HeLa cells bound to reporter transcripts in a GRE-dependent manner, and this binding led to transcript stabilization, demonstrating that NS5A has RNA-stabilizing activity in cells. A purified recombinant NS5A

polypeptide bound to GRE sequences in a zinc finger-dependent manner. Mutation of the zinc finger abolished the RNA-binding and the mRNA stabilizing activity of NS5A. Together, these data suggest that HCV manipulates host cellular mRNA decay through NS5A-mediated stabilization of host transcripts. Because GRE-containing NS5A target transcripts encode proto-oncogenes and other important regulators of cell growth and apoptosis, HCV-induced stabilization of these transcripts would prevent cell death and promote growth of virus-infected cells, allowing the virus to establish a chronic infection and thereby promote the development of hepatocellular carcinoma.

Materials and Methods

Cell culture.

The human hepatoma cell line Huh 7.5 (Huh) is a derivative of the Huh7 human hepatoma cell line attenuated in the RIG-I/interferon regulatory factor 3 (IRF-3) pathway (175). The Huh 7.5 SI cell line (Huh-HCV) stably expresses the HCV-Con1 replicon with an adaptive mutation in NS5A-coding sequence producing the S.2204.I variant (107). This cell line was generated by transfecting 1.6×10^6 Huh 7.5 cells with 2 µg of *in vitro* transcribed replicon RNA using TransMessenger transfection system (Qiagen). After transfection, 1×10^5 cells were seeded in 100-mm diameter dishes and 12-14 h later the cells were placed under G418 selection (500 µg/mL) for 3 weeks and colonies were further expanded. Huh and Huh-HCV cells were propagated in Dulbecco's modified eagle's medium (DMEM, Gibco) supplemented with 10% FBS (Atlanta

biologicals), 0.1 mM nonessential amino acids (Gibco), 1% L-Glutamine (Gibco) and 100 units/ml of penicillin/streptomycin (Gibco). For Huh-HCV cells, 500 µg/mL of G418 (Calbiochem) was added to the medium. HeLa Tet-off cells (Clontech) were cultured in minimal essential medium alpha (Gibco) containing 10% tetracycline-free FBS (Clontech), 1% L-Glutamine (Gibco) and 100 units/mL of penicillin/streptomycin (Gibco).

Plasmids.

The pTracerC green fluorescence protein (GFP) expression plasmid and the pcDNA3 plasmid were purchased from Invitrogen. The tet-responsive beta-globin expression plasmid pTetBBB (BBB) (176) was a gift from Dr. Ann-Bin Shyu (University of Texas-Houston). We previously described insertion of the *JUNB* GRE, mutated *JUNB* GRE, or *IL2* ARE sequences into the 3' UTR of the beta-globin sequence of the BBB plasmid to create the BBB-GRE, BBB-mGRE and BBB-ARE plasmids, respectively (44, 112). To generate pCDNA3.1-5A and pCDNA3.1-del32-5a NS5A was PCR-amplified from the plasmid pHCVbart.rep1b/Ava-II (177), a gift from Dr. Charles Rice (Rockefeller University) with primers FW-5a, 5'-GCGTCTAGAATGGGCTCCGGCTCGTGGCTA-3' or FW-del32-5a 5'-GCGTCTAGAATGGGCGGAGTCCCCTTCTTC-3' and RV-5a, 5'-GCGCAAGCTTCTATTAGCAGCAGACGACATC-3' and inserted into the XbaI and HindIII sites of pCDNA3.1 (Invitrogen). The NS5A expression plasmid pCDNA3.1-5A was used to express NS5A in HeLa cells and pCDNA3.1-del32-5a was used to express the NS5A ΔN mutation. The QuikChange Site-Directed

Mutagenesis Kit (Stratagene) was used to introduce four cysteine to serine mutations (C39S, C57S, C59S, and C80S) into these plasmids to create pCDNA3.1-5A-4C-4S and pCDNA3.1-del32-5a-4C-4S which express the NS5A 4C-4S and NS5A ΔN-4C-4S mutations, respectively.

Plasmids for expression of recombinant NS5A polypeptides in E. coli were created by cloning PCR amplified sequences from NS5A into the pSUMO plasmid (LifeSensors Inc). The following PCR primers were used to amplify the NS5A-domain 1+ coding sequence from the plasmid pHCVbart.rep1b/Ava-II (177): 5'-GCG GGT CTC AAG GTG GAG TCC CCT TC-3' and 5'-GCG CGC AAG CTT CTA TTA GGA GTC ATG CCT GGT AGT GCA TGT TGC-3'. The amplified product was subcloned into the pSUMO plasmid using the BsaI and HindIII sites to generate pSUMO-NS5A-domain1+. The QuikChange Site-Directed Mutagenesis Kit (Stratagene) was used to mutate four cysteines to serines (C39S, C57S, C59S and C80S) in pSUMO-NS5A-domain1+ to create pSUMO-5A-domain1+ 4C-4S.

Purification of NS5A-domain 1+ WT and 4C-4S proteins.

The NS5A polypeptides expressed from the pSUMO-based plasmids were expressed as fusion proteins with SUMO at the amino terminus. Overexpression of protein in this system was performed in the Rosetta (DE3) strain of *E.* coli and purified as described previously (178).

RNA sequencing and Actinomycin D mRNA decay assays.

To measure the decay of endogenous cellular transcripts in Huh or Huh-HCV cells, actinomycin D (5 μg/mL, Sigma) was added to the media, and total cellular RNA was collected after 0, 3 and 6 hours using the RNeasy kit (Qiagen). Genome-wide RNA sequencing was performed on technical duplicate samples to assess mRNA expression levels and mRNA decay rates as described previously (49). The zero time point was used to determine mRNA expression levels. Sequencing reads were mapped to the human genome (hg19) using Bowtie 2.0 with default settings. Tophat (v2.0.13) and Cufflinks (v2.2.1) were used subsequently to generate Fragments Per Kilobase of transcript per Million (FPKM) mapped reads that were quantified using custom R scripts. Transcript decay rates were determined following addition of actinomycin D based on a model of first order decay.

To measure the decay of beta-globin reporter transcripts in Huh and Huh-HCV cells, the cells were transfected in a 15 cm dish using 150 μL Lipofectamine 2000 (Invitrogen) and 15 μg of the beta-globin expression plasmids BBB, BBB-GRE, or BBB-ARE as well as 8 μg of the pTracerC GFP expression plasmid. After transfection, each 15 cm dish of cells was split into three 10 cm dishes. Cells were treated 48 hours later with 5 μg/ml of actinomycin D (Sigma), and total RNA was isolated after 0, 3, or 6 hours using the RNeasy kit (Qiagen), following manufacturer's recommendations. Residual genomic or plasmid DNA was removed by digesting 1 μg of each sample with 1 unit of DNAse I (NEB) for 30 min at 37 °C. cDNA was prepared with Superscript II enzyme (Invitrogen) and oligo dT_{15} primer from 1 μg of total RNA for each time point. Controls without RT

were also prepared from 1 µg of total RNA. Quantitative real time PCR was performed in triplicate for each sample, and relative concentrations were calculated based on standard curves for each primer set. The PCR reaction primers were:

Beta-globin: forward 5'-GAGGGTCTGAATCACCTGGA-3' and reverse 5'-GCCAAAATGATGAGACAGCA-3'.

GFP: forward 5'-TGGAAACATTCTCGGACACA-3' and reverse 5'-CTTTTCGTTGGGATCTTTCG-3'. These primers were mixed with the template and the IQ™ SYBR® Green Supermix (Biorad) and amplified SYBR-green amounts were measured in an iCycler (Biorad) over time. Beta-globin levels were normalized to GFP levels.

RNA-immunoprecipitation followed by RNA sequencing or RT-PCR.

To identify mRNA targets of NS5A, RNA-IP was performed as described previously (179) on Huh or Huh-HCV cells using a rabbit polyclonal antibody for NS5A which was produced at Covance Research Products (Denver, PA) using the purified recombinant protein NS5A-His as the antigen (107, 169), RNA was purified from the immunoprecipitated material using the RNeasy kit (Qiagen) following manufacturer's instructions. Genome-wide RNA sequencing was performed as described previously (49). For each transcript, we calculated a NS5A-binding parameter called the fold change in enrichment (FCE) defined as:

$$FCE = \frac{(\text{NS5A IP/input}) \text{ Huh-HCV}}{(\text{NS5A IP/input}) \text{ Huh}}$$

where the ratio of the RNA-Seq expression level for each transcript from the NS5A IP to the level from input RNA based on duplicate samples for Huh-HCV cells is divided by the same ratio for Huh cells.

To assess NS5A binding to reporter transcripts, Huh-HCV (15 cm dish) were transfected with 15 μg of BBB or BBB-GRE reporter plasmids and 8 μg of pTracerC plasmid in 100-150 μl of Lipofectamine 2000. RNA-IP was performed as described previously (179) using an anti-His antibody (Santa Cruz Biotech Inc.), anti-NS5A antibody (169), or anti-PABP antibody (Immuquest). RNA was purified from the input and immunoprecipitated material using the RNeasy kit (Qiagen) following manufacturer's recommendations. cDNA was prepared using Superscript II enzyme (Invitrogen), and PCR was performed with the beta-globin and GFP PCR primers described above.

In vitro RNA-protein binding assay.

The fluorescence polarization assay was performed using a Beacon fluorescence polarization system (Amersham Biosciences) as described previously (107). Recombinant NS5A domain 1+ protein (0-1500 nM) and the 3'-fluorescein-labeled GRE RNA oligonucleotides or mutant RNA oligonucleotides shown in Table 3.1 were gently mixed in binding reaction buffer (20 mM HEPES, pH 7.5, 5 mM $MgCl_2$, 10 mM 2-mercaptoethanol, 100 μM $ZnCl_2$ and 100 mM NaCl) and incubated briefly at 25 °C. Binding of NS5A domain 1+ was measured by the change in polarization. All steps were performed in reduced light. Data were fit to a hyperbola by using KaleidaGraph software (Synergy Software).

Tet-off mRNA decay assay.

HeLa Tet-off cells (15 cm dish) were transfected with 15 μg of the parental BBB reporter plasmid or BBB plasmids containing 3' UTR inserts along with 15 μg of the NS5A expression plasmid, mutated NS5A expression plasmids or mock expression plasmid, and 8 μg of the pTracerC GFP expression plasmid in 100-150 μl of Lipofectamine 2000. After transfection each 15 cm dish was split into five 10 cm dishes and 48 hours later cells were treated with 300 ng/ml of doxycycline. After 0, 1.5, 3, 4.5 or 6 hours, total RNA was extracted using the RNeasy kit (Qiagen) following manufacturer's recommendations, and for each sample, 10 μg of RNA was analyzed by northern blot using beta-globin and GFP probes as described previously (46). To ensure expression of NS5A or mutated NS5A, protein was extracted from cells in duplicate plates 48 hours after transfection and analyzed by western blotting as described previously (180) using an anti-NS5A antibody (169) and an anti-ERK 1/2 antibody (Cell signaling).

Results

Host cellular transcripts are stabilized in HCV-expressing cells.

We measured mRNA expression levels and mRNA decay rates on a genome-wide basis using Actinomycin D mRNA decay assay in the human hepatoma cell line, Huh 7.5 (Huh), and the same cell line expressing an HCV subgenomic replicon (Huh-HCV). Actinomycin D was added to Huh and Huh-HCV cells to block transcription and total cellular RNA was collected at 0, 3, and 6 hours. This RNA was analyzed by genome-wide RNA sequencing (RNA-Seq)

to calculate levels of transcript expression and transcript half-life based on a model of first order decay. We found a total of 16714 transcripts were expressed in either Huh or Huh-HCV cells, 14894 transcripts were expressed in Huh cells, 15542 transcripts were expressed in Huh-HCV cells, and 14359 transcripts were expressed in both. Of these, 6012 transcripts (36%) were up-regulated by >20% and 3903 transcripts (23%) were down-regulated by >20% in Huh-HCV cells compared to Huh cells. We calculated the half-life of each transcripts in both Huh and Huh-HCV cells and found 4945 transcripts (30%) were stabilized (the log of the decay slope increased by > 50%) and 5131 transcripts (31%) were destabilized (the log of the decay slope decreased by > 50%) in Huh-HCV cells compared to Huh cells. A master file containing all the primary gene expression and mRNA decay data is found in Supplementary Table 1. Overall, these data suggest that expression of the HCV subgenomic replicon had a dramatic impact on host gene expression and mRNA decay.

NS5A binding to host cellular transcripts correlates with transcript stabilization.

Since the HCV NS5A protein is an RNA-binding protein known to bind to HCV genomic RNA, we hypothesized that NS5A might also bind to host cellular mRNAs. To test this hypothesis, we used an anti-NS5A antibody to immunoprecipitate (IP) NS5A from cytoplasmic extracts prepared from Huh-HCV and Huh cells, and we used RNA-Seq to identify and quantify co-purified host cellular mRNA transcripts. The anti-NS5A antibody used in this study was previously shown to be specific for NS5A in Western blot and to specifically

immunoprecipitate NS5A from Huh cells expressing HCV replicon (107, 169). For each transcript, we calculated a NS5A-binding parameter called the fold change in enrichment (FCE) as defined in the Materials and Methods. We defined NS5A targets as host transcripts with a FCE > 3 or transcripts present in the NS5A IP from Huh-HCV cells but absent in the NS5A IP from Huh cells and identified 960 NS5A target transcripts. A pathway analysis of these NS5A target transcripts revealed that 701 transcripts were related to cancer, 294 transcripts were related to cell growth and proliferation, and 290 transcripts were related to cell death (Ingenuity Pathway Assistant software). Supplementary Table 2 shows examples of NS5A target transcripts, and a complete listing of target transcripts is found in Supplementary Table 3. Figure 3.1 shows examples of functional pathways that contain NS5A target transcripts involved in apoptosis (Figure 3.1A) and cell growth/proliferation (Figure 3.1B). Thus, we found that NS5A target transcripts were highly enriched for transcripts encoding regulators of cell growth, cell death, and cancer.

We hypothesized that cytoplasmic binding by NS5A to host cellular transcripts could alter their mRNA half-life. To evaluate this, we assessed changes in the mRNA decay rates of NS5A target transcripts in Huh-HCV cells compared to Huh cells. Of the 960 NS5A target transcripts, 556 (58%) were stabilized in Huh-HCV cells. In contrast, among 8731 transcripts that were not NS5A targets (FCE < or = 1), only 2116 (24%) were found to be stabilized (Figure 3.2A, blue bars). This difference was highly significant ($p < 2.2 \times 10^{-16}$). In addition to enrichment in transcript stabilization, we also found that NS5A target

transcripts were highly enriched for up-regulation and stabilization (Figure 3.2A, red bars; $p < 2.2 \times 10^{-16}$). For a subset of NS5A target transcripts, we used quantitative RT-PCR to verify that they were stabilized and upregulated in Huh-HCV cells (Supplementary Table 4). Overall, our data suggest NS5A targets are highly enriched for transcript stabilization and up-regulation in Huh-HCV cells.

GRE-containing reporter transcripts are stabilized in Huh-HCV cells.

The HCV NS5A protein functions as an RNA-binding protein with preference for G- and U-rich sequences (107). We showed that GU-rich sequences, known as GREs, present in the 3'UTR of certain human transcripts target them for rapid mRNA degradation (44). We found that 118 NS5A target transcripts contain GRE sequences in their 3' UTRs, as defined previously (44, 46). We derived a cumulative distribution of the FCE for NS5A target transcripts that contain a GRE or do not contain a GRE and found greater binding by NS5A to targets that contained a GRE ($p = 0.003$, two sample Kolmogorov-Smirnov test, Supplementary Figure 1). Many other NS5A targets contain 3' UTR sequences that are similar to the GRE and are rich in G or U residues. A *de novo* motif search was performed using Partek software to look for conserved sequences in the 3' UTRs of NS5A targets based on the RNA sequencing data. The top 12-mer motif, shown in Figure 3.2B (top sequence), is highly G rich and resembles a consensus sequence that was previously found in CELF1 target transcripts (bottom sequence) (46). Also, a motif resembling a polyU sequence was among the top 11-mer motifs identified as a consensus sequence present in

NS5A target transcripts (Supplementary Figure 2). These data are consistent with previous findings that NS5A could bind to polyU or polyG sequences (107). Since G and U rich sequences, similar to known NS5A binding sites, were conserved in the 3' UTRs of NS5A target transcripts, we hypothesized that NS5A could impact the decay of transcripts containing G and U rich sequences. Our finding that the consensus NS5A target sequences shown in Figure 3.2B (top) has similarity to previously published GRE sequences (46) suggested a possible relationship between NS5A binding sites and GREs.

To determine if GU-rich sequences regulate host mRNA decay in HCV-expressing cells, we transfected Huh or Huh-HCV cells with beta-globin reporter constructs in which the *JUNB* GRE (BBB-GRE) and the *IL2* ARE (BBB-ARE) were inserted into the 3' UTR. The *JUNB* GRE and the *IL2* ARE have been previously shown to function as mediators of rapid mRNA decay (20, 44). The cells were also co-transfected with a GFP reporter construct to control for transfection efficiency. Transcription was inhibited by the addition of actinomycin D, and total RNA was isolated after 0, 3 and 6 hours. Expression of the reporter transcripts was measured by quantitative RT-PCR and was normalized to the expression of the GFP transcripts. In this set of experiments, the BBB-GRE transcript decayed rapidly in Huh cells with a half-life of 80 ± 3 minutes and was stabilized ($p = 0.005$) in Huh-HCV cells with a half-life of 392 ± 18 minutes. In contrast, the BBB-ARE transcript decayed rapidly in Huh cells with a half-life of 133 ± 3 minutes but exhibited only minor and insignificant stabilization in Huh-HCV cells with a half-life of 158 ± 4 minutes (Figure 3.3). This finding that the

GRE-containing reporter transcript exhibited specific stabilization in replicon-containing cells suggests that a mechanism exists for selective recognition of the GRE in HCV replicon-containing cells.

Binding by the HCV NS5A protein to host cellular transcripts correlates with transcript stabilization.

Because the HCV NS5A protein binds preferentially to RNA containing GU-rich sequences, we speculated that NS5A could be responsible for the stabilization of GRE-containing transcripts in Huh-HCV cells. We performed RNA-IP assays to determine if we could identify a physical interaction between NS5A and the GRE in cells that contained the subgenomic HCV replicon. We transfected Huh-HCV cells with the beta-globin reporter construct (BBB) or the same reporter carrying the *JUNB* GRE in its 3'UTR (BBB-GRE). Two days after transfection, cell lysates were immunoprecipitated with an anti-His antibody (negative control), anti-PABP antibody (positive control) or anti-NS5A antibody, and RNA was isolated from the input material (I) and the immunoprecipitation pellet (P). Reverse transcription PCR was performed on this RNA to evaluate levels of beta-globin transcript and Hypoxanthine Phosphoribosyltransferase (HPRT) transcript, which is used as a housekeeping gene control (Figure 3.4). In cells transfected with the BBB-GRE construct, the beta-globin transcript was present in the NS5A pellet but the HPRT transcript was not (lane 10), whereas in cells transfected with the BBB construct, neither the beta-globin nor the HPRT transcripts were present in the NS5A pellet (lane 4). This result suggests that

NS5A bound specifically in cells only to beta-globin reporter transcript that contained a GRE. Thus, NS5A was capable of binding to the GRE in HCV replicon-containing cells.

We performed in vitro RNA-binding assays to measure the binding affinity (Kd) of NS5A for the GRE and other sequences, including RNA sequences derived from the consensus sequence shown in Figure 3.2B, top (Table 3.1). For these assays, we used a polypeptide that contained the amino terminal domain (domain 1) of NS5A. The structure of domain 1 of NS5A has been determined by X-ray crystallography (172, 173). The protein crystallized as a homodimer, and the structural integrity of the dimer was dependent on the tetra-cysteine-coordinated Zn^{2+} ion (Figure 3.5A). We purified a recombinant NS5A polypeptide that contained domain 1 plus 36 additional carboxy terminal amino acids; we refer to this protein as NS5A domain 1+. We also purified a NS5A derivative that was identical except the 4 cysteines in the zinc finger were changed to serines (referred to as 4C-4S). We used a fluorescence polarization assay (107) to measure binding of these NS5A polypeptides to fluorescein-labeled RNA oligonucleotides that contained a minimal GRE sequence (RNA #3 in Table 3.1). NS5A domain 1+ was titrated into a binding mixture containing a 3'-fluorescein labeled RNA substrate. The median polarization (mP) was plotted as a function of NS5A domain 1+ concentration, and the equilibrium dissociation constant was determined by fitting the data to a hyperbola. NS5A domain 1+ bound with high affinity to the GRE and this binding depended on the presence of zinc (Figure 3.5B). The mutated NS5A polypeptide (4C-4S), incapable of binding Zn^{2+}

because of complete disruption of the Zn^{2+}-binding site, failed to bind to the GRE (Figure 3.5C). Converting the GRE sequence into CU- or AU-rich sequences resulted in a 7- to 10-fold reduction in the observed affinity of NS5A domain 1+ for these RNAs (Table 3.1; compare RNA #4 and #5 to #3). Two RNA sequences derived from the consensus sequence in Figure 3.2B bound to NS5A domain 1+ with high affinities (Table 3.1, RNA #1 and #2). Overall, our data support a direct and specific interaction between NS5A and the GRE in cells and in vitro.

NS5A directly stabilizes GRE-containing transcripts.

Based on our findings that GRE-containing transcripts were stabilized in Huh-HCV cells and that the HCV NS5A protein was found to bind to GRE sequences, we hypothesized that binding by NS5A to GRE-containing transcripts mediates transcript stabilization. To test our hypothesis, we transfected HeLa cells with the BBB, BBB-GRE, BBB-mGRE, or BBB-ARE beta-globin reporter constructs and co-transfected them with constructs that expressed wild-type NS5A (NS5A) or the following NS5A derivatives: 4C-4S, ΔN, or ΔN-4C-4S. A GFP expression construct was also co-transfected to control for transfection efficiency. Transcription from the tet-responsive promoter was blocked by the addition of doxycycline, and total RNA was extracted after 0, 1.5, 3, 4.5 or 6 hours. Transcript degradation was measured over time by northern blot (Figure 3.6) and the expression of NS5A or derivatives thereof was monitored by western blot (Supplementary Figure 3). As expected, the BBB-reporter alone and the BBB-mGRE reporter were very stable, whereas the BBB-GRE reporter decayed

more rapidly (half-life = 337 ± 42 minutes). When the NS5A construct was co-transfected, however, the BBB-GRE transcript was stabilized (1091 ± 117 minutes; p = 0.0005). This stabilizing effect was not observed when the four cysteines that form the NS5A zinc finger were mutated to serine (4C-4S). This indicated that a zinc finger-mediated NS5A-GRE interaction was required for stabilization. Published reports showed that the N-terminal helix of NS5A is required for tethering the NS5A protein to the viral replication compartment of the endoplasmatic reticulum (181-183). Deletion of the N-terminal helix releases this protein into the cytoplasm and decreases viral replication (184). We found that deletion of the N-terminal 36 amino acids (ΔN) had no effect on the ability of NS5A to stabilize the GRE-containing reporter transcript. Deletion of the N-terminal 36 amino acids and perturbation of the NS5A zinc finger at the same time (ΔN-4C-4S), however, abrogated the stabilizing activity of NS5A. In contrast to the GRE-reporter, the ARE reporter transcript (BBB-ARE) displayed equal decay in the presence or absence of NS5A with half-life of 240 ± 15 minutes and 228 ± 25 minutes, respectively. This result indicates that NS5A specifically and selectively mediated the stabilization of GRE-containing, but not ARE-containing transcripts.

Discussion

Introduction of a HCV subgenomic replicon into Huh cells led to the selective stabilization of host cellular transcripts through a mechanism that involved binding of NS5A directly to GU-rich sequences. Not all stabilized

transcripts showed increased abundance. This could be due to other mechanisms that may affect transcript abundance to maintain homeostasis. For NS5A target transcripts we observed a significantly higher number of transcripts with increased abundance compared to non-NS5A target transcripts (Figure 3.2A). We showed that NS5A binds directly with high affinity to GRE sequences, and may bind to other G or U-rich sequences that were conserved in the 3' UTRs of NS5A target transcripts. Our finding in HeLa cells that exogenous expression of NS5A specifically stabilizes GRE-containing transcripts clearly demonstrates that NS5A possesses mRNA-stabilizing activity (Figure 3.6). This function of NS5A enables HCV to control host cellular gene expression.

The results presented here support previous work suggesting that NS5A functions as an RNA-binding protein. NS5A interacts with HCV genomic RNA (107, 171) and was shown to bind to polyU or polyG sequences (107). Our results indicate that a G-rich consensus sequence was present in the 3' UTRs of NS5A target transcripts (Figure 3.2B). This sequence resembles the G-rich consensus sequence previously found in CELF1 target transcripts (46). In addition, NS5A is also reported to bind to poly(U/UC) sequence in the 3'UTR of HCV RNA and downregulates viral RNA translation (185). We found similar poly(U/UC)-rich sequences were present within the 3'UTR of NS5A target transcripts (Figure S2). It is reported that GRE sequences are very common in the genome. Although GREs were found in NS5A target transcripts, they were not enriched. Our data shows that the GRE can function as a site for NS5A, but

not all GRE-containing transcripts are NS5A targets. This may be due to secondary structures, genomic context, or availability for binding sites.

Our results confirm the RNA-binding activity of NS5A and suggest that the GRE sequence, UGUUUGUUUGU (44), is a binding target for NS5A. We showed by RNA immunoprecipitation that an anti-NS5A antibody specifically co-immunoprecipitated GRE-containing reporter transcripts, but not reporter transcripts that lacked a GRE (Figure 3.4). These results suggest that the GRE functions as a target of NS5A within cells. Our in vitro binding experiments showed that NS5A binding to the GRE was dependent upon the C_4 zinc finger motif in domain 1 since no GRE-binding activity was observed when the four cysteines were mutated to serines (Figure 3.5C). Also, no binding presented in the absence of zinc (Figure 3.5B), suggesting that coordination of zinc is critical for binding. Crystal structures of domain 1 dimers revealed the presence of a cleft near the zinc-coordinating sites that may facilitate RNA binding (172, 173) (Figure 3.5A). Collectively, our findings suggest that the zinc finger motif contributes to the functional form of NS5A that enables specific interaction of NS5A with GRE RNA.

We previously showed that the GRE mediates rapid mRNA decay by binding to CELF1 (44), which appears to recruit components of the cellular mRNA decay machinery such as poly A ribonuclease (25). In the presence of NS5A, the rapid decay of the GRE-containing reporter was completely abolished (Figure 3.6), suggesting that NS5A might potentially antagonize the activity of CELF1. CELF1 and NS5A appear to have overlapping binding specificities since

they both bind directly to G-rich sequences, including the GRE, but a subset of NS5A target transcripts might not be targets of CELF1. These proteins have different mechanisms for RNA binding. NS5A binding involves zinc finger domains, whereas CELF1 binding involves RNA recognition motifs, yet their binding target sites appear to overlap, at least in the case of GRE sequences. Further work is needed to better define the sites for binding by these proteins to host transcripts.

Viruses have developed mechanisms to manipulate host gene expression at posttranscriptional levels in order to subvert antiviral defense mechanisms and to create an environment in the virus-infected cell that will prevent cell death and allow viral replication. Kaposi's sarcoma virus (156) and Herpes simplex virus (157) produce nucleases that mediate host mRNA decay. Herpes simplex virus also produces the ICP27 protein which mediates the stabilization of AU-rich element-containing host transcript (100) and Epstein-Barr virus infection leads to the stabilization of mRNAs through the activation of the stress activated protein kinase p38 (186). Several studies found differential host gene expression in cell cultures infected with HCV using high-throughput approaches and screens (187-191), but the mechanism of how the host gene expression is regulated by the virus is not well understood. Luna et al. proposed that microRNA-122 sequestration by HCV RNA may lead to stabilization of miR-122 targets, facilitating the oncogenesis of HCV (192). Moon et al. demonstrated another mechanism that HCV utilizes to affect host mRNA decay. They found the 5'UTR of HCV genomic RNA can stall and suppress the cellular 5'-3' exoribonuclease

Xrn1, leading to global stabilization of cellular transcripts (193). The mechanism by which HCV stabilizes GRE-containing transcripts, described in this report, depends on the direct interaction between the NS5A protein and GU-rich sequences within host cellular mRNA. Through this mechanism, HCV blocks the host mRNA degradation machinery and selectively stabilizes a set of GU-rich transcripts that may be necessary for establishment or maintenance of chronic HCV infection.

Many of the short-lived GRE-containing transcripts in mammalian cells encode proto-oncogenes and other important regulators of cell growth and apoptosis, constituting a network of coordinately regulated transcripts (116). These GRE-containing transcripts include proto-oncogene transcripts such as *JUN*, *JUNB*, *JUND*, and *ETS2*, transcripts encoding regulators of apoptosis such as *BCL10*, *BAG*, *MAP3K5*, and *TNFRSF1*, and transcripts encoding other regulators of cell growth including *EIF4EBP2*, *EIF4G3*, *SMAD7* and *HOXC10*. After infection with HCV, NS5A-mediated stabilization and overexpression of these GRE-containing transcripts would be predicted to promote cell growth and prevent cell death in order to allow a chronic infection to be established. It is possible that new drugs that block the NS5A interaction with the GRE could be developed that would prevent establishment of chronic HCV infections and inhibit the maintenance or propagation of infection. Indeed, drugs like ledipasvir that target NS5A but whose mechanism of action remain unclear (194) might function by perturbing the ability of NS5A to bind GREs or similar G or U rich sequences and modulate host gene expression.

Infection with HCV increases the risk for hepatocellular carcinoma development as well as certain lymphomas (195, 196). The onset of the tumors, however, occurs many years after HCV infection, suggesting that multiple events are required to transform hepatic cells to become malignant (197). Progression of liver fibrosis to cirrhosis in HCV-infected patients will generate a local milieu that predisposes to liver cancer. In this environment, changes occur to the hepatic parenchyma, with hepatocyte injury, which contributes to sequential genetic hits that culminate in malignant transformation (198). However, the mechanisms involved in this process are largely unknown. Moreover, multiple studies have showed a direct role for HCV in hepatic carcinogenesis and transgenic mice expressing the HCV polyprotein can develop liver cancer in the absence of inflammation, hepatic cirrhosis or immune recognition of the transgene (166, 199, 200). The stabilization and overexpression of GRE-containing transcripts including proto-oncogene transcripts and transcripts encoding regulators of apoptosis may contribute to the development of cancer by promoting cell growth and preventing the death of genetically damaged cells. Later events that finally lead to uncontrolled growth of these cells might destroy the fail-safe mechanisms that are initially able to cope with the increased stability of these important messages.

In conclusion, our findings describe a novel role of NS5A in stabilizing host GRE-containing transcripts, providing new insights into HCV pathogenesis and carcinogenesis that may lead to new treatments to prevent HCV infection and understand the progression to liver cancer.

Chapter 4:

Reovirus infection induces stabilization and up-regulation of cellular transcripts that encode regulators of TGF-β signaling

Liang Guo, Jennifer A. Smith, Michelle Abelson, Irina A. St-Louis-Vlasova, Leslie A. Schiff and Paul R. Bohjanen.

Introduction

Viral infection leads to changes in cellular steady state mRNA levels within infected cells. Some of these alterations represent the cell's innate antiviral response, while others are induced by the invading virus in an attempt to sequester host antiviral responses and usurp the cellular machinery for viral replication. Virus-induced changes in cellular gene expression are often regulated through transcriptional mechanisms. For example, infection with many viruses increases the transcription of genes involved in antiviral responses including the type I interferons (IFN) as well as numerous IFN-stimulated genes (ISGs) (reviewed in (201, 202)). Although transcriptional regulation is important for mammalian cells to respond to their environment, numerous mammalian genes are also regulated at the level of mRNA decay in response to a variety of external signals (reviewed in (26, 203). Virus-induced changes in cellular steady state mRNA levels have also been shown to be regulated at the level of mRNA decay (105, 204).

In this study, we utilized reovirus infection to evaluate the effect of viral infection on host cellular gene expression at the level of mRNA decay. Reovirus, a prototypic member of the *Reoviridae* family, is a non-enveloped double-stranded RNA virus that has been studied extensively as a model of viral infection (205). This virus was a valuable model for us to examine the effect of viral infection on mRNA stability for several reasons: i) the consequences of reovirus infection are well documented

and include induction of type I IFN, initiation of apoptosis, inhibition of cellular translation, and a G1/S cell cycle arrest (reviewed in (205)); ii) global studies on the impact of reovirus infection on cellular gene expression have been published (206-209); and iii) reovirus isolates vary in their effects on infected cells (208, 210-212). Since reovirus isolates induce distinct changes in cellular gene expression, as well as distinct cellular responses to infection, alterations in cellular gene expression following reovirus infection can be correlated to specific phenotypes (208). For example, in murine L929 cells, reovirus isolates Dearing and c87 induce high levels of type I IFN, whereas cells infected with isolate c8 have a poor IFN response (208). As a consequence, numerous ISG transcripts are induced following infection with isolates Dearing or c87, but not isolate c8 (208). Additionally, infection with c87 or c8 lead to an inhibition of cellular translation, whereas infection with Dearing does not (208, 210, 212). Mechanisms for inhibition of cellular translation in response to reovirus infection involve phosphorylation and inactivation of the alpha subunit of eukaryotic initiation factor-2 (eIF2α) by the dsRNA-dependent protein kinase (PKR) or the ER-stress-induced kinase PERK (208). We previously identified a specific subset of cellular transcripts that were induced following infection with c8 and c87, which inhibit cellular translation, but were not induced following infection with isolate Dearing, which does not inhibit cellular protein synthesis (208). The mechanisms for increased steady state expression of these cellular transcripts could

involve transcriptional and/or posttranscriptional mechanisms.

In this report, we investigate the role that mRNA decay plays in regulating host cellular gene expression following reovirus infection. We used oligonucleotide microarrays to measure mRNA decay rates in L929 cells that were mock-infected or infected with reovirus isolates Dearing, c8, or c87. We detected a subset of transcripts that were coordinately induced and stabilized upon infection with reovirus strains that induced host translational shutoff, i.e. strains c8 and c87. The induced and stabilized transcripts encoded multiple regulators of transforming growth factor-beta (TGF-β) signaling, including components of the Smad signaling network (SSN) and apoptosis/survival pathways. TGF-β is a cytokine that has multiple activities including immune modulation, promotion of fibrosis, control of cellular growth, and regulation of apoptosis (213-218). TGF-β production is activated following infection with a variety of viruses (219-226), including reovirus (227, 228), suggesting that the TGF-β signaling cascade plays a role in viral pathogenesis. In particular, regulation of apoptosis through TGF-β signaling may be part of a host response to viral infection. Thus, the coordinate stabilization and up-regulation of transcripts that encode components of TGF-β signaling pathways likely represent a cellular anti-viral response to reovirus infection.

Methods and Materials

Cells, viruses and viral infection. Murine L929 cells were maintained as suspension cultures as described previously (229). Reovirus isolates Dearing and c87/Abney are prototypic laboratory strains (230), and isolate c8 was previously described (229, 231). Purified virions were prepared by CsCl density gradient centrifugation of extracts from cells infected with third-passage L929 cell lysate stocks (232). In order to analyze three independent infections, each set of infections was initiated on separate days. L929 cells were plated in 150 x 25 mm tissue culture plates and were allowed to incubate at 37^{o}C for 4 h, after which time the medium was removed and cells were mock-infected or infected with purified virions (Dearing, c87 or c8) at a multiplicity of infection (MOI) of 80 plaque forming units (PFU)/cell. After a 1.5 h viral adsorption at 37^{o}C, medium was added and samples were incubated at 37^{o}C for an additional 18 h.

RNA isolation and microarray hybridization. At 19.5 h post-infection (p.i.), actinomycin D (Sigma, MO) was added at a final concentration of 10 μg/ml to stop transcription by RNA polymerase II and total RNA was isolated at 0, 45, 90 and 120 min post-actinomycin D treatment using Trizol reagent (Invitrogen, CA) according to the manufacturer's instructions. Total RNA was purified with the RNeasy column (QIAGEN, CA); 15 μg of RNA was converted to cDNA using the Superscript custom kit (Invitrogen) with an oligo dT-T7 primer (Geneset, CO). The purified

cDNA was used for an *in vitro* transcription reaction using T7 RNA polymerase and biotinylated nucleotides following the manufacturer's protocol (ENZO Bioarray, NY). Biotinylated anti-sense cRNA was purified with the RNeasy column; 15 µg was fragmented according to Affymetrix instructions' and hybridized to Affymetrix murine U74Av2 oligonucleotide microarrays (Affymetrix Inc., CA). Microarrays were scanned on a Hewlett Packard Agilent 2200 confocal scanner (Bio-Rad Laboratories, CA) and normalized signal intensities were obtained using Affymetrix MAS 5.0 software as described previously (208).

Microarray data analysis. Expressed transcripts levels were determined as the average signal values with 95% confidence intervals (95% CI) across three replicate arrays. Fold changes (FC) in expression between two infection conditions were determined as the ratio of average signal values. P values were calculated using a two-sample t test assuming equal variance. We fit the log signal values over time following actinomycin D treatment to a linear regression model to calculate transcript half-lives as described previously (44). A p-value of ≤ 0.05 was used to identify differences in mRNA decay rates in mock-infected cells compared to reovirus-infected cells.

Reverse Transcription Real-time PCR. Reverse transcription real time PCR (RT-PCR) was used to validate changes in transcript level and

mRNA decay rates of three transcripts that were found to be up-regulated and stabilized following infection with certain reovirus isolates: Gdf15, Tgif, and Myc. Total cellular RNA from the same reovirus infections as described above was used for real time RT-PCR. RNA was converted to cDNA by using StrataScript ™ reverse transcriptase (Stratagene) and gene specific primers. PCR amplifications were performed in a BioRad iCycler thermocycler by using the QuantiTect™ SYBR Green PCR Kit (QIAGEN) with the following cycling conditions: initial heating at 95°C for 13.5 min, followed by 40 cycles of 3-step temperature cycling at 95 °C for 10 s, 55.6 °C for 10 s, and 72 °C for 30 s. Data was analyzed using the iCycler software and standard curves were generated to measure transcripts levels, which were normalized to the level of HPRT transcript. The normalized values at each point were then used to generate mRNA decay curves. Oligonucleotide primers (Integrated DNA Technologies Inc) were: Gdf15 5' CCG AGA GGA CTC GAA CTC AG 3', 5' GTA GGC TTC GGG GAG ACC 3'; Hprt 5' GGT GAA AAG GAC CTC TCG AA 3', 5' AGT CAA GGG CAT ATC CAA CA 3'; c-Myc 5' TGA AGG CTG GAT TTC CTT TG 3', 5' TTC TCT TCC TCG TCG CAG AT 3'; Tgif 5' TCC TAG AAA CCC CAG CTT CA 3', 5' GCT GCT GAT GAG GAA AGG TC 3'.

Results and Discussion

We profiled the changes in L929 cellular gene expression and mRNA decay rates that occurred as a consequence of infection with reovirus isolates c87, c8 and Dearing. At 19.5 h p.i., ongoing transcription was arrested by addition of actinomycin D and global mRNA expression levels were measured after 0, 45, 90 and 120 min of actinomycin D treatment using Affymetrix U74Av2 microarrays. This experiment was performed three separate times for each reovirus isolate and the mRNA half-life with 95% confidence interval (95% CI) was calculated for over 6500 expressed transcripts based on a model of first order decay. We then defined subsets of transcripts with altered mRNA decay rates in reovirus-infected cells compared to mock-infected cells (Table 4.1).

We observed the stabilization ($p \leq 0.05$) of 349, 253, and 51 cellular transcripts after infection with reovirus isolates c87, c8, and Dearing, respectively. A complete list of the stabilized transcripts and their decay rates are displayed in S1 Table. Of the stabilized transcripts, 172 were stabilized following infection with both c87 and c8 isolates, whereas only 24 transcripts were stabilized after infection with all three isolates. We also noted the destabilization ($p \leq 0.05$) of a small number of transcripts in L929 cells following infection with these same reovirus isolates, but there was poor correlation between isolates; only four transcripts were destabilized following infection with both c87 and c8 and no destabilized transcripts were common to all three isolates.

We evaluated the steady state mRNA levels of stabilized cellular transcripts to determine whether or not stabilization following reovirus infection correlated with changes in overall levels of these transcripts. Following c87 infection, 70 cellular transcripts were up-regulated ($p \leq 0.05$) and stabilized ($p \leq 0.05$); 40 transcripts were up-regulated and stabilized following c8 infection (Table 4.1). Of these, 26 transcripts were up-regulated and stabilized following infection with both of these reovirus isolates. In contrast, only two transcripts were up-regulated and stabilized following infection with Dearing, the reovirus isolate that did not inhibit cellular translation. Using more strict criteria to identify transcripts that were up-regulated ($FC \geq 2.0$ and $p \leq 0.05$) in reovirus-infected cells, we identified 31 transcripts that were up-regulated and stabilized following c87 infection and 41 transcripts that were up-regulated and stabilized following c8 infection; 13 were up-regulated and stabilized following infection with both isolates that led to an inhibition of host protein synthesis. We did not identify any transcripts that were up-regulated ≥ 2-fold and stabilized following infection with strain Dearing.

A subset of the transcripts that were up-regulated ($p \leq 0.05$) and/or stabilized ($p \leq 0.05$) following infection of L929 cells with c87 or c8 are listed in Table 4.2. A complete list is found in S2 Table. These transcripts encode various components of the TGF-β signaling pathway (Figure 4.1), including cell cycle inhibitors and regulators of transcription, apoptosis and stress responses. In particular, many encode protein components of the

SSN, which regulates transcription associated with cell cycle arrest, differentiation and apoptosis (233-237). This suggests that the SSN is involved in a coordinated cellular response to infection with reovirus isolates c8 and c87. In contrast, none of the transcripts encoding components of this pathway were up-regulated and/or stabilized following infection with isolate Dearing, suggesting that reovirus isolates differ in their ability to induce changes in the decay of cellular transcripts encoding SSN components. The finding that strains that induced expression of the SSN network also induced cellular translational inhibition suggests that the SSN network and inhibition of translation could be linked.

Activation of the SSN could represent a cellular response to viral infection. Numerous viruses, including reovirus, induce increased expression of TGF-β as part of the host response to viral infection. Depending upon the integration of signals through the TGF-β receptor and other receptors, the SSN regulates the balance between apoptosis or cell growth and survival (reviewed in (238). In virus-infected cells, TGF-β signaling may play an antiviral role by promoting the apoptosis of virus-infected cells, whereas in uninfected cells, signaling through the SSN may play a role in protecting against apoptosis (227). In addition to activating the SSN, the TGF-β family of receptors interfaces with several other signaling pathways, including NF-κB, MAPK/ERK, p38 and JNK pathways (239-242). These pathways influence the SSN by regulating the phosphorylation of Smad proteins, which in turn, control cell proliferation,

differentiation and migration through their role as transcription factors (235, 237, 243-245). Smad transcription complexes are activated by TGF-β receptors 1 and 2. Following receptor activation, Smad 2,3 complexes or Smad 1,5,8 complexes become phosphorylated and interact with Smad 4, creating activated transcription complexes (234, 246). These newly formed Smad 4-containing complexes translocate into the nucleus, bind DNA, and activate target gene transcription. Depending on other signals, however, Smad 6 and Smad 7 can repress phosphorylation and prevent activation of Smad transcription complexes by blocking their translocation into the nucleus (235, 247, 248). Smad 7 can also act in a feedback loop to repress TGF-β signaling by inducing receptor ubiquitylation and protein degradation (249-251). Thus, depending on the integration of multiple signals, the SSN can activate or repress transcription of a specific subset of cellular genes.

Transcripts that were up-regulated and stabilized following reovirus infection included SMAD 1, 2, 6 &7, Tgif, c-Myc, CITED2 and KLF5, which encode components of the SSN that control transcription of genes that regulate apoptosis and cell growth (243, 246, 247, 249, 250). Of note, reovirus has been shown to preferentially infect and induce lysis of cells that express high levels of c-Myc or other oncoproteins, suggesting that reovirus might exploit this oncogenesis signaling pathways to preferentially kill cancer cells (252). For this reason, reovirus infection is a potential treatment of cancer (253). Other up-regulated and stabilized

transcripts encode growth regulatory cytokines that impact the SSN (see Figure 4.1). For example, the transcripts encoding Gdf15, a TGF-β superfamily cytokine, and Vegfa, an angiogenic endothelial cell growth factor, were dramatically stabilized and up-regulated following infection with reovirus isolates c8 and c87. Interestingly, Vegfa is induced by TGF-β and acts in concert with TGF-β to induce the apoptosis of endothelial cells (254, 255). In addition to growth factors, transcripts encoding downstream regulators of kinase pathways that can also impact the SSN, including Sos1, Sos2, Map3k3, Map3k1, Dusp1, and Dusp2, were also up-regulated and/or stabilized. The transcript encoding Stam, a cytokine signaling protein that interfaces with the SSN by activating c-Myc (256), was also up-regulated and stabilized in cells infected with reovirus isolates c87 or c8.

Since the SSN regulates the balance between apoptosis and survival, it is possible that the coordinate induction of SSN components through mRNA stabilization represents an attempt by the virus-infected cell to undergo apoptosis. Some up-regulated and stabilized transcripts encode components of receptor-mediated apoptosis pathways including: Bcl-10, which activates NF-κB (257); Tbk1, which promotes anti-viral responses (258) and activates NF-κB (259); Gadd45b, a NF-κB-inducible mediator of apoptosis (260); and Bid, an important component of caspase-induced apoptosis (261). TGF-β signaling also leads to activation of NF-κB and promotion of apoptosis through the signaling protein TGF-β

activating kinase 1 (Tak1) (241, 262, 263). The NF-κB signaling network interfaces with the SSN by activating Smad 7, which feeds back to repress TGF-β-induced transcription of genes that promote cell growth and survival (241, 264). Thus, the outcome of the SSN – cell growth and survival versus growth inhibition and cell death – is controlled by the coordinate integration of several signals. Following reovirus infection, not all cellular anti-viral responses lead to apoptosis; rather, a balance between death and survival occurs (265, 266). Cells attempt to avoid viral infection, but if unsuccessful, cell death pathways are frequently activated. Meanwhile, viruses need to prevent cell death for a period of time to ensure viral replication. Thus, the interplay between host anti-viral responses to promote death of infected cells and viral evasion mechanisms determines the fate of the cell. We have previously demonstrated that reovirus isolates that led to an inhibition of cellular translation (c87 and c8) also induced stress granule formation (8). Others have shown that reovirus particles are recruited to stress granules during infection, and the stress response induced by reovirus may be necessary for viral replication (267). Here we demonstrate that infection with the reovirus isolates that induced stress granule formation also caused the stabilization of numerous cellular transcripts, including transcripts encoding components of the SSN and regulators of apoptosis. Perhaps, stress granule formation leads to the stabilization and sequestration of certain cellular transcripts, such as the transcripts that encode the

regulators of the SSN and apoptosis pathways we identified here. Thus, the stabilization and up-regulation of transcripts that encode components of the SSN and associated apoptosis pathways may be part of a cellular stress response to reovirus infection.

Numerous other viruses have developed mechanisms to modulate or usurp TGF-β signaling pathways, perhaps to prevent cell death and promote viral replication. For example, Kaposi sarcoma herpes virus produces viral homologues of human interferon response factors that function to regulate TGF-β signaling (268, 269). Herpes simplex virus 1 down-regulates TGF-β and Smad 3 expression in infected cells (270, 271). Although this effect was reported to be due to an HSV-1-encoded microRNA (270), other groups were unable to reproduce those results (272). Human papillomavirus E6 and E7 proteins bind to specific Smad proteins, thereby inhibiting the SSN (273, 274), and the human T cell lymphotropic virus 1 tax protein inhibits TGF-β signaling through c-jun activation (275). Other viruses, such as cytomegalovirus and BK virus, usurp TGF-β signaling to promote viral replication (276, 277). The fact that numerous viruses have developed specific mechanisms to manipulate or evade the SSN suggests this pathway is important for host anti-viral responses.

To validate our microarray mRNA decay data, we utilized real time RT-PCR to measure mRNA levels from three selected genes: Tgif, Gdf15 and c-Myc. These transcripts encode important proteins that interface with

the SSN and, based upon our microarray data, were up-regulated and stabilized following infection with c87 and c8, but not Dearing. We generated decay curves for the three transcripts by real time RT-PCR using the same RNA that was used for the microarray analysis. Decay curves generated for these transcripts by real time RT-PCR were very similar to the mRNA decay curves generated from the microarray analysis (Figure 4.2). These data confirm that Tgif, Gdf-15, and c-Myc were up-regulated and stabilized following infection with reovirus isolates c87 and c8 (Table 4.3). In contrast, infection with strain Dearing led to little or no stabilization of these transcripts (Figure 4.2 and Table 4.3).

Conclusion

Our findings illustrate that multiple cellular transcripts encoding components of the SSN are coordinately up-regulated and stabilized following reovirus infection. We hypothesize this is a cellular response to reovirus infection meant to induce the apoptosis of infected cells, particularly following infection with reovirus isolates that lead to the inhibition of cellular translation. Our findings suggest that cells have unique regulatory mechanisms to selectively recognize and stabilize specific subsets of cellular transcripts. These transcripts may contain specific regulatory sequence(s) in common that allow them to be selectively recognized by RNA-binding proteins or microRNAs. Further work is needed to define the mechanism for the up-regulation and

stabilization following reovirus infection of the transcripts we identified which encode specific components of the SSN.

Chapter 5:

Discussion

The features of oncogenesis and chronic viral infection have considerable overlap. Both promote cell growth and prevent apoptosis, and achieve these ends using similar molecular mechanisms. Many of the ongoing studies of dysregulated cell signaling are still focused around the central dogma of biology; that is, they are aimed at studying the regulation of gene expression at the level of transcription, translation, or post-translation. There are very few studies related to disease pathogenesis that are focused at the level of post-transcriptional regulation, and even fewer on mRNA decay/stability. The work in this thesis represents a paradigm shift that fundamentally alters how we view dysregulation of cell signaling pathways in both oncogenesis and viral infection. In particular, the studies in this thesis provide evidence that mRNA decay plays a critical role in post-transcriptional regulation of gene expression in eukaryotic cells in malignancy and viral infection.

Dysregulation of mRNA decay is a critical step in the model systems that I studied: T cell malignancy, Hepatitis C infection, and Reovirus infection. Our findings raise the question of how many commonplace diseases are utilizing similar mechanisms of mRNA dysregulation.

According to the post-transcriptional RNA operon theory, the stabilities of functionally related mRNAs are regulated in coordination by one or more sequence-specific *trans*-acting factors, primarily RNA-binding proteins, but also microRNAs and other non-coding RNAs (23). The regulatory sequences within the targeted mRNAs (i.e. *cis*-elements) are usually located in the 3'- or 5'-untranslated regions. Some mRNAs may contain more than one such *cis*-

element, and can be influenced by the regulatory networks that are mediated by these *cis*-elements and their *trans*-acting factors concurrently. ARE-AREBP and GRE-GREBP form such regulatory networks to work in collaboration with each other or exclusively to control mRNA stability of many transcripts.

The mRNA decay profile is altered under both biological conditions and disease states, such as immune activation, development, cancer, and viral infection. By selectively regulating the expression of genes that are functionally related, cells can respond to stimuli with precision and efficiency. For instance, previous studies from our lab have shown that the GRE/CELF1 network is disrupted following T cell activation through CELF1 phosphorylation and alternative polyadenylation (APA). Under inactive conditions, unphosphorylated CELF1 binds to GRE-containing mRNAs, inducing their rapid decay and thereby silencing the expression of these transcripts. Soon after T cell stimulation, CELF1 becomes phosphorylated; this activation-dependent phosphorylation of CELF1 leads to altered affinity and decreased binding to GRE by CELF1. The end result is stabilization of GRE-containing transcripts that are involved in cell activation and proliferation (48). This alteration of GRE/CELF1 decay network seems to be a transient phenomenon, since T cells return back to a quiescent state after the stimulation signals disappear. Preliminary data indicates that CELF1 returns to an unphosphorylated state simultaneously. However, further studies are required to confirm these findings.

At the same time, our lab has also shown that a more permanent alteration of GRE/CELF1 regulatory networks plays a separate, yet related, role in T cell

activation. Our lab has found that CELF1 target transcripts preferentially undergo APA after T cell stimulation and the GREs are enriched immediately downstream of the excised APA site (49). The removal of GRE from the affected mRNAs frees them from GRE-mediated decay and may result in transcript stabilization. These findings suggest that the GRE and its binding protein CELF1 might be involved in the regulation of APA and that, in turn, the GRE/CELF1 networks are also influenced by APA.

These studies show that mRNA decay, particularly the GRE/CELF1 mediated mRNA decay network, plays a role in normal cell physiology; however, very few studies have examined the change of mRNA decay during disease states such as malignancy and viral infection. The projects described in this thesis dissertation aim to narrow this knowledge gap by addressing the mechanisms and consequences of mRNA decay regulation on cell growth and apoptosis networks in three contexts: T cell malignancy, HCV infection, and reovirus infection.

Aberrant mRNA decay regulation in malignancy

Based on the fact that GRE-containing CELF1 target transcripts are involved in cell growth, proliferation and apoptosis, we postulate that dysregulation of GRE/CELF1 network could lead to oncogenesis. As mentioned above, CELF1 is phosphorylated at the early stage after T cell activation and this phosphorylation is responsible for the decreased binding and subsequent increased stability of CELF1 target transcripts. Interestingly, both early stage T cell activation as well as aberrant T cell malignancies share certain

characteristics such as rapid cell growth and proliferation, as well as reduced apoptosis. In addition, many of the cell growth and apoptotic signaling pathways that are activated in T cells shortly after their stimulation have also shown abnormal regulation in cancer cells. Chief among these are the MAPK/ERK and the PKC signaling pathways (278, 279). Therefore, we hypothesize that in malignant cells, CELF1 becomes phosphorylated by the kinases that are activated in these signaling pathways, disrupting the GRE/CELF1 mRNA decay networks, thereby resulting in the stabilization or destabilization of cell growth and apoptosis regulatory transcripts, and drives the cells to malignant phenotypes.

Our investigation into the CELF1 phosphorylation and the changes of CELF1 target transcripts in two different malignant T cell types supported the above hypothesis. In the project described in Chapter 2, we did indeed observe CELF1 phosphorylation, or, to be more precise, hyperphosphorylation in both Jurkat and H9 cancer T cell lines. This hyperphosphorylation of CELF1 in malignant T cells is correlated with the loss of binding by CELF1 and subsequent stabilization of a subset of transcripts that had previously been identified as CELF1 targets in primary T cells. Interestingly, CELF1 hyperphosphorylation was also correlated with the gain of binding and subsequent destabilization of a new subset of transcripts. The combined net effect of the altered CELF1 targets is the promotion of cell growth and prevention of cell death. The exact mechanism of how CELF1 preferentially increases its binding to certain transcripts while simultaneously decreasing its binding to others is not clear. This knowledge gap

provides a clear-cut target for future work, which can aim to compare the binding patterns between target transcripts that increase their binding to CELF1 and those that decrease their binding. Similarly, binding patterns and transcript profiles of CELF1 targets can be compared between normal and cancer cells in other malignancies. In fact, dysregulation of CELF1 has already been shown to be associated with different types of cancer, including colorectal cancer, human oral squamous cell carcinomas, certain types of leukemias, and others (120, 123, 280) . Even though there is no consistent conclusion of CELF1's function in oncogenesis (some studies found CELF1 to be a tumor suppressor, while others suggest that CELF1 promotes tumor growth (123, 281), one common area of agreement is that CELF1 is a key regulator of cell growth, proliferation, and apoptosis in the process of malignant transformation. These disparate observations of CELF1's role in tumorigenesis could be due to the heterogeneity of cancer types that are investigated in different studies. Another possibility is that the inherent complexity of CELF1, a multi-functional protein involved in alternative splicing, alternative polyadenylation, mRNA decay as well as translation, allows for different aspects of its function to be targeted/disturbed in different cancer cells. The expression and post-translational modification of CELF1 in different types of cancer is a promising area of investigation; likewise, investigations into the presence CELF1 phosphorylation in other cancer cell lines and its impact on the mRNA stability of the GRE/CELF1 networks provides a promising and novel area for further research.

Altered cellular mRNA decay in viral infection

When infected with a virus, eukaryotic cells undergo a series of changes in response to the intruder; these changes originate from either the virus (i.e. viral factors promoting infection) or from the infected cells themselves (i.e. self-defense mechanisms). The changes often involve alterations in cellular gene expression that eventually lead to dysregulation of cellular processes, such as promotion/inhibition of growth, differentiation, proliferation, and apoptosis. Many studies have explored the impact of viral infection on cellular transcription and translation at length, but few studies have investigated the impact of viral infection on cellular mRNA decay. In Chapters 3 and 4, we utilized two viral infection systems-HCV and reovirus- to illustrate the changes of cellular mRNA stability and their consequences, particularly on the cell growth and apoptosis networks. These two viruses were chosen because they represent both possible outcomes of viral infection: HCV leads to chronic infection whereas reovirus infection ultimately induces the death of infected cells.

In the HCV infection system, our data showed that the HCV viral protein NS5A can bind to growth-regulating host transcripts that are enriched for G- and U-sequences. This binding stabilizes the mRNA transcripts, with the end result being the promotion of growth and prevention of apoptosis of the infected cells. From an evolutionary standpoint, one could postulate that the reason HCV exploits this mechanism in order to keep the host cells alive long enough for the virus to gain a solid enough foothold to establish long-term HCV infection. We may also surmise that these very same mechanisms would continue unchecked

and lead to malignancy. These suppositions are consistent with our basic knowledge of HCV; that is, HCV is known to cause chronic infection in most patients, and be capable of eventually progress to hepatocellular carcinoma.

In addition, our findings put forth a model in which CELF1, a promotor of degradation of GRE-containing transcripts, is antagonized by NS5A during HCV infection. In this model, we hypothesize that in uninfected cells, GRE-containing transcripts are destabilized through their interaction with CELF1, which recruits components of the mRNA decay machinery, such as polyA ribonuclease, to GRE-containing transcripts. While following HCV infection, virally-produced NS5A within host cells displaces CELF1 and binds to GREs, therefore selectively stabilizing these GRE-harboring transcripts. Confirmatory work on the competition between CELF1 and NS5A to their target binding sites as well as their antagonizing effects is needed to support this model.

In the reovirus infection system, our studies detected that infection with reovirus isolates c87 and c8 resulted in the stabilization and up-regulation of host transcripts involved in the TGF- β signaling pathway, particularly, the Smad signaling network (SSN). The SSN is known to regulate the balance between cell survival and apoptosis, and perturbation of this network occurs upon infection by several viruses (271, 273). This suggests two possibilities: (1) that the SSN might be a common target for many viruses seeking to manipulate host cell survival for the purpose of viral infection and propagation; or (2) the SSN is an important self-defense mechanism for infected host cells to trigger apoptosis in order to avoid viral replication and further infection. It is not unreasonable to speculate that the

SSN represents a focal point for the battle between host cell and virus.

Our data suggests a novel model for the regulation of the SSN at the level of mRNA decay following viral infection, with the goal being to control the survival and death of the infected cells. In addition, reovirus strain c87 and c8 have both been shown to induce inhibition of translation of host genes; our studies showed that only infection with these two strains caused the stabilization of the SSN transcripts, suggesting that there might be potential links between these two phenomena. Future studies are needed to identify the mechanism of the selective regulation of the transcript stability and its association with the virus-induced inhibition of cellular translation.

Conclusion

In summary, the work presented in this thesis has furthered our understanding of post-transcriptional regulation at the mRNA decay level in malignancy and viral infection, particularly on the cell growth and apoptosis networks. We have shown that in malignant T cell lines, CELF1 hyperphosphorylation disturbs the GRE/CELF1 mRNA decay networks, leading to stabilization and up-regulation of GRE-containing transcripts that promote cell growth and destabilization and down-regulation of other transcripts that suppress cell proliferation, resulting in malignant transformation. In our viral infection systems, we identified a molecular mechanism that HCV utilizes to manipulate host gene expression to stabilize cellular growth-regulatory transcripts to promote growth and prevent death of the infected cells. In addition, we revealed a novel

mechanism that host cell responds to reovirus infection through stabilization and up-regulation of transcripts that encode regulators of TGF-β signaling pathways, particularly the Smad signaling network, to determine cell survival and apoptosis. Future studies may investigate aberrant regulation of cellular mRNA in other types of cancer and viral infection systems, and its impact on important cellular networks other than growth and apoptosis. Special attention can be put on the GRE/CELF1 mRNA decay networks and other ARE-mediated decay networks.

Illustrations

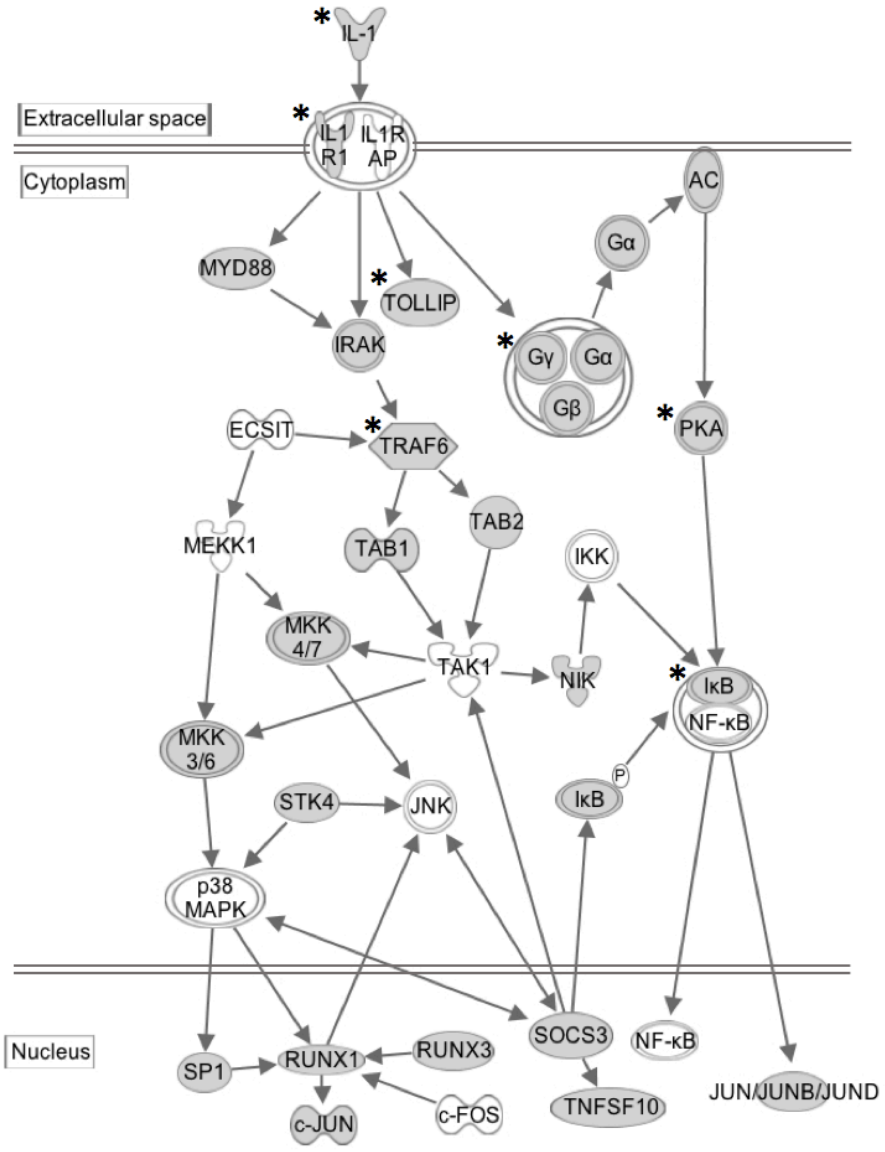

Figure 1. ARE- and GRE-containing transcripts that are targeted by HuR and CELF1 are enriched in the IL1 signaling pathway. Transcripts shown in grey nodes and labeled with an asterisk (*) contain AREs in their 3'UTRs. Transcripts shown in grey nodes contain GREs in their 3'UTRs. This pathway diagram was built using Ingenuity Pathway Assistant Software.

Table 1. Examples of ARE- and GRE-containing cytokine signaling transcripts.

Examples of ARE-containing cytokine transcripts	
Symbol	*Entrez Gene Name*
IL1A	interleukin 1, alpha
IL1B	interleukin 1, beta
IL2	interleukin 2
IL3	interleukin 3 (colony-stimulating factor, multiple)
IL4	interleukin 4
IL5	interleukin 5 (colony-stimulating factor, eosinophil)
IL6	interleukin 6 (interferon, beta 2)
IL8	interleukin 8
IL10	interleukin 10
IL11	interleukin 11
IL12	interleukin 12
IL17A	interleukin 17A
IFNA	interferon, alpha
IFNB	interferon, beta
IFNG	interferon, gamma
TNFA	tumor necrosis factor, alpha
CSF1	colony stimulating factor 1 (macrophage)
CSF2	colony stimulating factor 2 (granulocyte-macrophage)
LTA	lymphotoxin alpha (TNF superfamily, member 1)
Examples of GRE-containing cytokine signaling transcripts	
Symbol	*Entrez Gene Name*
IL1R	interleukin 1 receptor
IL6R	interleukin 6 receptor
IL7R	interleukin 7 receptor
IL17A	interleukin 17A
IFNG	interferon, gamma
IFNGR1	interferon gamma receptor
IFNAR1	interferon alpha receptor
TGFBR	tumor necrosis factor beta receptor
SOCS3	suppressor of cytokine signaling 3
MYD88	myeloid differentiation primary response 88
PKC	protein kinase C
AKT	protein kinase B
IKB	inhibitor of kappa B
TRAF5/6	TNF receptor-associated factor 5
SMAD1/5/7/8	SMAD family member 1/5/7/8
MKK3/4/6/7	mitogen-activated protein kinase kinase 3/4/6/7
MEKK1/5	mitogen-activated protein kinase kinase kinase 1/5
STAT1/3/5	signal transducer and activator of transcription 1/3/5
BCL2	B-cell lymphoma 2

Table 2.1. Expression and half-lives of GRE-containing transcripts that were CELF1 targets in malignant T cells but not normal T cells.

RefSeq ID	Gene symbol	Biological process	T HL (95% CI)	FC H9/T	H9 HL (95% CI)	FC JK/T	JK HL (95% CI)	FCE H9	FCE JK
Cell cycle and apoptosis regulators									
NM_001077440	BCLAF1	Regulator of apoptosis	484 (109,777)	0.7	290[a] (160,440)	0.6	306[a] (111,324)	2.0	1.6
NM_018685	ANLN	Arrest in mitosis	316 (96,891)	0.7	235[a] (103,373)	0.7	86 (45,573)	2.1	2.1
NM_001130524	AP1M1	Cell cycle	488 (421,544)	0.8	354[a] (65,857)	0.9	272[a] (56,511)	1.3	1.3
NM_001256834	AURKB	Arrest in mitosis	359 (312,1030)	1.0	241[a] (48,373)	1.1	184[a] (47,342)	1.6	1.5
NM_001032999	CBFA2T2	Transcription regulator	300 (139,438)	1.1	168[a] (145,381)	0.8	184[a] (63,332)	1.6	1.2
NM_006733	CENPI	Mitosis	640 (611,1732)	0.7	350[a] (134,933)	0.8	414[a] (302,515)	1.9	1.8
NM_017882	CLN6	Cell death	1097 (885,2878)	0.8	694[a] (457,770)	0.8	152[a] (45,741)	2.1	2.2
NM_001242481	EIF1AD	Protein translation	693 (233,1147)	0.7	182[a] (158,995)	0.6	189[a] (19,997)	1.5	1.6
NM_001184906	FBXL20	Arrest in mitosis	1305 (594,1904)	0.6	448[a] (78,935)	0.8	353[a] (98,471)	1.8	1.3
NM_017769	G2E3	Regulator of apoptosis	375 (301,851)	0.9	259[a] (109,569)	0.9	124[a] (69,417)	1.1	1.2
NM_001079518	MED24	Transcription regulator	345 (50,639)	0.7	129[a] (54,296)	0.6	213 (36,457)	2.2	2.5
NM_001003796	NHP2L1	S-phase regulation	390 (130,2280)	1.1	131 (111,297)	0.4	212[a] (105,698)	1.1	1.6
NM_138316	PANK1	S-phase regulation	477 (29,2483)	0.7	284 (43,727)	0.8	375 (47,996)	2.1	2.2
NM_012448	STAT5B	Transcription regulator	678 (435,3791)	0.6	245[a] (220,310)	0.6	292[a] (50,634)	2.1	1.8
NM_001006610	SIAH1	Negative regulator of cytokinesis	353 (93,1099)	0.7	138 (90,217)	0.7	113[a] (28,175)	1.5	1.6
NM_018423	STYK1	Cell cycle arrest	642 (253,3337)	0.5	143[a] (58,423)	0.6	196[a] (99,539)	1.8	2.1
NM_000430	PAFAH1B1	Arrest in mitosis	553 (431,1107)	0.8	89[a] (26,797)	0.5	108[a] (28,593)	1.3	1.4
NM_032354	TMEM107	Apoptosis	689 (218,1296)	0.4	295[a] (74,667)	0.5	377[a] (91,738)	1.5	1.3
Cellular metabolism regulators									
NM_018686	CMAS	Metabolism	922 (719,1875)	0.2	456 (311,532)	0.2	203[a] (109,615)	1.3	1.4
NM_147190	CERS5	Lipid metabolism	898 (28,1132)	0.8	399[a] (75,473)	0.7	236[a] (102,529)	2.0	2.2
NM_024345	DCAF10	Protein ubiquitination	514 (54,882)	0.7	217 (64,898)	0.7	359[a] (96,524)	2.1	2.0
NM_032138	KBTBD7	Protein metabolism	593 (416,1129)	0.8	219 (39,350)	0.8	283 (26,592)	1.5	1.6
NM_005723	TSPAN5	Motility	349 (126,624)	0.8	233[a] (52,701)	0.7	145[a] (72,656)	1.2	1.6
NM_014820	TOMM70A	Protein transport	187 (19,693)	0.8	77[a] (14,207)	0.7	171[a] (34,204)	1.3	1.2
NM_001195677	VAPB	Vesicle transport	748 (202,3698)	0.5	126[a] (14,267)	0.9	394[a] (95,907)	1.4	1.3
NM_007187	WBP4	Metabolism	137 (89,687)	0.9	103 (18,267)	0.4	170[a] (46,486)	1.7	1.8

(RefSeq ID) Reference sequence annotated in NCBI; (Biological process) annotated in NCBI; (T) T cells; (JK, H9) Jurkat or H9 cells; (HL) median half-life; (CI) confidence interval as measured by microarrays (as described in Materials and Methods); (FC) fold change; (FCE) fold change in enrichment.

[a]The *P*-value for the difference in transcript half-life between normal and malignant T cells is ≤0.05.

Table 2.2. Expression and half-lives of GRE-containing transcripts that were CELF1 targets in normal T cells but not malignant T cells.

RefSeq Transcript ID	Gene Symbol	Biological process	T HL (95% CI)	FC H9/T	H9 HL (95% CI)	FC JK/T	JK HL (95% CI)	FCE H9	FCE JK
Cell growth and motility									
NM_001017415	USP1	Protein ubiquitination	49 (18,80)	1.6	156[a] (49,262)	1.6	581[a] (184,1881)	0.43	0.36
NM_000462	UBE3A	Protein ubiquitination	67 (46,139)	1.5	346[a] (246,746)	1.7	1511[a] (586,6560)	0.64	0.70
NM_001017371	SP3	Transcription regulator	70 (14,126)	1.6	186 (55,316)	1.5	627[a] (241,2987)	0.44	0.51
NM_012197	RABGAP1	RAB GTPase activating protein 1	91 (12,168)	1.5	638[a] (279,2056)	1.5	616[a] (408,3741)	0.47	0.44
NM_005028	PIP4K2A	Cytoskeleton signaling	119 (34,204)	1.5	454 (69,2839)	1.4	1235[a] (148,3518)	0.48	0.57
NM_002806	PSMC6	Protein ubiquitination	88 (55,132)	1.8	259[a] (25,843)	1.9	717[a] (334,4900)	0.52	0.50
NM_005542	INSIG1	Insulin induced gene 1	86 (53,140)	1.7	124[a] (87,336)	1.5	788[a] (378,5455)	0.52	0.53
NM_006496	GNAI3	Cytoskeleton signaling	98 (30,1249)	1.7	547[a] (42,2135)	1.5	1081[a] (93,1405)	0.45	0.48
NM_012297	G3BP2	Scaffold protein	130 (98,501)	1.5	509[a] (81,358)	1.4	654[a] (131,2620)	0.44	0.42
NM_012300	FBXW11	Transcription regulator	71 (8,134)	1.4	366[a] (88,820)	1.5	146[a] (76,3603)	0.50	0.54
NM_001193416	DDX3X	Translation regulator	80 (15,145)	1.5	472[a] (117,1061)	1.5	459[a] (302,2221)	0.41	0.49
NM_001127192	CNBP	Transcription regulator	69 (16,121)	2.0	346[a] (99,1306)	1.8	477[a] (90,1345)	0.39	0.41
NM_014918	CHSY1	Cytoskeleton signaling	64 (31,131)	1.5	146[a] (66,227)	1.5	3614[a] (441,8067)	0.63	0.58
NM_005194	CEBPB	Transcription regulator	58 (23,94)	1.4	88 (27,150)	1.4	229[a] (58,815)	0.57	0.60
NM_001838	CCR7	Chemokine receptor	83 (27,138)	1.2	229[a] (72,529)	1.3	372[a] (124,1068)	0.52	0.55
NM_001008540	CXCR4	Chemokine receptor	61 (30,92)	1.4	49 (31,67)	1.5	271[a] (28,571)	0.46	0.33
Cell stress and cell survival									
NM_006948	HSPA13	Heat shock response	90 (3,182)	1.2	280[a] (161,722)	1.5	319[a] (114,507)	0.50	0.37
NM_003574	VAPA	Vesicle assembly protein	86 (19,153)	1.4	332[a] (90,753)	1.4	760[a] (596,1107)	0.55	0.59
NM_001010989	HERPUD1	Stress-inducible protein	133 (29,298)	1.4	79 (37,320)	1.4	331[a] (117,1834)	0.42	0.39
NM_019058	DDIT4	DNA-damage-inducible	50 (11,89)	1.7	738[a] (528,3248)	1.5	127[a] (79,432)	0.46	0.50
NM_005038	PPID	Oxidative stress response protein	67 (35,99)	1.4	437[a] (102,749)	1.4	445[a] (288,1199)	0.41	0.45

(RefSeq ID) Reference sequence annotated in NCBI; (Biological process) annotated in NCBI; (T) T cell; (JK, H9) Jurkat or H9 cells; (HL) median half-life; (CI) confidence interval, as measured by microarrays; (FC) fold change; (FCE) fold change in enrichment.
[a]The *P*-value for the difference in transcript half-life between normal and malignant T cells is ≤0.05.

Table 2.3. Biological pathways, which were enriched among CELF1 target transcripts from malignant T cells.

Diseases and disorders	Cancer
	Neurological disease
	Developmental abnormalities
Molecular and cellular function	Cell cycle
	Cellular organization
	Cell death and survival
Physiological system development and function	Tumor morphology
	Tissue morphology
	Organ morphology

Table 2.4. CELF1 targets in resting T cells are stabilized and overexpressed in malignant T-cell lines and primary T-cell tumors.

RefSeq ID	Gene symbol	FC H9/T	FC JK/T	FC T-ALL/T	T cells HL	H9 HL[a]	JK HL[a]	T-ALL HL[a]
NM_001066	TNFRSF1B	3.5	9.0	7.2	59 (38,182)	790 (486,866)	376 (5,587)	245 (117,374)
NM_006282	STK4	1.8	1.9	2.4	77 (57,199)	684 (194,813)	308 (61,491)	351 (101,498)
NM_005542	INSIG1	2.5	1.7	6.7	87 (65,216)	204 (54,385)	233 (60,407)	220 (51,409)
NM_002806	PSMC6	2.3	2.4	1.9	48 (9,314)	297 (72,470)	367 (74,545)	254 (80,411)
NM_025164	SIK3	1.5	1.8	6.2	99 (28,129)	790 (486,896)	376 (56,587)	270 (13,519)
NM_003340	UBE2D3	1.4	2.0	3.8	53 (19,229)	423 (119,568)	461 (96,623)	113 (27,349)
NM_002577	PAK2	1.5	1.8	6.4	58 (44,143)	333 (68,517)	308 (61,706)	409 (36,709)
NM_001252036	RAB5B	1.7	2.1	4.6	55 (22,218)	839 (276,958)	597 (273,711)	177 (30,447)
NM_005627	TGFBR2	6.5	3.8	5.7	50 (40,238)	511 (96,615)	511 (72,638)	422 (75,548)
NM_006908	RAC1	1.9	2.0	1.4	69 (48,153)	369 (38,159)	329 (50,152)	227 (8,197)
NM_005354	JUND	2.0	2.3	1.7	77 (10,100)	369 (52,520)	283 (87,396)	271 (21,498)
NM_005349	RBPJ	1.2	1.7	1.1	44 (11,252)	519 (415,622)	673 (224,794)	374 (127,509)
NM_005342	HMGB3	1.7	2.2	4.6	98 (20,274)	310 (146,435)	433 (204,552)	249 (41,472)
NM_000462	UBE3A	1.4	2.0	1.3	63 (59,166)	214 (17,610)	367 (261,474)	364 (99,471)
NM_015633	FGFR1OP2	2.4	6.3	7.6	51 (11,238)	505 (346,612)	518 (173,645)	177 (160,512)

(RefSeq ID) Reference sequence annotated in NCBI; (JK) Jurkat; (HL) mean half-life; (CI) confidence interval; (FC) fold change; (FCE) fold change in enrichment.
[a]The *P*-value for the difference in all transcript half-lives compared with normal T cells is ≤ 0.05. Statistical significance was determined based on $n = 3$ experiments for each malignant T-cell line, and $n = 4$ donors for primary T cells or T-ALL tumors.

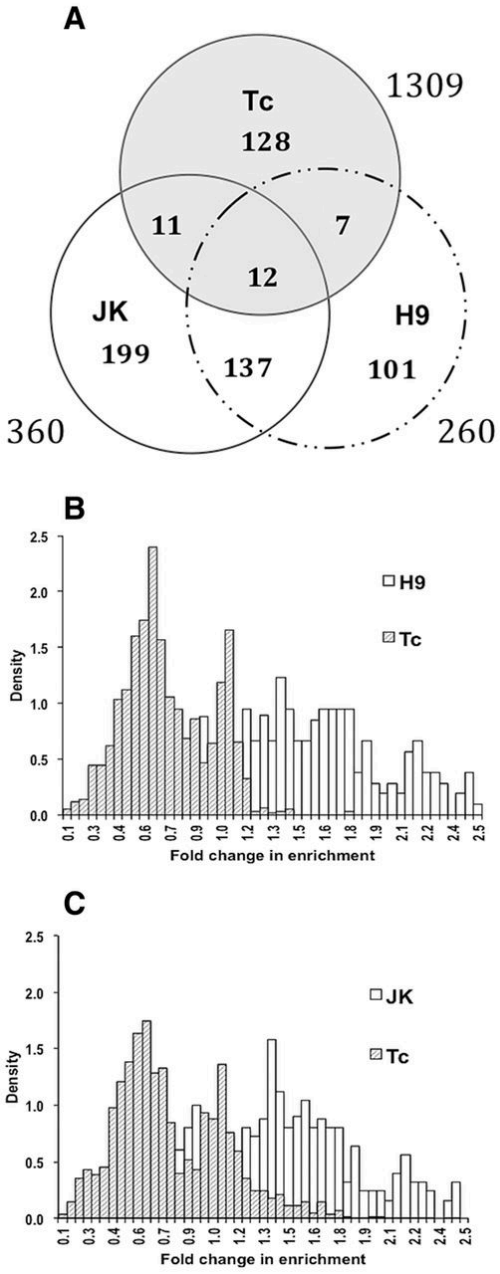

Figure 2.1. (A) Distinct CELF1 targets in normal and malignant T cells. The Venn diagram shows the number of transcripts identified in the CELF1 IP from normal T cells (Tc), H9 T cells (H9), and Jurkat T cells (JK). **(B,C) Altered association of CELF1 with target transcripts in malignant T cells compared with normal T cells.** For H9 (*B*) and Jurkat (*C*) T-cell lines, the fold change in enrichment (FCE) was calculated as described in the text. Histograms showing

the distribution of these values are depicted for CELF1 target transcripts in normal T cells (Tc, hatched gray bars) and H9 or Jurkat (JK) malignant T cells (empty bars). For each group of histograms, density on the *y*-axis is the normalized number of transcripts falling in a given FCE bin.

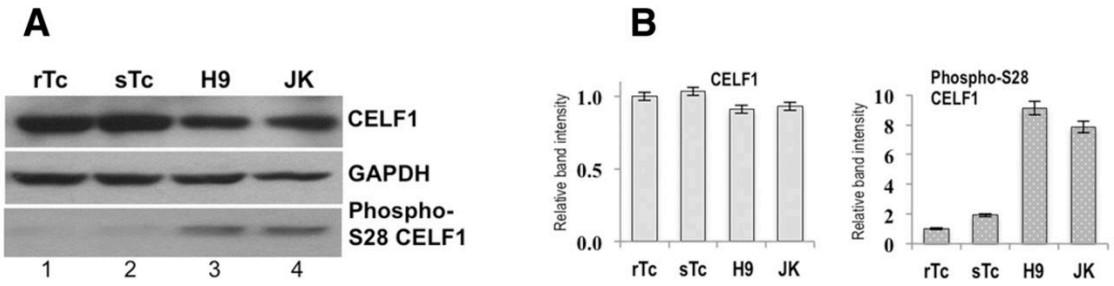

Figure 2.2. The levels of CELF1 and phopho-S28 CELF1 expression in normal and malignant T cells. (A) Cytoplasmic extracts were prepared from resting normal T cells (rTc), normal T cells that had been stimulated for 6 h with anti-CD3 and CD28 antibodies (sTc), H9 T cells, or Jurkat (JK) T cells. Equal amounts of cytoplasmic protein from each cell type were separated by SDS-polyacrylamide gel electrophoresis and the gels were blotted onto PVDF membranes which were probed with an anti-CELF1 antibody, an anti-phopho-S28 CELF1 antibody, and an anti-GAPDH antibody (loading control). (B) The experiment shown in A was performed three times and the images were quantified using Image J. For each experiment, the density of each CELF1 band or phospho-S28 CELF1 band was normalized to the density of the corresponding GAPDH band, and the average normalized densities were graphed. The error bars represent the ±SE for each average value.

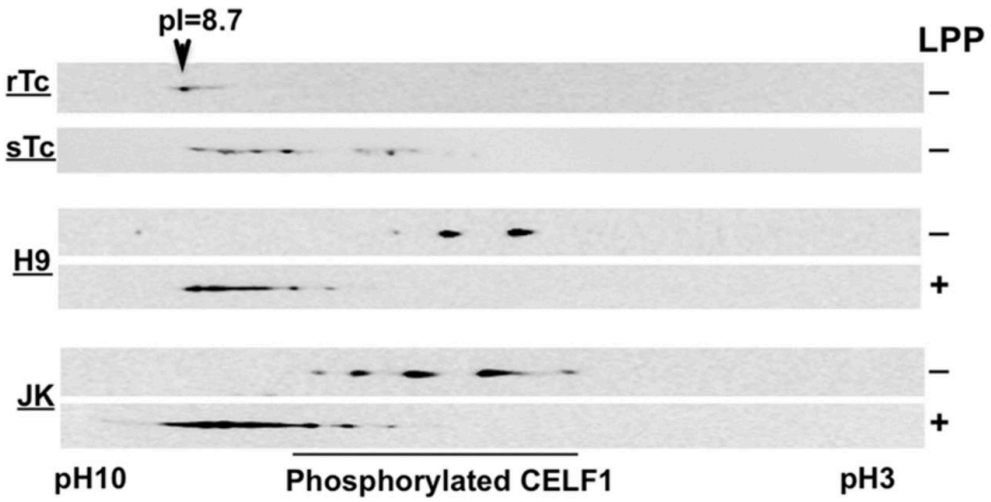

Figure 2.3. The CELF1 phosphorylation pattern differs in malignant T cells compared with normal stimulated T cells. Cytoplasmic lysates were prepared from normal resting T cells (rTc), normal T cells that were stimulated for 6 h with anti-CD3 and anti-CD28 antibodies (sTc), H9 T cells (H9), and Jurkat (JK) T cells. The lysates were treated with λ-protein phosphatase (LPP +) or mock-treated (LPP −). Samples were then separated by two-dimensional gel electrophoresis, and CELF1 was identified by Western blot analysis as described in Materials and Methods. The arrow represents the position of migration of the unphosphorylated form of CELF1, localized at pH 8.7. The results are representative of four independent experiments.

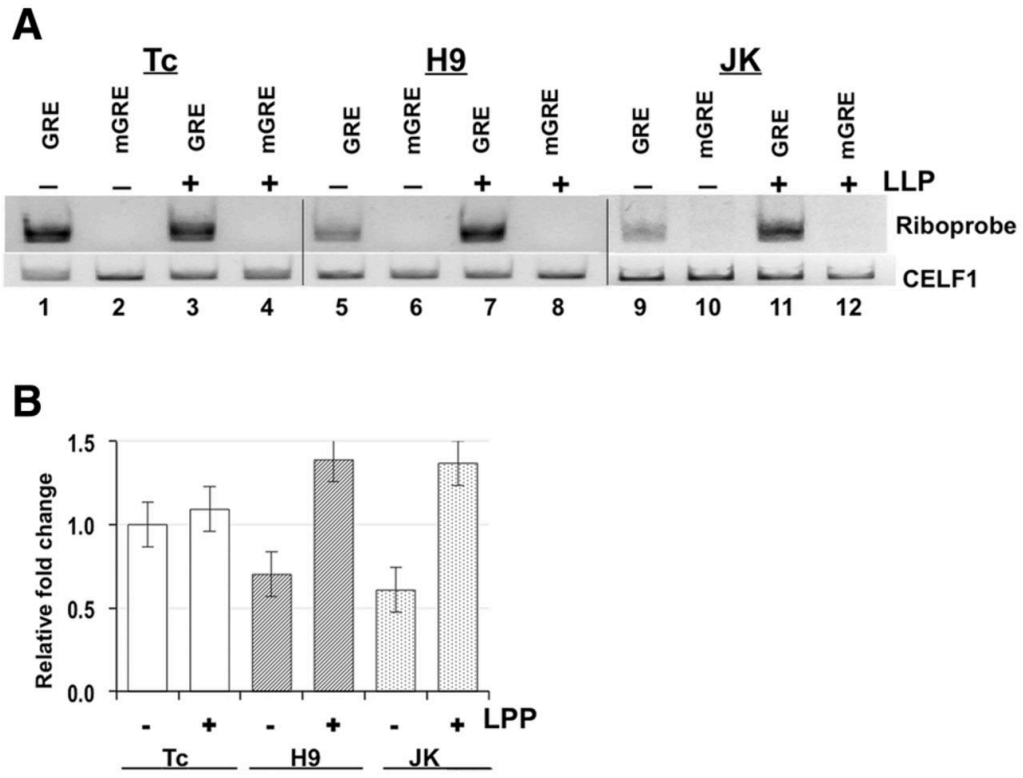

Figure 2.4. Dephosphorylation of CELF1 improves its in vitro binding to a GRE-riboprobe. (A) CELF1 protein was immunopurified on agarose beads from cytoplasmic extracts (100 µg of protein) from normal resting T cells (Tc), H9 T cells, or Jurkat (JK) T cells that were treated with either λ-protein phosphatase (LPP +) or mock-treated (LPP −). A biotinylated 35-nt GRE-riboprobe (GRE) or a mutated GRE RNA riboprobe (mGRE) was mixed with immunopurified CELF1. Complexes were then UV-crosslinked, separated by SDS electrophoresis, and transferred onto a nylon membrane. CELF1 binding to the biotinylated RNA riboprobe was visualized by probing the membrane with labeled streptavidin (top panel, Riboprobe). Subsequently, the same membranes were probed with an anti-CELF1 antibody to determine the amount of total CELF1 protein

immunopurified on beads (bottom panel, CELF1). (B) The experiment shown in A was performed four times. In each experiment the amount of bound riboprobe signal in each lane was normalized to the corresponding signal for total CELF1 protein. For lanes where the GRE-riboprobe was used, LPP+ signal was normalized to relative LPP− signal for bound riboprobe and graphed as the average and ±SE from each condition.

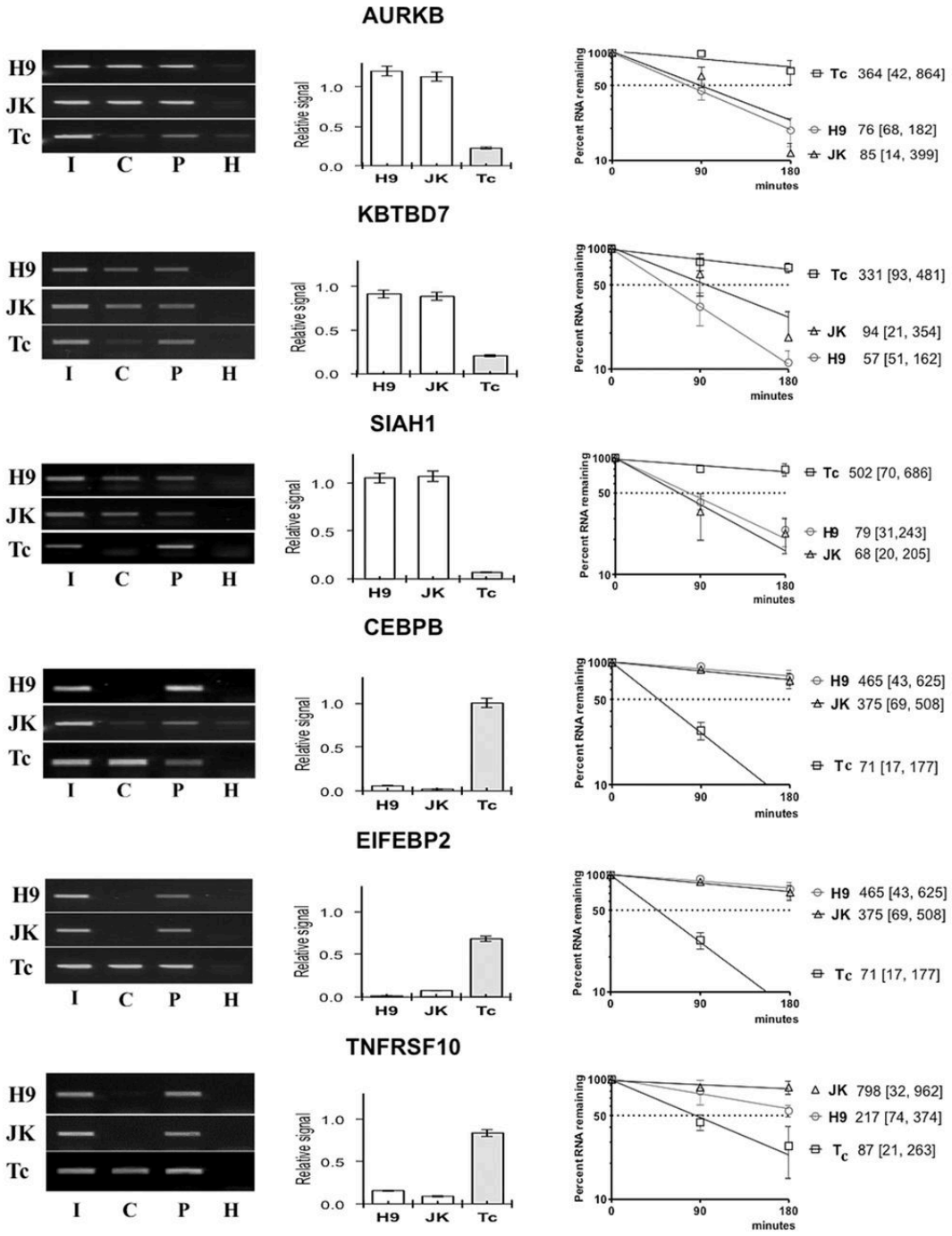

Figure 2.5. Binding by CELF1 is associated with mRNA destabilization. (Left) Cytoplasmic lysates were prepared from normal T cells (Tc), H9 T cells (H9), and Jurkat T cells (JK), and material from these lysates was

immunoprecipitated on beads coated with an anti-CELF1 antibody (C), an anti-Hemagglutinin antibody (H), or an anti-poly(A) binding protein antibody (P). RNA isolated from the input cytoplasmic lysates (I) and the immunoprecipitated material was analyzed by reverse transcription PCR using transcript-specific primers to amplify the indicated transcripts. (Middle) The experiment shown in A was performed three times, and band intensities were determined using Image J. For each band, the intensity of the corresponding HA (H) band was subtracted, and then the CELF1 (C) signal was normalized to the PABP (P) signal for each transcript. The normalized relative signal intensity of the CELF1 band was graphed for each transcript in each cell line as the average signal and ± standard error, SE, from three experiments. (Right) Real-time quantitative PCR was used to measure the half-lives of the transcripts shown in A and B in normal and malignant T cells. Actinomycin D was added to primary human T cells (T), H9 or Jurkat (JK) T-cell cultures, and total cellular RNA was harvested at 0-, 90-, and 180-min time points. mRNA levels were measured by quantitative real-time PCR using transcript-specific primers, and transcript levels were normalized to the level of the HPRT transcript. The normalized level of each transcript was set at 100% at time zero, and the other time points were graphed relative to that value using Graph Prism Software. Each point represents the mean and standard error of the mean from three or four independent experiments. To the right of the graph, the mean half-life (in minutes) and 95% confidence interval is shown for each transcript in each cell type.

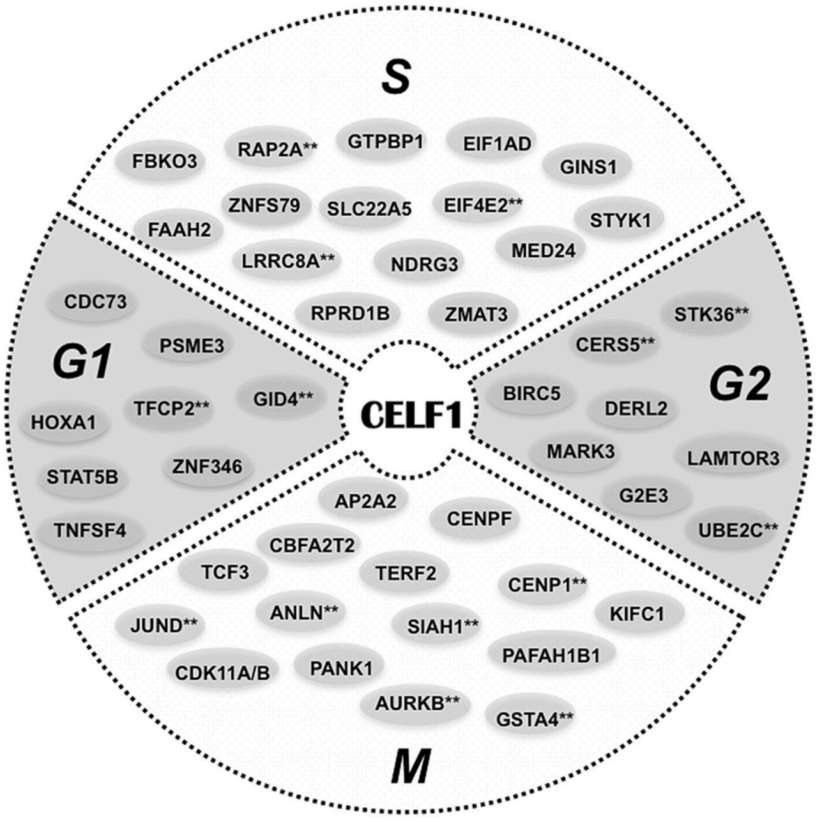

Figure 2.6. CELF1 targets in malignant T-cell lines encode cell cycle regulators. Ingenuity pathway analysis identified regulators of cell cycle as the top molecular network overrepresented among CELF1 targets in malignant T cells. This figure shows transcripts that were CELF1 targets in both H9 and Jurkat malignant T cells, but not normal T cells. The phases of the cell cycle (G1, S, G2, M) indicate the cell cycle phase where the proteins encoded by these transcripts are thought to function (Ingenuity Knowledge Database). Transcripts indicated with double asterisks (**) were also found to be CELF1 targets in the malignant HeLa cell line. This figure was built using Ingenuity Pathway Analysis, Canonical Pathways.

Table 3.1. NS5A affinity (Kd) for binding to RNA oligonucleotides

RNA	Sequence	K_d (nM)
1	GGCUGAGGCAGG	10 ± 1.5
2	GGGUGGGGGUGG	20 ± 2.7
3	UGUUUGUUUGUCCC	100 ± 10
4	UCUUUCUUUCUCCC	700 ± 200
5	UAUUUAUUUAUCCC	1000 ± 400
6	AAAAAAAAAAAAAA	1000 ± 150

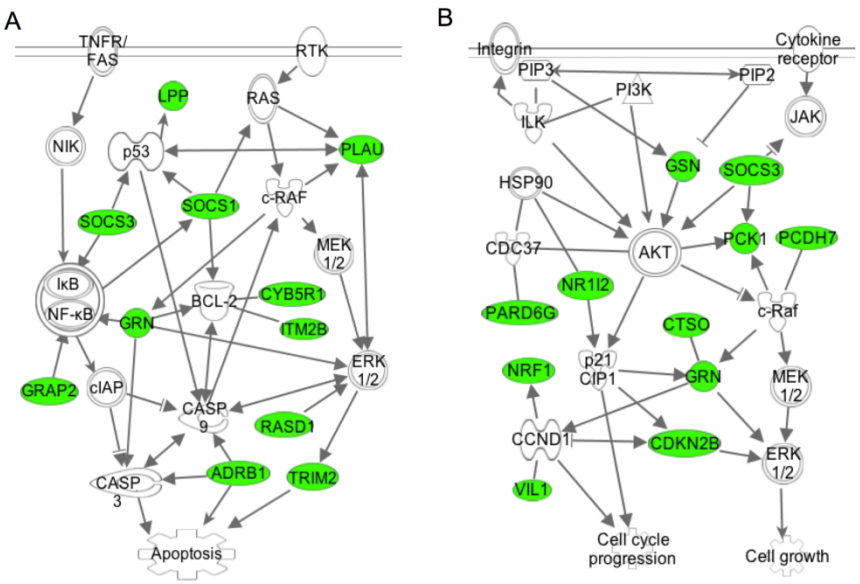

Figure 3.1. GRE-containing NS5A target transcripts encode regulators of apoptosis (A) and cell growth/proliferation (B). Transcripts depicted in green are NS5A target transcripts that contain GREs based on a FCE > 3 as defined in the Materials and Methods. These pathway figures were created using Ingenuity Pathway Assist software (Qiagen Inc).

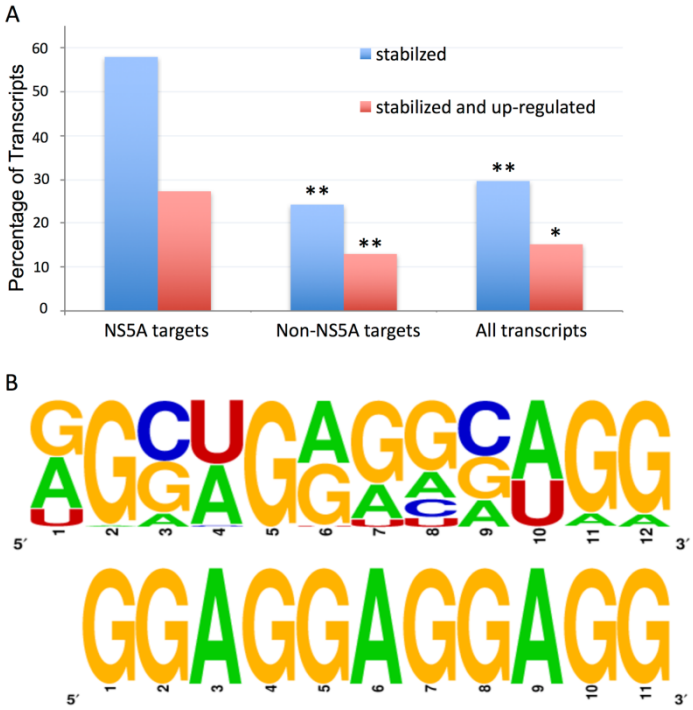

Figure 3.2. NS5A target transcripts are highly enriched for transcript stabilization and up-regulation. (A) The percentage of NS5A target transcripts, non-NS5A target transcripts and all transcripts that were stabilized (blue bars) or stabilized and up-regulated (red bars) is shown. **represents statistically significant differences (p-value<10^{-16}, Fisher's exact test with R) and *represents statistically significant differences (p-value<10^{-11}, Fisher's extact test, R) in the percentages comparing NS5A target transcripts to Non-NS5A target transcripts or all transcripts. (B) Top: A motif search was performed to look for conserved consensus sequences in the 3' UTRs of NS5A target transcripts. The top 12-mer motif is shown. The position in the signal (bases) is depicted on the horizontal axis. The height of each stack of letters on the vertical axis is proportional to the

residue frequency in the given position. Bottom: The motif previously found in CELF1 target transcripts that resembles the top 12-mer motif shown above.

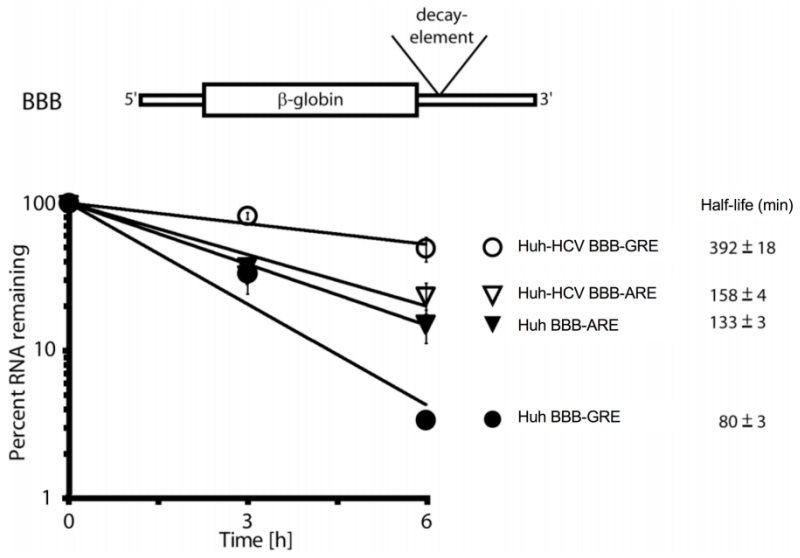

Figure 3.3. GRE-containing host mRNA transcripts are stabilized in Huh cells stably expressing an HCV subgenomic replicon (Huh-HCV). Huh or Huh-HCV cells were transfected with the BBB-GRE or BBB-ARE beta-globin reporter constructs. Actinomycin D was added to stop transcription and total cellular RNA was isolated after 0, 3 or 6 hours. Specific mRNA levels were determined by quantitative real time RT-PCR. Beta-globin transcript levels at each time point were normalized to the transcript levels from a co-transfected GFP reporter. Transcript levels at the 0 time point were set to 100%, and the percent mRNA remaining was plotted as a function of time. The error bars indicate the standard error of the mean (SEM) from three experiments. Transcript half-life and SEM are shown to the right of each graph.

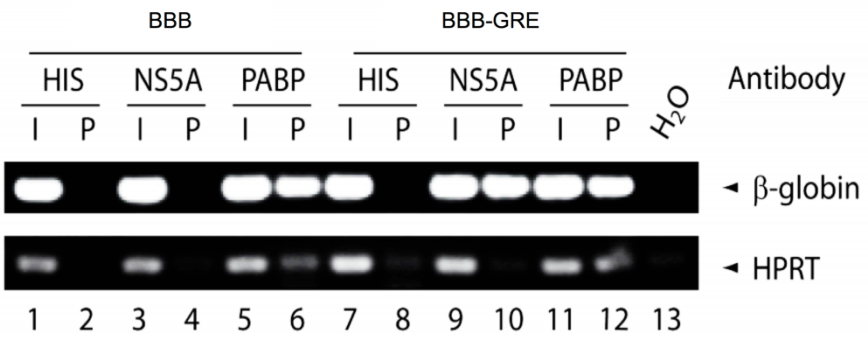

Figure 3.4. NS5A binds to GRE-containing transcripts in cells. Huh7-HCV cells were transfected with the BBB, or BBB-GRE reporter plasmids. Cell lysates were immunoprecipitated using specific antibodies against the His-tag (HIS), NS5A or the poly A binding protein (PABP). RNA isolated from the input (I) or the pellet fraction (P) was reverse transcribed and amplified by PCR using beta-globin and HPRT specific primers, and the RNA was separated by electrophoresis. Water (H_2O) was used as a contamination control for the PCR.

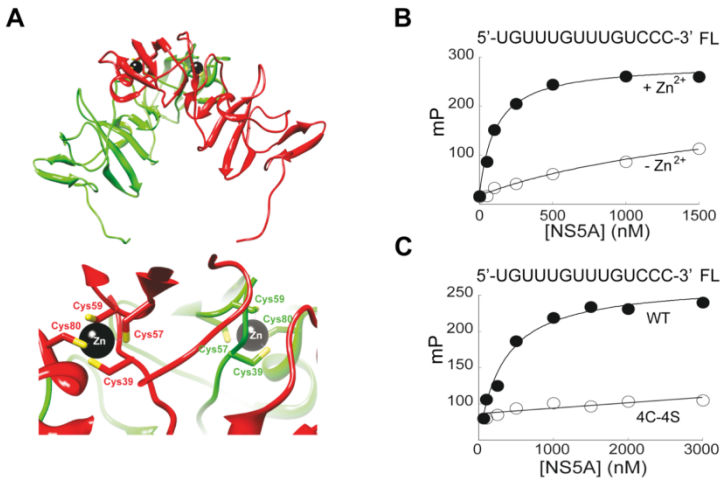

Figure 3.5. Recombinant NS5A binds to GRE RNA in a manner that is dependent on an intact zinc-binding site and the presence of zinc. (A) The upper panel shows a ribbon diagram of dimeric NS5A domain 1 that was prepared by using reference number 1ZH1 from the Protein Data Bank. One subunit is colored red and the other is colored green. The lower panel zooms in on the zinc-binding site of each subunit. Four conserved cysteines are required for zinc binding. (B) The NS5A domain 1+ polypeptide was titrated into a binding reaction buffer (20 mM HEPES pH 7.5, 5 mM $MgCl_2$, 10 mM 2-mercaptoethanol, 100 mM NaCl) in the absence ($-Zn^{2+}$) or presence ($+Zn^{2+}$) of 100 μM $ZnCl_2$ and incubated briefly at 25 °C in a final volume of 100 μl. Binding of NS5A was measured by the change in polarization (mP). The change in fluorescence

polarization was plotted as a function of NS5A domain 1+ concentration and fit to a hyperbola by using KaleidaGraph (Synergy Software). (C) Experiments were performed as described in panel B in the presence of zinc using the NS5A domain 1+ polypeptide or the derivative whose zinc-binding site was inactivated by converting the four cysteine residues to serine residues (4C-4S).

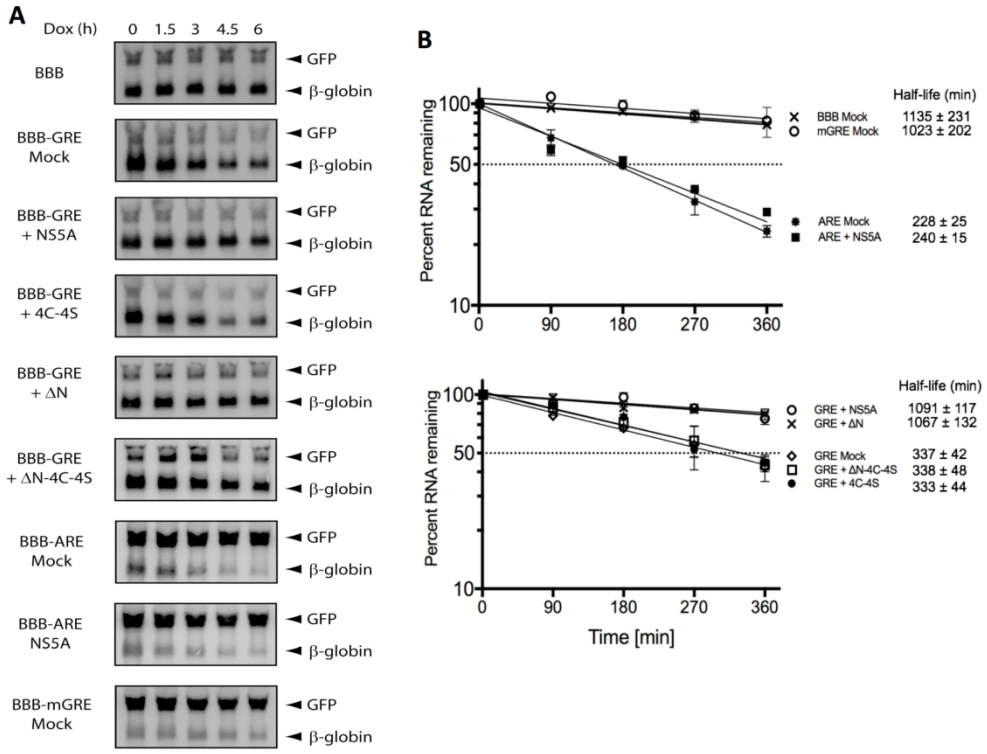

Figure 3.6. Exogenously expressed NS5A stabilizes GRE-containing reporter genes. (A) HeLa tet-off cells were transfected with BBB, BBB-GRE, BBB-ARE or BBB-mGRE reporter plasmids as well as a plasmid that express NS5A, NS5A-4C-4S, ΔN-NS5A, ΔN-NS5A-4C-4S or a mock control plasmid. A GFP expression plasmid was included in each to control for transfection efficiency. Transcription from the tet-responsive promoter was stopped with 300 ng of doxycycline and RNA harvested after 0, 1.5, 3, 4.5 or 6 hours was analyzed by northern blotting using GFP and beta-globin probes. (B) The experiment shown in (A) was performed 3 times, and the northern blot signals were quantified by a Storm 820 phosphorimager (Amersham Biosciences). For each time point, the

intensity of the beta-globin reporter was normalized to the intensity of the GFP band, and the band intensity at the 0 time point was set to 100%. The percent of mRNA remaining was plotted over time. The error bars indicate the standard error of the mean (SEM) from three experiments. The calculated transcript half-life and SEM are shown to the right of each graph.

Table 4.1. Number of cellular transcripts that were stabilized and up-regulated following reovirus infection.

	Strain c87	Strain c8	Strain Dearing	Strains c87 and c8	All 3 Strains
Stabilized ($p < 0.05$)	349	253	52	172	24
Stabilized and Up-regulated ($p < 0.05$)	70	49	2	26	0
Stabilized and Up-regulated (FC > 2-fold, $p < 0.05$)	31	41	0	13	0

Table 4.2. Subset of transcripts that were stabilized or up-regulated following reovirus infection.

Transcript Description	Gene Symbol	Mock HL(min)	Mock 95% CI	Strain c87 FC	Strain c87 HL(min)	Strain c87 95% CI	Strain c8 FC	Strain c8 HL(min)	Strain c8 95% CI
Up-regulated ($p \leq 0.05$) and Stabilized ($p \leq 0.05$); c87 and c8									
*growth differentiation factor 15	Gdf15	69	[47,124]	18.24	>480	[101,>480]	12.07	>480	[115,>480]
*MAD homolog 7 (Drosophila)	Smad7	67	[52,95]	4.03	197	[89,>480]	1.87	199	[90,>480]
*dual specificity phosphatase 1	Dusp1	50	[39,68]	3.65	>480	[112,>480]	3.65	104	[57,>480]
*myelocytomatosis oncogene	Myc	44	[37,55]	2.59	366	[108,>480]	2.20	183	[83,>480]
*vascular endothelial growth factor A	Vegfa	119	[79,240]	2.44	>480	[226,>480]	3.49	>480	[156,>480]
*TG interacting factor	Tgif	94	[76,124]	2.33	>480	[217,>480]	2.59	468	[174,>480]
*Kruppel-like factor 5	Klf5	115	[82,192]	2.18	>480	[149,>480]	1.78	>480	[179,>480]
coagulation factor III	F3	77	[55,130]	7.79	>480	[115,>480]	5.16	>480	[128,>480]
nuclear receptor subfamily 1, group D, member 1	Nr1d1	125	[89,207]	4.97	>480	[294,>480]	3.79	>480	[174,>480]
nuclear factor, interleukin 3, regulated	Nfil3	65	[49,100]	2.77	171	[75,>480]	2.85	184	[77,>480]
B-cell translocation gene 1, anti-proliferative	Btg1	152	[109,250]	1.68	>480	[398,>480]	2.15	>480	[209,>480]
CDC like kinase 4	Clk4	78	[59,115]	3.29	>480	[128,>480]	2.99	>480	[174,>480]
Up-regulated ($p \leq 0.05$) and Stabilized ($p \leq 0.05$); c87									
*dual specificity phosphatase 2	Dusp2	91	[60,180]	3.31	>480	[120,>480]	1.57	371	[96,>480]
*growth arrest and DNA-damage-inducible 45 beta	Gadd45 b	53	[40,79]	2.18	139	[63,>480]	3.21	80	[48,259]
*MAD homolog 2 (Drosophila)	Smad2	216	[153,368]	1.28	>480	[286,>480]	1.15	>480	[335,>480]
immediate early response 3	Ier3	49	[37,71]	4.22	230	[75,>480]	2.17	113	[56,>480]
nucleoporin 62	Nup62	146	[101,264]	1.73	>480	[196,>480]	1.06	188	[104,>480]
seven in absentia 2	Siah2	72	[56,100]	1.78	>480	[174,>480]	1.29	454	[129,>480]
Up-regulated ($p \leq 0.05$) and Stabilized ($p \leq 0.05$); c8									
*signal transducing adaptor molecule 1	Stam	222	[142,>480]	1.45	>480	[341,>480]	1.81	>480	[340,>480]
*MAD homolog 1 (Drosophila)	Smad1	163	[123,242]	1.16	>480	[>480,>480]	1.36	>480	[252,>480]
B-cell leukemia/lymphoma 6	Bcl6	49	[41,61]	1.01	>480	[130,>480]	1.86	273	[105,>480]
cyclin G2	Ccng2	93	[71,134]	0.67	>480	[215,>480]	2.41	>480	[229,>480]
TGFB inducible early growth response	Tieg / Klf10	61	[51,75]	0.69	287	[126,>480]	1.49	145	[88,397]
E4F transcription factor 1	E4f1	373	[216,>480]	1.24	>480	[443,>480]	1.58	>480	[>480,>480]
Stabilized ($p \leq 0.05$); c87 and c8									
*mitogen activated protein kinase kinase kinase 1	Map3k1	77	[59,108]	0.48	>480	[157,>480]	1.27	399	[128,>480]
*Cbp/p300-interacting transactivator, CITED2	Cited2	71	[56,97]	0.69	>480	[138,>480]	1.47	264	[110,>480]
*BCL2-like 11	Bcl2l11	67	[52,94]	0.86	348	[112,>480]	0.79	261	[102,>480]
*Son of sevenless homolog 2, (Drosophila)	Sos2	93	[63,174]	0.97	>480	[120,>480]	1.57	>480	[121,>480]
*B-cell leukemia/lymphoma 10	Bcl10	374	[239,>480]	1.10	>480	[>480,>480]	1.18	>480	[455,>480]
*TANK-binding kinase 1	Tbk1	121	[85,210]	1.04	>480	[142,>480]	1.20	>480	[170,>480]

*Transcripts shown in Fig 4.1.

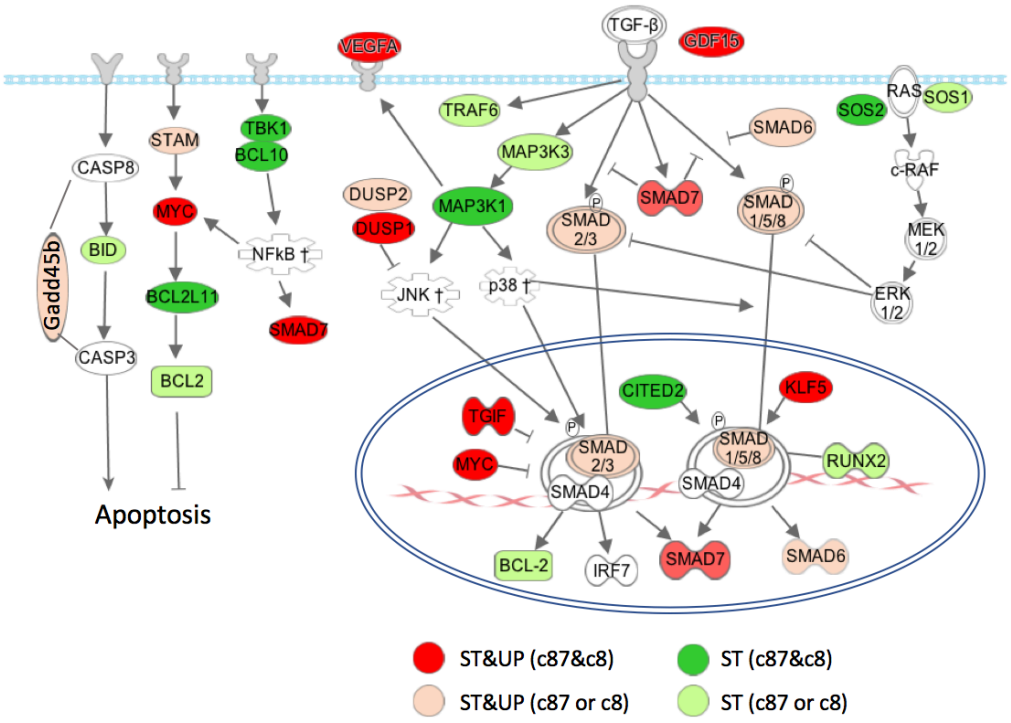

Figure 4.1. Transcripts that encode components of the SSN or related proteins were up-regulated and/or stabilized following reovirus infection. Signaling through the TGF-β family of receptors activate several pathways, including NF-κB, MAPK/ERK, p38, and JNK pathways. These pathways regulate phosphorylation of Smad proteins, which in turn regulate cell survival and apoptosis. Transcripts shown in red were up-regulated and stabilized following infection of L929 cells with reovirus isolates c87 and c8, transcripts shown in light orange were up-regulated and stabilized following infection with isolate c87 or c8, transcripts shown in dark green were stabilized (but not up-regulated) following infection with isolates c87 and c8, and transcripts shown in light green were stabilized (but not up-regulated) following infection with isolate c87 or c8.

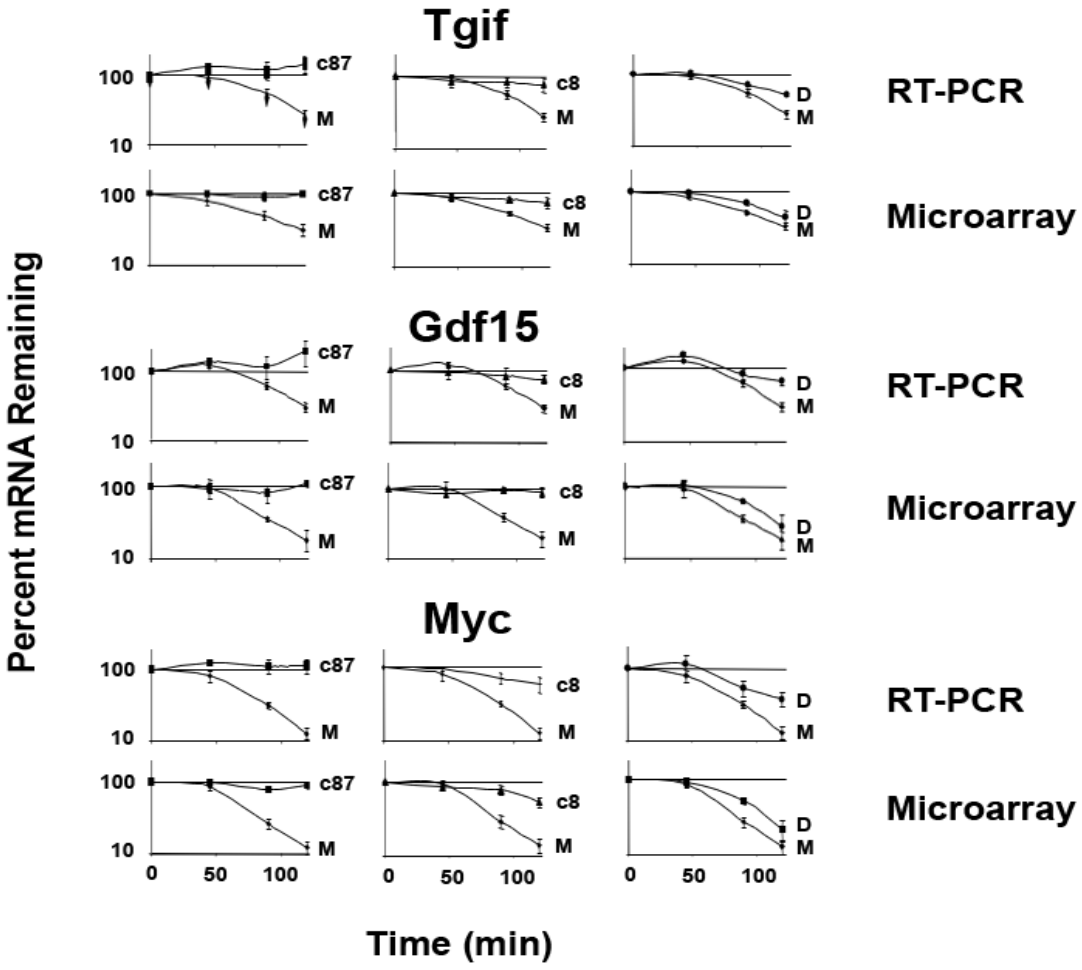

Figure 4.2. Real time RT-PCR validation of transcript up-regulation and stabilization. Murine L929 cells were infected for 19.5 h with reovirus isolates c87, c8 and Dearing or mock (M) infected. Actinomycin D was added to stop transcription and total cellular RNA was purified 0, 45, 90, and 120 min post-actinomycin D treatment. The same RNA was used for both microarry and real time RT-PCR. Tgif, Gdf-15 and c-Myc mRNA levels were measured by real-time RT-PCR using gene specific primers and transcript levels were normalized to the level of the HPRT transcript. Data shown are from three independent experiments. Each point represents the mean ± standard error of the mean.

Table 4.3. Comparison of transcript expression and half-life data obtained using real time RT-PCR or microarrays.

Transcript	Mock		Strain c87			Strain c8			Strain Dearing		
	HL(min)	95% CI	FC	HL(min)	95% CI	FC	HL(min)	95% CI	FC	HL(min)	95% CI
Tgif											
RT-PCR	83	[71,103]	3.49	>480	[>480]	3.69	>480	[>480]	2.78	171	[147,195]
Microarray	94	[76,124]	2.33	>480	[217,>480]	2.59	468	[174,>480]	1.55	113	[80,191]
Gdf15											
RT-PCR	124	[85,174]	20.45	>480	[>480]	18.24	>480	[458,>480]	14.19	226	[151,>480]
Microarray	69	[47,124]	18.24	>480	[101,>480]	12.07	>480	[115,>480]	3.83	63	[40,149]
Myc											
RT-PCR	54	[47,61]	1.43	>480	[>480]	2.60	339	[223,443]	1.85	86	[75,98]
Microarray	44	[37,55]	2.59	366	[108,>480]	2.20	183	[83,>480]	1.89	56	[41,88]

Bibliography

1. Elmore S. Apoptosis: a review of programmed cell death. Toxicol Pathol. 2007;35(4):495-516.
2. Favaloro B, Allocati N, Graziano V, Di Ilio C, De Laurenzi V. Role of apoptosis in disease. Aging (Albany NY). 2012;4(5):330-49.
3. Adams JM, Harris AW, Pinkert CA, Corcoran LM, Alexander WS, Cory S, et al. The c-myc oncogene driven by immunoglobulin enhancers induces lymphoid malignancy in transgenic mice. Nature. 1985;318(6046):533-8.
4. Romeo MM, Ko B, Kim J, Brady R, Heatley HC, He J, et al. Acetylation of the c-MYC oncoprotein is required for cooperation with the HTLV-1 p30(II) accessory protein and the induction of oncogenic cellular transformation by p30(II)/c-MYC. Virology. 2015;476:271-88.
5. Moody CA, Laimins LA. Human papillomavirus oncoproteins: pathways to transformation. Nat Rev Cancer. 2010;10(8):550-60.
6. Aerts I, Lumbroso-Le Rouic L, Gauthier-Villars M, Brisse H, Doz F, Desjardins L. Retinoblastoma. Orphanet J Rare Dis. 2006;1:31.
7. Henderson S, Rowe M, Gregory C, Croom-Carter D, Wang F, Longnecker R, et al. Induction of bcl-2 expression by Epstein-Barr virus latent membrane protein 1 protects infected B cells from programmed cell death. Cell. 1991;65(7):1107-15.
8. Jaiswal S, Traver D, Miyamoto T, Akashi K, Lagasse E, Weissman IL. Expression of BCR/ABL and BCL-2 in myeloid progenitors leads to myeloid leukemias. Proc Natl Acad Sci U S A. 2003;100(17):10002-7.
9. Hewitt EW. The MHC class I antigen presentation pathway: strategies for viral immune evasion. Immunology. 2003;110(2):163-9.
10. Garcia-Lora A, Algarra I, Garrido F. MHC class I antigens, immune surveillance, and tumor immune escape. J Cell Physiol. 2003;195(3):346-55.
11. zur Hausen H. Viruses in human cancers. Science. 1991;254(5035):1167-73.
12. Parkin DM. The global health burden of infection-associated cancers in the year 2002. Int J Cancer. 2006;118(12):3030-44.
13. McLaughlin-Drubin ME, Munger K. Viruses associated with human cancer. Biochim Biophys Acta. 2008;1782(3):127-50.
14. Munchel SE, Shultzaberger RK, Takizawa N, Weis K. Dynamic profiling of mRNA turnover reveals gene-specific and system-wide regulation of mRNA decay. Mol Biol Cell. 2011;22(15):2787-95.
15. Schwanhausser B, Busse D, Li N, Dittmar G, Schuchhardt J, Wolf J, et al. Global quantification of mammalian gene expression control. Nature. 2011;473(7347):337-42.
16. Shyu AB, Belasco JG, Greenberg ME. Two distinct destabilizing elements in the c-fos message trigger deadenylation as a first step in rapid mRNA decay. Genes Dev. 1991;5(2):221-31.
17. Song MG, Li Y, Kiledjian M. Multiple mRNA decapping enzymes in mammalian cells. Mol Cell. 2010;40(3):423-32.
18. Decker CJ, Parker R. A turnover pathway for both stable and unstable mRNAs in yeast: evidence for a requirement for deadenylation. Genes Dev. 1993;7(8):1632-43.

19. Hsu CL, Stevens A. Yeast cells lacking 5'-->3' exoribonuclease 1 contain mRNA species that are poly(A) deficient and partially lack the 5' cap structure. Mol Cell Biol. 1993;13(8):4826-35.
20. Chen CY, Gherzi R, Ong SE, Chan EL, Raijmakers R, Pruijn GJ, et al. AU binding proteins recruit the exosome to degrade ARE-containing mRNAs. Cell. 2001;107(4):451-64.
21. Liu H, Rodgers ND, Jiao X, Kiledjian M. The scavenger mRNA decapping enzyme DcpS is a member of the HIT family of pyrophosphatases. EMBO J. 2002;21(17):4699-708.
22. Chen CY, Shyu AB. Mechanisms of deadenylation-dependent decay. Wiley Interdiscip Rev RNA. 2011;2(2):167-83.
23. Keene JD. RNA regulons: coordination of post-transcriptional events. Nat Rev Genet. 2007;8(7):533-43.
24. Lai WS, Kennington EA, Blackshear PJ. Tristetraprolin and its family members can promote the cell-free deadenylation of AU-rich element-containing mRNAs by poly(A) ribonuclease. Mol Cell Biol. 2003;23(11):3798-812.
25. Moraes KC, Wilusz CJ, Wilusz J. CUG-BP binds to RNA substrates and recruits PARN deadenylase. RNA. 2006;12(6):1084-91.
26. Wu X, Brewer G. The regulation of mRNA stability in mammalian cells: 2.0. Gene. 2012;500(1):10-21.
27. Caput D, Beutler B, Hartog K, Thayer R, Brown-Shimer S, Cerami A. Identification of a common nucleotide sequence in the 3'-untranslated region of mRNA molecules specifying inflammatory mediators. Proc Natl Acad Sci U S A. 1986;83(6):1670-4.
28. Chen CY, Shyu AB. AU-rich elements: characterization and importance in mRNA degradation. Trends Biochem Sci. 1995;20(11):465-70.
29. Bakheet T, Frevel M, Williams BR, Greer W, Khabar KS. ARED: human AU-rich element-containing mRNA database reveals an unexpectedly diverse functional repertoire of encoded proteins. Nucleic Acids Res. 2001;29(1):246-54.
30. Vlasova-St Louis I, Bohjanen PR. Post-transcriptional regulation of cytokine and growth factor signaling in cancer. Cytokine Growth Factor Rev. 2017;33:83-93.
31. Hodge DL, Berthet C, Coppola V, Kastenmuller W, Buschman MD, Schaughency PM, et al. IFN-gamma AU-rich element removal promotes chronic IFN-gamma expression and autoimmunity in mice. J Autoimmun. 2014;53:33-45.
32. Jacob CO, Hwang F, Lewis GD, Stall AM. Tumor necrosis factor alpha in murine systemic lupus erythematosus disease models: implications for genetic predisposition and immune regulation. Cytokine. 1991;3(6):551-61.
33. Gillis P, Malter JS. The adenosine-uridine binding factor recognizes the AU-rich elements of cytokine, lymphokine, and oncogene mRNAs. J Biol Chem. 1991;266(5):3172-7.
34. Lai WS, Carballo E, Strum JR, Kennington EA, Phillips RS, Blackshear PJ. Evidence that tristetraprolin binds to AU-rich elements and promotes the deadenylation and destabilization of tumor necrosis factor alpha mRNA. Mol Cell Biol. 1999;19(6):4311-23.
35. Brennan CM, Steitz JA. HuR and mRNA stability. Cell Mol Life Sci. 2001;58(2):266-77.

36. Raghavan A, Robison RL, McNabb J, Miller CR, Williams DA, Bohjanen PR. HuA and tristetraprolin are induced following T cell activation and display distinct but overlapping RNA binding specificities. J Biol Chem. 2001;276(51):47958-65.
37. Matsushita K, Takeuchi O, Standley DM, Kumagai Y, Kawagoe T, Miyake T, et al. Zc3h12a is an RNase essential for controlling immune responses by regulating mRNA decay. Nature. 2009;458(7242):1185-90.
38. Fan J, Ishmael FT, Fang X, Myers A, Cheadle C, Huang SK, et al. Chemokine transcripts as targets of the RNA-binding protein HuR in human airway epithelium. J Immunol. 2011;186(4):2482-94.
39. Lopez de Silanes I, Zhan M, Lal A, Yang X, Gorospe M. Identification of a target RNA motif for RNA-binding protein HuR. Proc Natl Acad Sci U S A. 2004;101(9):2987-92.
40. Mukherjee N, Lager PJ, Friedersdorf MB, Thompson MA, Keene JD. Coordinated posttranscriptional mRNA population dynamics during T-cell activation. Mol Syst Biol. 2009;5:288.
41. Stellato C, Gubin MM, Magee JD, Fang X, Fan J, Tartar DM, et al. Coordinate regulation of GATA-3 and Th2 cytokine gene expression by the RNA-binding protein HuR. J Immunol. 2011;187(1):441-9.
42. Winzen R, Gowrishankar G, Bollig F, Redich N, Resch K, Holtmann H. Distinct domains of AU-rich elements exert different functions in mRNA destabilization and stabilization by p38 mitogen-activated protein kinase or HuR. Mol Cell Biol. 2004;24(11):4835-47.
43. Jing Q, Huang S, Guth S, Zarubin T, Motoyama A, Chen J, et al. Involvement of microRNA in AU-rich element-mediated mRNA instability. Cell. 2005;120(5):623-34.
44. Vlasova IA, Tahoe NM, Fan D, Larsson O, Rattenbacher B, Sternjohn JR, et al. Conserved GU-rich elements mediate mRNA decay by binding to CUG-binding protein 1. Mol Cell. 2008;29(2):263-70.
45. Vlasova-St Louis I, Dickson AM, Bohjanen PR, Wilusz CJ. CELFish ways to modulate mRNA decay. Biochim Biophys Acta. 2013;1829(6-7):695-707.
46. Rattenbacher B, Beisang D, Wiesner DL, Jeschke JC, von Hohenberg M, St Louis-Vlasova IA, et al. Analysis of CUGBP1 targets identifies GU-repeat sequences that mediate rapid mRNA decay. Mol Cell Biol. 2010;30(16):3970-80.
47. Halees AS, Hitti E, Al-Saif M, Mahmoud L, Vlasova-St Louis IA, Beisang DJ, et al. Global assessment of GU-rich regulatory content and function in the human transcriptome. RNA Biol. 2011;8(4):681-91.
48. Beisang D, Rattenbacher B, Vlasova-St Louis IA, Bohjanen PR. Regulation of CUG-binding protein 1 (CUGBP1) binding to target transcripts upon T cell activation. J Biol Chem. 2012;287(2):950-60.
49. Beisang D, Reilly C, Bohjanen PR. Alternative polyadenylation regulates CELF1/CUGBP1 target transcripts following T cell activation. Gene. 2014;550(1):93-100.
50. Vlasova IA, McNabb J, Raghavan A, Reilly C, Williams DA, Bohjanen KA, et al. Coordinate stabilization of growth-regulatory transcripts in T cell malignancies. Genomics. 2005;86(2):159-71.

51. Chu PC, Kulp SK, Chen CS. Insulin-like growth factor-I receptor is suppressed through transcriptional repression and mRNA destabilization by a novel energy restriction-mimetic agent. Carcinogenesis. 2013;34(12):2694-705.
52. Hitti E, Bakheet T, Al-Souhibani N, Moghrabi W, Al-Yahya S, Al-Ghamdi M, et al. Systematic Analysis of AU-Rich Element Expression in Cancer Reveals Common Functional Clusters Regulated by Key RNA-Binding Proteins. Cancer Res. 2016;76(14):4068-80.
53. Al-Ahmadi W, Al-Ghamdi M, Al-Haj L, Al-Saif M, Khabar KS. Alternative polyadenylation variants of the RNA binding protein, HuR: abundance, role of AU-rich elements and auto-Regulation. Nucleic Acids Res. 2009;37(11):3612-24.
54. Mukherjee N, Jacobs NC, Hafner M, Kennington EA, Nusbaum JD, Tuschl T, et al. Global target mRNA specification and regulation by the RNA-binding protein ZFP36. Genome Biol. 2014;15(1):R12.
55. Raghavan A, Ogilvie RL, Reilly C, Abelson ML, Raghavan S, Vasdewani J, et al. Genome-wide analysis of mRNA decay in resting and activated primary human T lymphocytes. Nucleic Acids Res. 2002;30(24):5529-38.
56. Calaluce R, Gubin MM, Davis JW, Magee JD, Chen J, Kuwano Y, et al. The RNA binding protein HuR differentially regulates unique subsets of mRNAs in estrogen receptor negative and estrogen receptor positive breast cancer. BMC Cancer. 2010;10:126.
57. Kotta-Loizou I, Giaginis C, Theocharis S. Clinical significance of HuR expression in human malignancy. Med Oncol. 2014;31(9):161.
58. Sanduja S, Blanco FF, Young LE, Kaza V, Dixon DA. The role of tristetraprolin in cancer and inflammation. Front Biosci (Landmark Ed). 2012;17:174-88.
59. Suswam E, Li Y, Zhang X, Gillespie GY, Li X, Shacka JJ, et al. Tristetraprolin down-regulates interleukin-8 and vascular endothelial growth factor in malignant glioma cells. Cancer Res. 2008;68(3):674-82.
60. Nabors LB, Gillespie GY, Harkins L, King PH. HuR, a RNA stability factor, is expressed in malignant brain tumors and binds to adenine- and uridine-rich elements within the 3' untranslated regions of cytokine and angiogenic factor mRNAs. Cancer Res. 2001;61(5):2154-61.
61. Nabors LB, Suswam E, Huang Y, Yang X, Johnson MJ, King PH. Tumor necrosis factor alpha induces angiogenic factor up-regulation in malignant glioma cells: a role for RNA stabilization and HuR. Cancer Res. 2003;63(14):4181-7.
62. Griseri P, Bourcier C, Hieblot C, Essafi-Benkhadir K, Chamorey E, Touriol C, et al. A synonymous polymorphism of the Tristetraprolin (TTP) gene, an AU-rich mRNA-binding protein, affects translation efficiency and response to Herceptin treatment in breast cancer patients. Hum Mol Genet. 2011;20(23):4556-68.
63. Upadhyay R, Sanduja S, Kaza V, Dixon DA. Genetic polymorphisms in RNA binding proteins contribute to breast cancer survival. Int J Cancer. 2013;132(3):E128-38.
64. Blanco FF, Jimbo M, Wulfkuhle J, Gallagher I, Deng J, Enyenihi L, et al. The mRNA-binding protein HuR promotes hypoxia-induced chemoresistance through posttranscriptional regulation of the proto-oncogene PIM1 in pancreatic cancer cells. Oncogene. 2016;35(19):2529-41.

65. Lafarga V, Cuadrado A, Lopez de Silanes I, Bengoechea R, Fernandez-Capetillo O, Nebreda AR. p38 Mitogen-activated protein kinase- and HuR-dependent stabilization of p21(Cip1) mRNA mediates the G(1)/S checkpoint. Mol Cell Biol. 2009;29(16):4341-51.
66. Gabai VL, Meng L, Kim G, Mills TA, Benjamin IJ, Sherman MY. Heat shock transcription factor Hsf1 is involved in tumor progression via regulation of hypoxia-inducible factor 1 and RNA-binding protein HuR. Mol Cell Biol. 2012;32(5):929-40.
67. Zhang J, Modi Y, Yarovinsky T, Yu J, Collinge M, Kyriakides T, et al. Macrophage beta2 integrin-mediated, HuR-dependent stabilization of angiogenic factor-encoding mRNAs in inflammatory angiogenesis. Am J Pathol. 2012;180(4):1751-60.
68. Carrick DM, Blackshear PJ. Comparative expression of tristetraprolin (TTP) family member transcripts in normal human tissues and cancer cell lines. Arch Biochem Biophys. 2007;462(2):278-85.
69. Lee HH, Yang SS, Vo MT, Cho WJ, Lee BJ, Leem SH, et al. Tristetraprolin down-regulates IL-23 expression in colon cancer cells. Mol Cells. 2013;36(6):571-6.
70. Patial S, Curtis AD, 2nd, Lai WS, Stumpo DJ, Hill GD, Flake GP, et al. Enhanced stability of tristetraprolin mRNA protects mice against immune-mediated inflammatory pathologies. Proc Natl Acad Sci U S A. 2016;113(7):1865-70.
71. Ross CR, Brennan-Laun SE, Wilson GM. Tristetraprolin: roles in cancer and senescence. Ageing Res Rev. 2012;11(4):473-84.
72. Van Tubergen E, Vander Broek R, Lee J, Wolf G, Carey T, Bradford C, et al. Tristetraprolin regulates interleukin-6, which is correlated with tumor progression in patients with head and neck squamous cell carcinoma. Cancer. 2011;117(12):2677-89.
73. Brennan SE, Kuwano Y, Alkharouf N, Blackshear PJ, Gorospe M, Wilson GM. The mRNA-destabilizing protein tristetraprolin is suppressed in many cancers, altering tumorigenic phenotypes and patient prognosis. Cancer Res. 2009;69(12):5168-76.
74. Bourcier C, Griseri P, Grepin R, Bertolotto C, Mazure N, Pages G. Constitutive ERK activity induces downregulation of tristetraprolin, a major protein controlling interleukin8/CXCL8 mRNA stability in melanoma cells. Am J Physiol Cell Physiol. 2011;301(3):C609-18.
75. Bohjanen PR, Moua ML, Guo L, Taye A, Vlasova-St Louis IA. Altered CELF1 binding to target transcripts in malignant T cells. RNA. 2015;21(10):1757-69.
76. Liu L, Ouyang M, Rao JN, Zou T, Xiao L, Chung HK, et al. Competition between RNA-binding proteins CELF1 and HuR modulates MYC translation and intestinal epithelium renewal. Mol Biol Cell. 2015;26(10):1797-810.
77. Lebedeva S, Jens M, Theil K, Schwanhausser B, Selbach M, Landthaler M, et al. Transcriptome-wide analysis of regulatory interactions of the RNA-binding protein HuR. Mol Cell. 2011;43(3):340-52.
78. Zhu Z, Wang B, Bi J, Zhang C, Guo Y, Chu H, et al. Cytoplasmic HuR expression correlates with P-gp, HER-2 positivity, and poor outcome in breast cancer. Tumour Biol. 2013;34(4):2299-308.
79. Kuyumcu-Martinez NM, Wang GS, Cooper TA. Increased steady-state levels of CUGBP1 in myotonic dystrophy 1 are due to PKC-mediated hyperphosphorylation. Mol Cell. 2007;28(1):68-78.

80. Vlasova-St Louis I, Bohjanen PR. Feedback Regulation of Kinase Signaling Pathways by AREs and GREs. Cells. 2016;5(1).
81. Simone LE, Keene JD. Mechanisms coordinating ELAV/Hu mRNA regulons. Curr Opin Genet Dev. 2013;23(1):35-43.
82. Zhang L, Lee JE, Wilusz J, Wilusz CJ. The RNA-binding protein CUGBP1 regulates stability of tumor necrosis factor mRNA in muscle cells: implications for myotonic dystrophy. J Biol Chem. 2008;283(33):22457-63.
83. Dean JL, Wait R, Mahtani KR, Sully G, Clark AR, Saklatvala J. The 3' untranslated region of tumor necrosis factor alpha mRNA is a target of the mRNA-stabilizing factor HuR. Mol Cell Biol. 2001;21(3):721-30.
84. Khabar KS, Young HA. Post-transcriptional control of the interferon system. Biochimie. 2007;89(6-7):761-9.
85. Khabar KS. Post-transcriptional control of cytokine gene expression in health and disease. J Interferon Cytokine Res. 2014;34(4):215-9.
86. Rivas HG, Schmaling SK, Gaglia MM. Shutoff of Host Gene Expression in Influenza A Virus and Herpesviruses: Similar Mechanisms and Common Themes. Viruses. 2016;8(4):102.
87. Esclatine A, Taddeo B, Evans L, Roizman B. The herpes simplex virus 1 UL41 gene-dependent destabilization of cellular RNAs is selective and may be sequence-specific. Proc Natl Acad Sci U S A. 2004;101(10):3603-8.
88. Shu M, Taddeo B, Roizman B. Tristetraprolin Recruits the Herpes Simplex Virion Host Shutoff RNase to AU-Rich Elements in Stress Response mRNAs To Enable Their Cleavage. J Virol. 2015;89(10):5643-50.
89. Kuroshima T, Aoyagi M, Yasuda M, Kitamura T, Jehung JP, Ishikawa M, et al. Viral-mediated stabilization of AU-rich element containing mRNA contributes to cell transformation. Oncogene. 2011;30(26):2912-20.
90. Barnhart MD, Moon SL, Emch AW, Wilusz CJ, Wilusz J. Changes in cellular mRNA stability, splicing, and polyadenylation through HuR protein sequestration by a cytoplasmic RNA virus. Cell Rep. 2013;5(4):909-17.
91. Dickson AM, Anderson JR, Barnhart MD, Sokoloski KJ, Oko L, Opyrchal M, et al. Dephosphorylation of HuR protein during alphavirus infection is associated with HuR relocalization to the cytoplasm. J Biol Chem. 2012;287(43):36229-38.
92. Qiu Y, Ye X, Hanson PJ, Zhang HM, Zong J, Cho B, et al. Hsp70-1: upregulation via selective phosphorylation of heat shock factor 1 during coxsackieviral infection and promotion of viral replication via the AU-rich element. Cell Mol Life Sci. 2016;73(5):1067-84.
93. Laroia G, Cuesta R, Brewer G, Schneider RJ. Control of mRNA decay by heat shock-ubiquitin-proteasome pathway. Science. 1999;284(5413):499-502.
94. Wong J, Si X, Angeles A, Zhang J, Shi J, Fung G, et al. Cytoplasmic redistribution and cleavage of AUF1 during coxsackievirus infection enhance the stability of its viral genome. FASEB J. 2013;27(7):2777-87.
95. Lee N, Pimienta G, Steitz JA. AUF1/hnRNP D is a novel protein partner of the EBER1 noncoding RNA of Epstein-Barr virus. RNA. 2012;18(11):2073-82.

96. Corcoran JA, Khaperskyy DA, Johnston BP, King CA, Cyr DP, Olsthoorn AV, et al. Kaposi's sarcoma-associated herpesvirus G-protein-coupled receptor prevents AU-rich-element-mediated mRNA decay. J Virol. 2012;86(16):8859-71.
97. Wang HW, Boshoff C. Linking Kaposi virus to cancer-associated cytokines. Trends Mol Med. 2005;11(7):309-12.
98. McCormick C, Ganem D. The kaposin B protein of KSHV activates the p38/MK2 pathway and stabilizes cytokine mRNAs. Science. 2005;307(5710):739-41.
99. Yoo J, Kang J, Lee HN, Aguilar B, Kafka D, Lee S, et al. Kaposin-B enhances the PROX1 mRNA stability during lymphatic reprogramming of vascular endothelial cells by Kaposi's sarcoma herpes virus. PLoS Pathog. 2010;6(8):e1001046.
100. Corcoran JA, Hsu WL, Smiley JR. Herpes simplex virus ICP27 is required for virus-induced stabilization of the ARE-containing IEX-1 mRNA encoded by the human IER3 gene. J Virol. 2006;80(19):9720-9.
101. Green J, Khabar KS, Koo BC, Williams BR, Polyak SJ. Stability of CXCL-8 and related AU-rich mRNAs in the context of hepatitis C virus replication in vitro. J Infect Dis. 2006;193(6):802-11.
102. Wagoner J, Austin M, Green J, Imaizumi T, Casola A, Brasier A, et al. Regulation of CXCL-8 (interleukin-8) induction by double-stranded RNA signaling pathways during hepatitis C virus infection. J Virol. 2007;81(1):309-18.
103. Friedrich S, Schmidt T, Schierhorn A, Lilie H, Szczepankiewicz G, Bergs S, et al. Arginine methylation enhances the RNA chaperone activity of the West Nile virus host factor AUF1 p45. RNA. 2016;22(10):1574-91.
104. Rozovics JM, Chase AJ, Cathcart AL, Chou W, Gershon PD, Palusa S, et al. Picornavirus modification of a host mRNA decay protein. MBio. 2012;3(6):e00431-12.
105. Guo L, Sharma SD, Debes J, Beisang D, Rattenbacher B, Louis IV, et al. The hepatitis C viral nonstructural protein 5A stabilizes growth-regulatory human transcripts. Nucleic Acids Res. 2018;46(5):2537-47.
106. de Chassey B, Navratil V, Tafforeau L, Hiet MS, Aublin-Gex A, Agaugue S, et al. Hepatitis C virus infection protein network. Mol Syst Biol. 2008;4:230.
107. Huang L, Hwang J, Sharma SD, Hargittai MR, Chen Y, Arnold JJ, et al. Hepatitis C virus nonstructural protein 5A (NS5A) is an RNA-binding protein. J Biol Chem. 2005;280(43):36417-28.
108. Raghavan A, Bohjanen PR. Microarray-based analyses of mRNA decay in the regulation of mammalian gene expression. Brief Funct Genomic Proteomic. 2004;3(2):112-24.
109. Turner M, Hodson D. Regulation of lymphocyte development and function by RNA-binding proteins. Curr Opin Immunol. 2012;24(2):160-5.
110. Khabar KS. Post-transcriptional control during chronic inflammation and cancer: a focus on AU-rich elements. Cellular and Molecular Life Sciences. 2010;67(17):2937-55.
111. Blackinton JG, Keene JD. Post-transcriptional RNA regulons affecting cell cycle and proliferation. Semin Cell Dev Biol. 2014;34:44-54.
112. Ogilvie RL, Abelson M, Hau HH, Vlasova I, Blackshear PJ, Bohjanen PR. Tristetraprolin down-regulates IL-2 gene expression through AU-rich element-mediated mRNA decay. J Immunol. 2005;174(2):953-61.

113. Ogilvie RL, Sternjohn JR, Rattenbacher B, Vlasova IA, Williams DA, Hau HH, et al. Tristetraprolin mediates interferon-gamma mRNA decay. Journal of Biological Chemistry. 2009;284(17):11216-23.
114. Vlasova-St Louis I, Bohjanen PR. Post-transcriptional regulation of cytokine signaling by AU-rich and GU-rich elements. J Interferon Cytokine Res. 2014;34(4):233-41.
115. Beisang D, Bohjanen PR. Perspectives on the ARE as it turns 25 years old. Wiley Interdiscip Rev RNA. 2012;3(5):719-31.
116. Vlasova IA, Bohjanen PR. Posttranscriptional regulation of gene networks by GU-rich elements and CELF proteins. RNA Biol. 2008;5(4):201-7.
117. Lee JE, Lee JY, Wilusz J, Tian B, Wilusz CJ. Systematic analysis of cis-elements in unstable mRNAs demonstrates that CUGBP1 is a key regulator of mRNA decay in muscle cells. PLoS One. 2010;5(6):e11201.
118. Wu J, Li C, Zhao S, Mao B. Differential expression of the Brunol/CELF family genes during Xenopus laevis early development. Int J Dev Biol. 2010;54(1):209-14.
119. Beisang D, Bohjanen P, Vlasova-St Louis I. CELF1, a Multifunctional Regulator of Posttranscriptional Networks. In: Kotb Abdelmohsen editor. 2012;Binding Protein. Chapter 8. InTech(Open Access):p.181-206.
120. Starr TK, Allaei R, Silverstein KA, Staggs RA, Sarver AL, Bergemann TL, et al. A transposon-based genetic screen in mice identifies genes altered in colorectal cancer. Science. 2009;323(5922):1747-50.
121. Gareau C, Fournier MJ, Filion C, Coudert L, Martel D, Labelle Y, et al. p21(WAF1/CIP1) upregulation through the stress granule-associated protein CUGBP1 confers resistance to bortezomib-mediated apoptosis. PLoS One. 2011;6(5):e20254.
122. Iakova P, Timchenko L, Timchenko NA. Intracellular signaling and hepatocellular carcinoma. Semin Cancer Biol. 2011;21(1):28-34.
123. Talwar S, Balasubramanian S, Sundaramurthy S, House R, Wilusz CJ, Kuppuswamy D, et al. Overexpression of RNA-binding protein CELF1 prevents apoptosis and destabilizes pro-apoptotic mRNAs in oral cancer cells. RNA Biol. 2013;10(2):277-86.
124. Wang GL, Salisbury E, Shi X, Timchenko L, Medrano EE, Timchenko NA. HDAC1 promotes liver proliferation in young mice via interactions with C/EBP beta. J Biol Chem. 2008.
125. Arnal-Estape A, Tarragona M, Morales M, Guiu M, Nadal C, Massague J, et al. HER2 silences tumor suppression in breast cancer cells by switching expression of C/EBPss isoforms. Cancer Res. 2010;70(23):9927-36.
126. Guerzoni C, Bardini M, Mariani SA, Ferrari-Amorotti G, Neviani P, Panno ML, et al. Inducible activation of CEBPB, a gene negatively regulated by BCR/ABL, inhibits proliferation and promotes differentiation of BCR/ABL-expressing cells. Blood. 2006;107(10):4080-9.
127. Benjamini Y, Hochberg Y. Controlling the False Discovery Rate - a Practical and Powerful Approach to Multiple Testing. J Roy Stat Soc B Met. 1995;57(1):289-300.
128. Neuwald AF, Liu JS, Lawrence CE. Gibbs motif sampling: detection of bacterial outer membrane protein repeats. Protein Sci. 1995;4(8):1618-32.

129. Favorov AV, Gelfand MS, Gerasimova AV, Ravcheev DA, Mironov AA, Makeev VJ. A Gibbs sampler for identification of symmetrically structured, spaced DNA motifs with improved estimation of the signal length. Bioinformatics. 2005;21(10):2240-5.
130. Yang X, An L, Li X. NDRG3 and NDRG4, two novel tumor-related genes. Biomed Pharmacother. 2013;67(7):681-4.
131. Darvin P, Joung YH, Yang YM. JAK2-STAT5B pathway and osteoblast differentiation. JAKSTAT. 2013;2(4):e24931.
132. Lokody I. Signalling: FOXM1 and CENPF: co-pilots driving prostate cancer. Nat Rev Cancer. 2014;14(7):450-1.
133. Crawford DF, Piwnica-Worms H. The G(2) DNA damage checkpoint delays expression of genes encoding mitotic regulators. J Biol Chem. 2001;276(40):37166-77.
134. Li Y, Du X, Li F, Deng Y, Yang Z, Wang Y, et al. A novel zinc-finger protein ZNF436 suppresses transcriptional activities of AP-1 and SRE. Molecular biology reports. 2006;33(4):287-94.
135. Parikh N, Hilsenbeck S, Creighton CJ, Dayaram T, Shuck R, Shinbrot E, et al. Effects of TP53 mutational status on gene expression patterns across 10 human cancer types. J Pathol. 2014;232(5):522-33.
136. Ting SB, Deneault E, Hope K, Cellot S, Chagraoui J, Mayotte N, et al. Asymmetric segregation and self-renewal of hematopoietic stem and progenitor cells with endocytic Ap2a2. Blood. 2012;119(11):2510-22.
137. Bemmo A, Dias C, Rose AA, Russo C, Siegel P, Majewski J. Exon-level transcriptome profiling in murine breast cancer reveals splicing changes specific to tumors with different metastatic abilities. PLoS One. 2010;5(8):e11981.
138. Hernandez JM, Floyd DH, Weilbaecher KN, Green PL, Boris-Lawrie K. Multiple facets of junD gene expression are atypical among AP-1 family members. Oncogene. 2008;27(35):4757-67.
139. McDaniel LD, Schultz RA, Friedberg EC. TERF2-XPF: caught in the middle; beginnings from the end. DNA Repair (Amst). 2006;5(7):868-72.
140. Valdivia MM, Hamdouch K, Ortiz M, Astola A. CENPA a genomic marker for centromere activity and human diseases. Curr Genomics. 2009;10(5):326-35.
141. Zimdahl B, Ito T, Blevins A, Bajaj J, Konuma T, Weeks J, et al. Lis1 regulates asymmetric division in hematopoietic stem cells and in leukemia. Nat Genet. 2014;46(3):245-52.
142. Hu D, Valentine M, Kidd VJ, Lahti JM. CDK11(p58) is required for the maintenance of sister chromatid cohesion. J Cell Sci. 2007;120(Pt 14):2424-34.
143. Choi HH, Choi HK, Jung SY, Hyle J, Kim BJ, Yoon K, et al. CHK2 kinase promotes pre-mRNA splicing via phosphorylating CDK11(p110). Oncogene. 2014;33(1):108-15.
144. Roy D, Arason GA, Chowdhury B, Mitra A, Calaf GM. Profiling of cell cycle genes of breast cells exposed to etodolac. Oncology reports. 2010;23(5):1383-91.
145. Hahn MA, Dickson KA, Jackson S, Clarkson A, Gill AJ, Marsh DJ. The tumor suppressor CDC73 interacts with the ring finger proteins RNF20 and RNF40 and is required for the maintenance of histone 2B monoubiquitination. Hum Mol Genet. 2012;21(3):559-68.

146. Kramer OH, Stauber RH, Bug G, Hartkamp J, Knauer SK. SIAH proteins: critical roles in leukemogenesis. Leukemia. 2013;27(4):792-802.
147. Goldenson B, Crispino JD. The aurora kinases in cell cycle and leukemia. Oncogene. 2014.
148. Zhao L, Birdwell LD, Wu A, Elliott R, Rose KM, Phillips JM, et al. Cell-type-specific activation of the oligoadenylate synthetase-RNase L pathway by a murine coronavirus. J Virol. 2013;87(15):8408-18.
149. Kang JH, Toita R, Kim CW, Katayama Y. Protein kinase C (PKC) isozyme-specific substrates and their design. Biotechnol Adv. 2012;30(6):1662-72.
150. Navarro MN, Cantrell DA. Serine-threonine kinases in TCR signaling. Nat Immunol. 2014;15(9):808-14.
151. Edwards J, Malaurie E, Kondrashov A, Long J, de Moor CH, Searle MS, et al. Sequence determinants for the tandem recognition of UGU and CUG rich RNA elements by the two N--terminal RRMs of CELF1. Nucleic Acids Res. 2011;39(19):8638-50.
152. Edwards JM, Long J, de Moor CH, Emsley J, Searle MS. Structural insights into the targeting of mRNA GU-rich elements by the three RRMs of CELF1. Nucleic Acids Res. 2013.
153. Teplova M, Song J, Gaw HY, Teplov A, Patel DJ. Structural insights into RNA recognition by the alternate-splicing regulator CUG-binding protein 1. Structure. 2010;18(10):1364-77.
154. Mayr C, Bartel DP. Widespread shortening of 3'UTRs by alternative cleavage and polyadenylation activates oncogenes in cancer cells. Cell. 2009;138(4):673-84.
155. Vlasova-St Louis I, Bohjanen PR. Coordinate regulation of mRNA decay networks by GU-rich elements and CELF1. Curr Opin Genet Dev. 2011;21(4):444-51.
156. Glaunsinger B, Chavez L, Ganem D. The exonuclease and host shutoff functions of the SOX protein of Kaposi's sarcoma-associated herpesvirus are genetically separable. J Virol. 2005;79(12):7396-401.
157. Elgadi MM, Hayes CE, Smiley JR. The herpes simplex virus vhs protein induces endoribonucleolytic cleavage of target RNAs in cell extracts. J Virol. 1999;73(9):7153-64.
158. Lindenbach BD, Rice, C.M. Flaviviridae: The viruses and their replication. Fourth ed ed. Knipe D.M. HPM, editor. Philadelphia: Lippincott-Raven; 2001. 991-1041 p.
159. Grakoui A, McCourt DW, Wychowski C, Feinstone SM, Rice CM. Characterization of the hepatitis C virus-encoded serine proteinase: determination of proteinase-dependent polyprotein cleavage sites. J Virol. 1993;67(5):2832-43.
160. Thrift AP E-SH, Kanwal F. Global epidemiology and burden of HCV infection and HCV-related disease. Nat Rev Gastroenterol Hepatol. 2016.
161. Poynard T, Yuen MF, Ratziu V, Lai CL. Viral hepatitis C. Lancet. 2003;362(9401):2095-100.
162. Jose D Debes HLAJ, Andre Boonstra. Hepatitis C treatment and liver cancer recurrence: cause for concern? The Lancet Gastroenterology & Hepatology. 2017;2(2):78-80.
163. Reig M, Marino Z, Perello C, Inarrairaegui M, Ribeiro A, Lens S, et al. Unexpected high rate of early tumor recurrence in patients with HCV-related HCC undergoing interferon-free therapy. J Hepatol. 2016;65(4):719-26.

164. Majumder M, Ghosh AK, Steele R, Ray R, Ray RB. Hepatitis C virus NS5A physically associates with p53 and regulates p21/waf1 gene expression in a p53-dependent manner. J Virol. 2001;75(3):1401-7.
165. Ghosh AK, Steele R, Meyer K, Ray R, Ray RB. Hepatitis C virus NS5A protein modulates cell cycle regulatory genes and promotes cell growth. J Gen Virol. 1999;80 (Pt 5):1179-83.
166. Lan KH, Sheu ML, Hwang SJ, Yen SH, Chen SY, Wu JC, et al. HCV NS5A interacts with p53 and inhibits p53-mediated apoptosis. Oncogene. 2002;21(31):4801-11.
167. Arima N, Kao CY, Licht T, Padmanabhan R, Sasaguri Y, Padmanabhan R. Modulation of cell growth by the hepatitis C virus nonstructural protein NS5A. J Biol Chem. 2001;276(16):12675-84.
168. Shirota Y, Luo H, Qin W, Kaneko S, Yamashita T, Kobayashi K, et al. Hepatitis C virus (HCV) NS5A binds RNA-dependent RNA polymerase (RdRP) NS5B and modulates RNA-dependent RNA polymerase activity. J Biol Chem. 2002;277(13):11149-55.
169. Huang L, Sineva EV, Hargittai MR, Sharma SD, Suthar M, Raney KD, et al. Purification and characterization of hepatitis C virus non-structural protein 5A expressed in Escherichia coli. Protein Expr Purif. 2004;37(1):144-53.
170. Shimakami T, Hijikata M, Luo H, Ma YY, Kaneko S, Shimotohno K, et al. Effect of interaction between hepatitis C virus NS5A and NS5B on hepatitis C virus RNA replication with the hepatitis C virus replicon. J Virol. 2004;78(6):2738-48.
171. Ivanov AV, Tunitskaya VL, Ivanova ON, Mitkevich VA, Prassolov VS, Makarov AA, et al. Hepatitis C virus NS5A protein modulates template selection by the RNA polymerase in in vitro system. FEBS Lett. 2009;583(2):277-80.
172. Tellinghuisen TL, Marcotrigiano J, Rice CM. Structure of the zinc-binding domain of an essential component of the hepatitis C virus replicase. Nature. 2005;435(7040):374-9.
173. Love RA, Brodsky O, Hickey MJ, Wells PA, Cronin CN. Crystal structure of a novel dimeric form of NS5A domain I protein from hepatitis C virus. J Virol. 2009;83(9):4395-403.
174. Graindorge A, Le Tonqueze O, Thuret R, Pollet N, Osborne HB, Audic Y. Identification of CUG-BP1/EDEN-BP target mRNAs in Xenopus tropicalis. Nucleic Acids Res. 2008;36(6):1861-70.
175. Zhong J, Gastaminza P, Cheng G, Kapadia S, Kato T, Burton DR, et al. Robust hepatitis C virus infection in vitro. Proc Natl Acad Sci U S A. 2005;102(26):9294-9.
176. Peng SS, Chen CY, Shyu AB. Functional characterization of a non-AUUUA AU-rich element from the c-jun proto-oncogene mRNA: evidence for a novel class of AU-rich elements. Mol Cell Biol. 1996;16(4):1490-9.
177. Blight KJ, Kolykhalov AA, Rice CM. Efficient initiation of HCV RNA replication in cell culture. Science. 2000;290(5498):1972-4.
178. Hwang J, Huang L, Cordek DG, Vaughan R, Reynolds SL, Kihara G, et al. Hepatitis C virus nonstructural protein 5A: biochemical characterization of a novel structural class of RNA-binding proteins. J Virol. 2010;84(24):12480-91.

179. Tenenbaum SA, Lager PJ, Carson CC, Keene JD. Ribonomics: identifying mRNA subsets in mRNP complexes using antibodies to RNA-binding proteins and genomic arrays. Methods. 2002;26(2):191-8.
180. Kiser KF, Colombi M, Moroni C. Isolation and characterization of dominant and recessive IL-3-independent hematopoietic transformants. Oncogene. 2006;25(50):6595-603.
181. Penin F, Brass V, Appel N, Ramboarina S, Montserret R, Ficheux D, et al. Structure and function of the membrane anchor domain of hepatitis C virus nonstructural protein 5A. J Biol Chem. 2004;279(39):40835-43.
182. Brass V, Bieck E, Montserret R, Wolk B, Hellings JA, Blum HE, et al. An amino-terminal amphipathic alpha-helix mediates membrane association of the hepatitis C virus nonstructural protein 5A. J Biol Chem. 2002;277(10):8130-9.
183. Sapay N, Montserret R, Chipot C, Brass V, Moradpour D, Deleage G, et al. NMR structure and molecular dynamics of the in-plane membrane anchor of nonstructural protein 5A from bovine viral diarrhea virus. Biochemistry. 2006;45(7):2221-33.
184. Sauter D, Himmelsbach K, Kriegs M, Carvajal Yepes M, Hildt E. Localization determines function: N-terminally truncated NS5A fragments accumulate in the nucleus and impair HCV replication. J Hepatol. 2009;50(5):861-71.
185. Hoffman B, Li Z, Liu Q. Downregulation of viral RNA translation by hepatitis C virus non-structural protein NS5A requires the poly(U/UC) sequence in the 3' UTR. J Gen Virol. 2015;96(8):2114-21.
186. Vockerodt M, Pinkert D, Smola-Hess S, Michels A, Ransohoff RM, Tesch H, et al. The Epstein-Barr virus oncoprotein latent membrane protein 1 induces expression of the chemokine IP-10: importance of mRNA half-life regulation. Int J Cancer. 2005;114(4):598-605.
187. Hojka-Osinska A, Budzko L, Zmienko A, Rybarczyk A, Maillard P, Budkowska A, et al. RNA-Seq-based analysis of differential gene expression associated with hepatitis C virus infection in a cell culture. Acta Biochim Pol. 2016;63(4):789-98.
188. Woodhouse SD, Narayan R, Latham S, Lee S, Antrobus R, Gangadharan B, et al. Transcriptome sequencing, microarray, and proteomic analyses reveal cellular and metabolic impact of hepatitis C virus infection in vitro. Hepatology. 2010;52(2):443-53.
189. Papic N, Maxwell CI, Delker DA, Liu S, Heale BS, Hagedorn CH. RNA-sequencing analysis of 5' capped RNAs identifies many new differentially expressed genes in acute hepatitis C virus infection. Viruses. 2012;4(4):581-612.
190. Walters KA, Syder AJ, Lederer SL, Diamond DL, Paeper B, Rice CM, et al. Genomic analysis reveals a potential role for cell cycle perturbation in HCV-mediated apoptosis of cultured hepatocytes. PLoS Pathog. 2009;5(1):e1000269.
191. Blackham S, Baillie A, Al-Hababi F, Remlinger K, You S, Hamatake R, et al. Gene expression profiling indicates the roles of host oxidative stress, apoptosis, lipid metabolism, and intracellular transport genes in the replication of hepatitis C virus. J Virol. 2010;84(10):5404-14.
192. Luna JM, Scheel TK, Danino T, Shaw KS, Mele A, Fak JJ, et al. Hepatitis C virus RNA functionally sequesters miR-122. Cell. 2015;160(6):1099-110.

193. Moon SL, Blackinton JG, Anderson JR, Dozier MK, Dodd BJ, Keene JD, et al. XRN1 stalling in the 5' UTR of Hepatitis C virus and Bovine Viral Diarrhea virus is associated with dysregulated host mRNA stability. PLoS Pathog. 2015;11(3):e1004708.
194. Kwon HJ, Xing W, Chan K, Niedziela-Majka A, Brendza KM, Kirschberg T, et al. Direct binding of ledipasvir to HCV NS5A: mechanism of resistance to an HCV antiviral agent. PLoS One. 2015;10(4):e0122844.
195. Craxi A, Laffi G, Zignego AL. Hepatitis C virus (HCV) infection: a systemic disease. Mol Aspects Med. 2008;29(1-2):85-95.
196. Hassan M, Selimovic D, Ghozlan H, Abdel-kader O. Hepatitis C virus core protein triggers hepatic angiogenesis by a mechanism including multiple pathways. Hepatology. 2009;49(5):1469-82.
197. Hanahan D, Weinberg RA. The hallmarks of cancer. Cell. 2000;100(1):57-70.
198. Debes JD, de Knegt RJ, Boonstra A. The path to cancer, and back: Immune modulation during hepatitis C virus infection, progression to fibrosis and cancer, and unexpected roles of new antivirals. Transplantation. 2016.
199. Moriya K, Fujie H, Shintani Y, Yotsuyanagi H, Tsutsumi T, Ishibashi K, et al. The core protein of hepatitis C virus induces hepatocellular carcinoma in transgenic mice. Nat Med. 1998;4(9):1065-7.
200. Fukutomi T, Zhou Y, Kawai S, Eguchi H, Wands JR, Li J. Hepatitis C virus core protein stimulates hepatocyte growth: correlation with upregulation of wnt-1 expression. Hepatology. 2005;41(5):1096-105.
201. Sadler AJ, Williams BR. Interferon-inducible antiviral effectors. Nat Rev Immunol. 2008;8(7):559-68.
202. Schoggins JW, Rice CM. Interferon-stimulated genes and their antiviral effector functions. Curr Opin Virol. 2011;1(6):519-25.
203. Schoenberg DR, Maquat LE. Regulation of cytoplasmic mRNA decay. Nat Rev Genet. 2012;13(4):246-59.
204. Guo L, Vlasova-St Louis I, Bohjanen PR. Viral manipulation of host mRNA decay. Future Virol. 2018;13(3):211-23.
205. Schiff LA, Nibert ML, Tyler KL. **Chapter 52: Orthoreoviruses and Their Replication**. In: Knipe DM, Howley PM, editors. Fields Virology, Fifth Edition. Philadelphia, PA: Lippincott Williams & Wilkins; 2007. p. 1854-915.
206. DeBiasi RL CP, Meintzer S, Jotte R, Kleinschmidt-Demasters BK, Johnson GL, Tyler KL. Reovirus-induced alteration in expression of apoptosis and DNA repair genes with potential roles in viral pathogenesis. Journal of Virology. 2003;77(16):8934-47.
207. O'Donnell SM, Holm GH, Pierce JM, Tian B, Watson MJ, Chari RS, et al. Identification of an NF-kappaB-dependent gene network in cells infected by mammalian reovirus. J Virol. 2006;80(3):1077-86.
208. Smith JA, Schmechel SC, Raghavan A, Abelson M, Reilly C, Katze MG, et al. Reovirus induces and benefits from an integrated cellular stress response. J Virol. 2006;80(4):2019-33.
209. Tyler KL, Leser JS, Phang TL, Clarke P. Gene expression in the brain during reovirus encephalitis. J Neurovirol. 2010;16(1):56-71.

210. Schmechel S, Chute M, Skinner P, Anderson R, Schiff L. Preferential translation of reovirus mRNA by a sigma3-dependent mechanism. Virology. 1997;232(1):62-73.
211. Sharpe AH, Fields BN. Reovirus inhibition of cellular RNA and protein synthesis: role of the S4 gene. Virology. 1982;122(2):381-91.
212. Smith JA, Schmechel SC, Williams BR, Silverman RH, Schiff LA. Involvement of the interferon-regulated antiviral proteins PKR and RNase L in reovirus-induced shutoff of cellular translation. J Virol. 2005;79(4):2240-50.
213. Liu F. Smad3 phosphorylation by cyclin-dependent kinases. Cytokine Growth Factor Rev. 2006;17(1-2):9-17.
214. Varga J, Pasche B. Antitransforming growth factor-beta therapy in fibrosis: recent progress and implications for systemic sclerosis. Curr Opin Rheumatol. 2008;20(6):720-8.
215. Li MO, Flavell RA. TGF-beta: a master of all T cell trades. Cell. 2008;134(3):392-404.
216. Massague J. TGFbeta in Cancer. Cell. 2008;134(2):215-30.
217. Massague J. TGFbeta signalling in context. Nat Rev Mol Cell Biol. 2012;13(10):616-30.
218. Kubiczkova L, Sedlarikova L, Hajek R, Sevcikova S. TGF-beta - an excellent servant but a bad master. J Transl Med. 2012;10:183.
219. Dosanjh A. Transforming growth factor-beta expression induced by rhinovirus infection in respiratory epithelial cells. Acta Biochim Biophys Sin (Shanghai). 2006;38(12):911-4.
220. Mendez-Samperio P, Hernandez M, Ayala HE. Induction of transforming growth factor-beta 1 production in human cells by herpes simplex virus. J Interferon Cytokine Res. 2000;20(3):273-80.
221. Rowan AG, Fletcher JM, Ryan EJ, Moran B, Hegarty JE, O'Farrelly C, et al. Hepatitis C virus-specific Th17 cells are suppressed by virus-induced TGF-beta. J Immunol. 2008;181(7):4485-94.
222. Malizia AP, Keating DT, Smith SM, Walls D, Doran PP, Egan JJ. Alveolar epithelial cell injury with Epstein-Barr virus upregulates TGFbeta1 expression. Am J Physiol Lung Cell Mol Physiol. 2008;295(3):L451-60.
223. Jiang Y, Yang M, Sun X, Chen X, Ma M, Yin X, et al. IL-10(+) NK and TGF-beta(+) NK cells play negative regulatory roles in HIV infection. BMC Infect Dis. 2018;18(1):80.
224. Li N, Ren A, Wang X, Fan X, Zhao Y, Gao GF, et al. Influenza viral neuraminidase primes bacterial coinfection through TGF-beta-mediated expression of host cell receptors. Proc Natl Acad Sci U S A. 2015;112(1):238-43.
225. Denney L, Branchett W, Gregory LG, Oliver RA, Lloyd CM. Epithelial-derived TGF-beta1 acts as a pro-viral factor in the lung during influenza A infection. Mucosal Immunol. 2017.
226. Gibbs JD, Ornoff DM, Igo HA, Zeng JY, Imani F. Cell cycle arrest by transforming growth factor beta1 enhances replication of respiratory syncytial virus in lung epithelial cells. J Virol. 2009;83(23):12424-31.

227. Beckham JD, Tuttle K, Tyler KL. Reovirus activates transforming growth factor beta and bone morphogenetic protein signaling pathways in the central nervous system that contribute to neuronal survival following infection. J Virol. 2009;83(10):5035-45.
228. Stanifer ML, Rippert A, Kazakov A, Willemsen J, Bucher D, Bender S, et al. Reovirus intermediate subviral particles constitute a strategy to infect intestinal epithelial cells by exploiting TGF-beta dependent pro-survival signaling. Cell Microbiol. 2016;18(12):1831-45.
229. Kedl R, S. Schmechel, and L. Schiff. Comparative sequence analysis of the reovirus S4 genes from 13 serotype 1 and serotype 3 field isolates. Journal of Virology. 1995;69:552-9.
230. Jacobs BL, Ferguson RE. The Lang strain of reovirus serotype 1 and the Dearing strain of reovirus serotype 3 differ in their sensitivities to beta interferon. J Virol. 1991;65(9):5102-4.
231. Rosen L, Hovis JF, Mastrota FM, Bell JA, Huebner RJ. Observations on a newly recognized virus (Abney) of the reovirus family. Am J Hyg. 1960;71:258-65.
232. Furlong DB, Nibert ML, Fields BN. Sigma 1 protein of mammalian reoviruses extends from the surfaces of viral particles. J Virol. 1988;62(1):246-56.
233. Ibarrola N, Kratchmarova I, Nakajima D, Schiemann WP, Moustakas A, Pandey A, et al. Cloning of a novel signaling molecule, AMSH-2, that potentiates transforming growth factor beta signaling. BMC Cell Biol. 2004;5:2.
234. Kucich U, Rosenbloom JC, Abrams WR, Rosenbloom J. Transforming growth factor-beta stabilizes elastin mRNA by a pathway requiring active Smads, protein kinase C-delta, and p38. Am J Respir Cell Mol Biol. 2002;26(2):183-8.
235. Massague J. How cells read TGF-beta signals. Nat Rev Mol Cell Biol. 2000;1(3):169-78.
236. Sanchez-Capelo A. Dual role for TGF-beta1 in apoptosis. Cytokine Growth Factor Rev. 2005;16(1):15-34.
237. Shi Y, Massague J. Mechanisms of TGF-beta signaling from cell membrane to the nucleus. Cell. 2003;113(6):685-700.
238. Rahimi RA, Leof EB. TGF-beta signaling: a tale of two responses. J Cell Biochem. 2007;102(3):593-608.
239. Zhang YE. Non-Smad Signaling Pathways of the TGF-beta Family. Cold Spring Harb Perspect Biol. 2017;9(2).
240. Zhang YE. Non-Smad pathways in TGF-beta signaling. Cell Res. 2009;19(1):128-39.
241. Freudlsperger C, Bian Y, Contag Wise S, Burnett J, Coupar J, Yang X, et al. TGF-beta and NF-kappaB signal pathway cross-talk is mediated through TAK1 and SMAD7 in a subset of head and neck cancers. Oncogene. 2013;32(12):1549-59.
242. Yamashita M, Fatyol K, Jin C, Wang X, Liu Z, Zhang YE. TRAF6 mediates Smad-independent activation of JNK and p38 by TGF-beta. Mol Cell. 2008;31(6):918-24.
243. Derynck R, Zhang YE. Smad-dependent and Smad-independent pathways in TGF-beta family signalling. Nature. 2003;425(6958):577-84.

244. Heldin CH, Landstrom M, Moustakas A. Mechanism of TGF-beta signaling to growth arrest, apoptosis, and epithelial-mesenchymal transition. Curr Opin Cell Biol. 2009;21(2):166-76.
245. Syed V. TGF-beta Signaling in Cancer. J Cell Biochem. 2016;117(6):1279-87.
246. Itoh S, Itoh F, Goumans MJ, Ten Dijke P. Signaling of transforming growth factor-beta family members through Smad proteins. Eur J Biochem. 2000;267(24):6954-67.
247. Moustakas A, Souchelnytskyi S, Heldin CH. Smad regulation in TGF-beta signal transduction. J Cell Sci. 2001;114(Pt 24):4359-69.
248. Heldin CH, Moustakas A. Role of Smads in TGFbeta signaling. Cell Tissue Res. 2012;347(1):21-36.
249. Ebisawa T, Fukuchi M, Murakami G, Chiba T, Tanaka K, Imamura T, et al. Smurf1 interacts with transforming growth factor-beta type I receptor through Smad7 and induces receptor degradation. J Biol Chem. 2001;276(16):12477-80.
250. Kavsak P, Rasmussen RK, Causing CG, Bonni S, Zhu H, Thomsen GH, et al. Smad7 binds to Smurf2 to form an E3 ubiquitin ligase that targets the TGF beta receptor for degradation. Mol Cell. 2000;6(6):1365-75.
251. Inoue Y, Imamura T. Regulation of TGF-beta family signaling by E3 ubiquitin ligases. Cancer Sci. 2008;99(11):2107-12.
252. Kim M, Chung YH, Johnston RN. Reovirus and tumor oncolysis. J Microbiol. 2007;45(3):187-92.
253. Gong J, Sachdev E, Mita AC, Mita MM. Clinical development of reovirus for cancer therapy: An oncolytic virus with immune-mediated antitumor activity. World J Methodol. 2016;6(1):25-42.
254. Ferrari G, Pintucci G, Seghezzi G, Hyman K, Galloway AC, Mignatti P. VEGF, a prosurvival factor, acts in concert with TGF-beta1 to induce endothelial cell apoptosis. Proc Natl Acad Sci U S A. 2006;103(46):17260-5.
255. Ferrari G, Terushkin V, Wolff MJ, Zhang X, Valacca C, Poggio P, et al. TGF-beta1 induces endothelial cell apoptosis by shifting VEGF activation of p38(MAPK) from the prosurvival p38beta to proapoptotic p38alpha. Mol Cancer Res. 2012;10(5):605-14.
256. Takeshita T, Arita T, Higuchi M, Asao H, Endo K, Kuroda H, et al. STAM, signal transducing adaptor molecule, is associated with Janus kinases and involved in signaling for cell growth and c-myc induction. Immunity. 1997;6(4):449-57.
257. Wang D, You Y, Lin PC, Xue L, Morris SW, Zeng H, et al. Bcl10 plays a critical role in NF-kappaB activation induced by G protein-coupled receptors. Proc Natl Acad Sci U S A. 2007;104(1):145-50.
258. Guo B, Cheng G. Modulation of the interferon antiviral response by the TBK1/IKKi adaptor protein TANK. J Biol Chem. 2007;282(16):11817-26.
259. Moser CV, Stephan H, Altenrath K, Kynast KL, Russe OQ, Olbrich K, et al. TANK-binding kinase 1 (TBK1) modulates inflammatory hyperalgesia by regulating MAP kinases and NF-kappaB dependent genes. J Neuroinflammation. 2015;12:100.
260. De Smaele E, Zazzeroni F, Papa S, Nguyen DU, Jin R, Jones J, et al. Induction of gadd45beta by NF-kappaB downregulates pro-apoptotic JNK signalling. Nature. 2001;414(6861):308-13.

261. Billen LP, Shamas-Din A, Andrews DW. Bid: a Bax-like BH3 protein. Oncogene. 2008;27 Suppl 1:S93-104.
262. Schuman J, Chen Y, Podd A, Yu M, Liu HH, Wen R, et al. A critical role of TAK1 in B-cell receptor-mediated nuclear factor kappaB activation. Blood. 2009;113(19):4566-74.
263. Weng T, Koh CG. POPX2 phosphatase regulates apoptosis through the TAK1-IKK-NF-kappaB pathway. Cell Death Dis. 2017;8(9):e3051.
264. Yan X, Liu Z, Chen Y. Regulation of TGF-beta signaling by Smad7. Acta Biochim Biophys Sin (Shanghai). 2009;41(4):263-72.
265. Holm GH, Pruijssers AJ, Li L, Danthi P, Sherry B, Dermody TS. Interferon regulatory factor 3 attenuates reovirus myocarditis and contributes to viral clearance. J Virol. 2010;84(14):6900-8.
266. Knowlton JJ, Dermody TS, Holm GH. Apoptosis induced by mammalian reovirus is beta interferon (IFN) independent and enhanced by IFN regulatory factor 3- and NF-kappaB-dependent expression of Noxa. J Virol. 2012;86(3):1650-60.
267. Qin Q, Hastings C, Miller CL. Mammalian orthoreovirus particles induce and are recruited into stress granules at early times postinfection. J Virol. 2009;83(21):11090-101.
268. Offermann MK. Kaposi sarcoma herpesvirus-encoded interferon regulator factors. Curr Top Microbiol Immunol. 2007;312:185-209.
269. Baresova P, Pitha PM, Lubyova B. Distinct roles of Kaposi's sarcoma-associated herpesvirus-encoded viral interferon regulatory factors in inflammatory response and cancer. J Virol. 2013;87(17):9398-410.
270. Gupta A, Gartner JJ, Sethupathy P, Hatzigeorgiou AG, Fraser NW. Anti-apoptotic function of a microRNA encoded by the HSV-1 latency-associated transcript. Nature. 2006;442(7098):82-5.
271. Nie Y, Cui D, Pan Z, Deng J, Huang Q, Wu K. HSV-1 infection suppresses TGF-beta1 and SMAD3 expression in human corneal epithelial cells. Mol Vis. 2008;14:1631-8.
272. Umbach JL, Kramer MF, Jurak I, Karnowski HW, Coen DM, Cullen BR. MicroRNAs expressed by herpes simplex virus 1 during latent infection regulate viral mRNAs. Nature. 2008;454(7205):780-3.
273. Meyers JM, Uberoi A, Grace M, Lambert PF, Munger K. Cutaneous HPV8 and MmuPV1 E6 Proteins Target the NOTCH and TGF-beta Tumor Suppressors to Inhibit Differentiation and Sustain Keratinocyte Proliferation. PLoS Pathog. 2017;13(1):e1006171.
274. Roman A, Munger K. The papillomavirus E7 proteins. Virology. 2013;445(1-2):138-68.
275. Arnulf B, Villemain A, Nicot C, Mordelet E, Charneau P, Kersual J, et al. Human T-cell lymphotropic virus oncoprotein Tax represses TGF-beta 1 signaling in human T cells via c-Jun activation: a potential mechanism of HTLV-I leukemogenesis. Blood. 2002;100(12):4129-38.
276. Abend JR, Imperiale MJ. Transforming growth factor-beta-mediated regulation of BK virus gene expression. Virology. 2008;378(1):6-12.

277. Kossmann T, Morganti-Kossmann MC, Orenstein JM, Britt WJ, Wahl SM, Smith PD. Cytomegalovirus production by infected astrocytes correlates with transforming growth factor-beta release. J Infect Dis. 2003;187(4):534-41.
278. Yang X, Wang W, Fan J, Lal A, Yang D, Cheng H, et al. Prostaglandin A2-mediated stabilization of p21 mRNA through an ERK-dependent pathway requiring the RNA-binding protein HuR. J Biol Chem. 2004;279(47):49298-306.
279. Okkenhaug K, Vanhaesebroeck B. PI3K in lymphocyte development, differentiation and activation. Nat Rev Immunol. 2003;3(4):317-30.
280. Choi WT, Folsom MR, Azim MF, Meyer C, Kowarz E, Marschalek R, et al. C/EBPbeta suppression by interruption of CUGBP1 resulting from a complex rearrangement of MLL. Cancer Genet Cytogenet. 2007;177(2):108-14.
281. Lewis K, Valanejad L, Cast A, Wright M, Wei C, Iakova P, et al. RNA Binding Protein CUGBP1 Inhibits Liver Cancer in a Phosphorylation-Dependent Manner. Mol Cell Biol. 2017;37(16).